Evaluation of Novel Ventilation Designs for Increasing Local Exhaust Ventilation Performance in Traditional Settings and Concrete Dowel Drilling

by

James R. Couch

A dissertation submitted in partial fulfillment
of the requirements for the degree of
Doctor of Philosophy
(Environmental Health Sciences)
in the University of Michigan
2016

Doctoral Committee:

Professor John D. Meeker, Chair
Kenneth Mead, National Institute for Occupational Safety and Health
Professor Bhramar Mukherjee
Assistant Professor Richard Neitzel

“It is not the critic who counts; not the man who points out how the strong man stumbles, or where the doer of deeds could have done them better. The credit belongs to the man who is actually in the arena, whose face is marred by dust and sweat and blood; who strives valiantly; who errs, who comes short again and again, because there is no effort without error and shortcoming; but who does actually strive to do the deeds; who knows great enthusiasms, the great devotions; who spends himself in a worthy cause; who at the best knows in the end the triumph of high achievement, and who at the worst, if he fails, at least fails while daring greatly, so that his place shall never be with those cold and timid souls who neither know victory nor defeat”.

-Theodore Roosevelt

This dissertation is dedicated to my wonderful wife Melissa, my loving parents Willie and Rosemary, my brother Willie and his family, and all of Melissa's family especially Wendy Bennett.

Acknowledgements

I would like to acknowledge my doctoral committee for their advice, patience, and wisdom. I would like to especially thank Dr. John Meeker for being my research advisor.

Thank you to my wife Melissa who sacrificed so much to allow me to pursue my dream. Without your love and support, this would have never became a reality. I cannot thank God enough for blessing me with such an amazing wife.

I would also like to acknowledge the National Institute for Occupational Safety and Health for allowing me to participate in the Long Term Training Program. Thank you to my NIOSH colleagues Alan Echt, Donald Booher, Dan Farwick, Ron Kovein, Jerry Kratzer, Kevin H. Dunn, Alberto Garcia, Duane Hammond, Scott Brueck, and all the Hazard Evaluation and Technical Assistance Branch, Engineering and Physical Hazards Branch, and Four Seasons Environmental folks that helped me along the way. Without your expertise, support, and assistance I would have never completed this research.

Table of Contents

List of Figures

List of Tables

ABSTRACT

Evaluation of Novel Ventilation Designs for Increasing Local Exhaust Ventilation Performance in Traditional Settings and Concrete Dowel Drilling

by

James Robert Couch

Chair: John D. Meeker

Over 2 million workers are potentially exposed to respirable crystalline silica with the overwhelming majority in the construction industry. Occupational exposure to respirable crystalline silica can lead to silicosis, lung cancer, and other adverse diseases. The present research evaluated novel designs in both traditional ventilation and local exhaust ventilation for a concrete dowel drill to reduce occupational exposures such as silica. The first study investigated traditional ventilation novel designs to increase capture velocities without increasing fan speeds or power consumption. Limited success was observed and further research is needed to refine the novel design to reach full potential. The second and third study focused on improving a concrete dowel drill local exhaust ventilation design to reduce potential respirable crystalline silica exposures during large concrete construction project such as airport runways. Previous research indicated that the manufacturer's local exhaust ventilation system reduced

respirable crystalline silica exposures by over 90 percent but the system was susceptible to filter and hose clogging which reduced performance. In the second study, a laboratory study evaluated two novel local exhaust ventilation hoods, one commercially available hood, and the dowel drill manufacturer's hood for hood efficiency and airflow characteristics. The novel design hoods increased the measured hood coefficient of entry from 0.59 for the manufacturer's hood to 0.64 indicating increased efficiency. Novel simple hood analysis found an average hood coefficient of entry of 0.81 which indicates that further improvements can be made to increase overall hood efficiency. In the third study, simulated workplace conditions were used to evaluate the best performance hood identified in laboratory testing along with other local exhaust ventilation modifications such as replacing the manufacturer's corrugated hose with smooth-bore hose and including a cyclone pre-separator to reduce the dust transport burden within the exhaust system. The most effective local exhaust ventilation configuration consisted of the novel design hood, smooth-bore hose, and cyclone which reduced average accumulated hose weight (manufacturer's configuration = 0.3 pounds per trial vs. most effective configuration = 0.05 pounds per trial) and increased average cleanout bucket capture (0.95 pounds per trial to 6.30 pounds per trial). These metrics indicated potential concrete dowel drill ventilation system efficiency and capture performance increases that address the ventilation system limitations indicated by previous research.

CHAPTER I

Introduction

1.1 Introduction

Local Exhaust Ventilation (LEV) is a commonly used engineering control to capture airborne contaminants, normally hazardous substances, which are generated in the form of dust, fume, mist, or vapor. LEV is an essential tool for occupational safety and health professionals to reduce potential worker exposures. It can also be used to capture and recycle materials to decrease economic costs and increase production yields. LEV systems have been utilized in a wide variety of industries from healthcare and research laboratories to the construction and mining industries.

Occupational safety and health impacts include the increased ability to capture and control contaminants in a more efficient manner and increased system performance metrics. These impacts provide better exposure control methods than previously available. The ability to better capture contaminants leads to increase protection of worker's health by reducing occupational exposures.

1.2 Background

From an occupational health and safety perspective, LEV systems are used for processes that require more ventilation near the worker or the process point of generation than general dilution ventilation can provide in order to reduce contaminant concentrations to maintain a safe working environment. LEV is traditionally positioned near the point of generation to minimize the amount of air that is required to be controlled but this is not feasible in every situation. This positioning also decreases the influences of deleterious system factors such as cross-drafts, uneven air distribution, and disturbances due to equipment/workers (Flynn 1995). In turn, these factors lessen the economic impact of initial installation costs (increased fan costs, increased materials, etc.) and operating costs (heating/cooling, greater electricity consumption of larger fans, etc.).

1.3 Ventilation System Components

LEV systems are categorized as either fixed or portable systems. Fixed LEV systems are permanent installations normally located at work stations for dedicated work processes or tasks, i.e. paint booths, welding lines, biosafety cabinets. Portable LEV systems are designed to allow for easy relocation for processes that are mobile in nature or require temporary engineering controls. Because of their portability and versatility, these LEV systems would be ideal for industries with temporary work sites or intermittent, potentially hazardous work such as the construction industry. However, despite widespread availability and proven track record of reducing potential worker

exposures, they are infrequently used in the construction industry (Flynn and Susi 2012; Meeker, Susi, and Flynn 2007; Shepherd et al. 2009).

While LEV system designs can vary greatly, they are generally comprised of four components: 1) Hood, 2) Duct, 3) Fan, and 4) Filter. Figure 1.1 illustrates a basic example of a LEV system. These basic four components can be modified in numerous ways to customize the LEV system to ensure the system sufficiently controls the airborne contaminants of concern.

Often, the main duct is branched in order to provide ventilation to a number of different areas while utilizing only one fan and filtration mechanism. The branches are smaller in diameter than the main duct. If the volumetric flow rate (Q) is constant, then velocity (V) will increase when the area (A) of the duct decreases (equation 1). This direct relationship between flow rate, velocity, and cross-sectional area of the duct, is such that a duct with a smaller cross-sectional area will have a higher air velocity for a given flow rate compared to a larger duct.

$$Q = VxA \qquad \text{Equation 1}$$

Q = Volumetric Flow Rate (cubic feet per minute or CFM)
V = Velocity (feet per minute or fpm)
A = Area (square feet or ft^2)

1.5 Ventilation System Performance Measures

Industrial ventilation utilizes three pressures when evaluating a system: total; static; and velocity. Each pressure metric can be measured in a number of ways and by using various instruments and techniques (ACGIH 2016; ACGIH Committee on

Industrial Ventilation. 1991; Burgess, Ellenbecker, and Treitman 2004; Goodfellow and Tähti 2001; Popendorf 2006; United States. Occupational Safety and Health Administration. 1999). In the United States, pressure measurements are typically recorded in non-International System of Units (SI) units such as inches of water column (“wc) or inches of water gauge (“w.g.). A number of other pressure metrics are used in reporting pressure measurements including inches of mercury, pascals, millibars, atmospheres, and others. For the purposes of this dissertation, pressure measurements will be reported in “w.g.

1.4 Ventilation and Local Exhaust Ventilation Fundamentals

Air is a state of matter that assumes the volume and shape of its container and is the most compressible state of matter. Molecules within air move randomly and cause pressure on its surroundings. In theory, it is often assumed that contaminants mix evenly and completely within air, even though this may not be the case in practice. Air movement is due to the difference in pressure with air flowing from areas of higher pressure to areas of lower pressure.

In industrial ventilation, air movement is created by a fan creating pressure differential within a workplace atmosphere. Ventilation systems carry moisture, dust or particulates, vapors, and heating and cooling air and often carried them all under pressure.

The American Conference of Governmental Industrial Hygienists (ACGIH®) states that the first step in the life cycle of any industrial ventilation system is an exposure assessment to define and determine the issues to be addressed (ACGIH 2016). LEV is often used for specific tasks that have been identified through qualitative

or quantitative exposure characterization as having a high potential of exposing workers to unacceptable contaminant concentrations.

ACGIH® has a storied history of publishing premiere ventilation manuals and information for ventilation design and use. Many of the ACGIH® equations and recommendations are taken from the early work of ventilation pioneers such as Dallavalle, Hatch, and Silverman (Dallavalle 1932; DallaValle 1952; Silverman 1942; Wabeke 1998). This early work focused on testing various hood designs and velocity contour mapping to indicate at what distances certain velocities where obtained (Dallavalle 1932; Silverman 1942; DallaValle 1944, 1952). The research led to the determination that the centerline velocity was the most impactful and influential of the parameters tested (Dallavalle 1932; DallaValle 1952; Silverman 1942). Based upon this research, the measurement of centerline capture velocities was selected as the best indicator of capture velocity performance (Garrison 1981).

Equations derived to determine centerline velocities are pulled directly from these early pioneers and are still used today, despite being nearly 80 years old (ACGIH 2016; Goodfellow and Tähti 2001; Wabeke 1998; Burgess, Ellenbecker, and Treitman 2004). It is also important to note that these equations were determined in ideal conditions under laboratory settings and therefore are, at best, estimates as to how LEVs will perform in the field when considering system performance variables such as cross-drafts, particle characteristics (size, speed, momentum, etc.), and other factors (Flynn 1995).

1.5.1 Total Pressure

The total pressure (TP) at any location in an industrial ventilation duct is the summation of all the air pressures exerted at that point in the system. The TP is equal to the static pressure (SP) plus the velocity pressure (VP). The TP at any point in the ventilation system can be either positive or negative depending on the purpose of the system and the location of the measurements. TP varies throughout the industrial ventilation system and across the duct. Despite the name, TP only has limited use when evaluating an industrial ventilation system.

1.5.2 Static Pressure

Static pressure is the potential pressure induced within a duct by a fan that either pulls the duct walls towards the duct center (negative static pressure) or pushes the duct walls away from the duct center (positive static pressure). Positive or negative SP is determined by the relationship between the fan and the point of measurement. Figure 1.2 illustrates this relationship between the fan and SP. For a fully-developed flow, SP is quantitatively the same across the duct cross-section. It is not modified by wall losses as we will see occurs with velocity pressure later.

1.5.3 Velocity Pressure

Velocity pressure (VP) is a measurement of the kinetic energy of air moving within the duct. VP is unidirectional and is the only pressure measurement that is only positive. This is reflective of the kinetic energy component in that air is only moving in one general direction through the duct.

VP cannot be directly measured using a pitot tube but is determined by subtracting the SP from the TP measured at a specific point within the duct. Because VP is affected by wall losses, turbulence, vena contracta, and other system factors, VP varies across a cross-section of a duct. The variance of VP across a duct cross-section necessitates averaging multiple measurements taken throughout the duct cross-section. This process is known as a pitot traverse and is discussed in detail later in this chapter.

1.5.4 Velocity

Velocity (V) is the quantitative measurement of air speed per unit of time within a duct or at specific points with the industrial ventilation system. In industrial ventilation, velocity is typically reported in feet per minute (fpm) in the United States. The formulaic relationship between velocity and VP is given by equation 2 where “df” is equal to the density factor. Density factors are discussed later in this chapter.

$$V = 4005\sqrt{\frac{VP}{df}} \qquad \text{Equation 2}$$

Velocities can also be measured directly using a thermal anemometer. However, velocities within a duct are rarely measured using a thermal anemometer because they have diminished sensitivity in high velocities, can be damaged by materials being transported within the duct, and are more susceptible to false reading due to turbulence within the duct. Thermal anemometers also do not measure velocities close to the duct wall with precision due to their susceptibility to air turbulences. However, thermal anemometers are a preferred method to measure velocities outside the duct such as

capture, face, and inlet velocities. The preferred method for determining duct velocity is to conduct a multi-point pitot traverse of VP measurements, converting each VP measurement into a corresponding V using equation 2, then calculating an arithmetically averaged determination.

1.5.5 Pitot Tube and Pitot Traverse

A pitot tube is an air pressure measurement device used in the recording of total, static pressure and velocity pressures. It is a long, cylindrical, L-shaped probe with two tubes, one within the other. The outer tube contains small, punched holes on the outside tube (perpendicular to the airflow) that measure static pressure while a hole in the tip (parallel to the airflow) allows the smaller, inner tube to measure total pressure. The two tubes are connected to a differential pressure instrument, such as a manometer or a Magnehelic® gauge, via two, equidistant tubes. Manufacturer instructions often require that each tube is made of the same material and are equidistant so that the losses across the connection tubing is the same. This ensures no artificial fluctuations in measured pressures from tubing friction loss. Depending on the configuration, a pitot tube can directly measure total and static pressure. Velocity pressure can be indirectly determined by subtracting the static pressure from the total pressure. Most manometers allow this determination to be made automatically.

Pitot traverses are used to test and balance systems, determine transport velocities, identify obstructions, compare current system performance to commissioning specifications, and to determine the emission stack velocity pressure which can be converted to velocity. A pitot traverse is an important tool in evaluating duct velocities

because it accounts for the uneven air distributions within a duct. As the air moves through the duct, it is subject to wall losses. Wall losses are due to the friction between the moving air and the duct walls. The friction slows the air velocity near the walls. Therefore, velocities within the duct are generally lower as you approach the wall and greater as you approach the center of the duct. This uneven air distribution necessitates taking velocity pressure measurements at multiple positions (representing equal areas) within the duct. Guidelines for determining pitot traverse measurements can be found in Appendix C of the ACGIH® Industrial Ventilation Manual (ACGIH 2016).

Each VP measurement of a pitot traverse allows calculation of the velocity at that point within the duct. The arithmetic average of all the individual calculated velocities is the calculated duct velocity at that point in the duct. Equation 3 illustrates the duct velocity calculation.

$$V\text{duct} = \frac{Vpitot1 + Vpitot2 \ldots + Vpitotn}{n} \qquad \text{Equation 3}$$

where:

Vpitot = the V calculated from the VP measurement at that point in the traverse

n = the number of VP measurement locations in the pitot traverse

Pitot traverses are routinely conducted using two orthogonal vertices, one vertical and one horizontal. Table 1.1 illustrates an example of an orthogonal pitot traverse and subsequent velocity and flowrate calculations.

1.5.6 Capture Velocity

Capture velocity refers to the velocity needed to capture contaminants outside of the hood and pull them into the LEV system. Capture velocity does not refer to only the centerline velocity in front of the hood, but rather refers to the entire area surrounding the hood. ACGIH® defines capture velocity as the “air velocity at any point in front of the hood or at the hood opening necessary to overcome opposing air currents and to capture the contaminated air at that point by causing it to flow into the hood” (ACGIH 2016). Each numbered line shows equal velocities and how the airstream contours around the hood. While the capture velocity metric refers to the entire capture field, most LEVs are designed and positioned to take advantage of greater centerline velocities.

The required capture velocity can also change depending upon the generated contaminant. For example, the capture velocity for a vapor is much lower than the capture velocity for a particulate. Thus for identical LEV systems, the vapor point of generation can occur further from the LEV’s hood than that required for particulate capture because the capture velocity needed to capture a vapor can be as low as 100 fpm vs capture velocity requirements exceeding 2,000 fpm for some particulate contaminant scenarios (ACGIH 2016).

The release energy or energy of dispersion can also greatly influence the capture velocity required. ACGIH® recommends a range of capture velocities that increase in direct proportion to the energy of dispersion (ACGIH 2016). For low energy of dispersion i.e. vapor naturally off-gassing from a degreasing tank, the capture velocity recommended would only be 100 fpm. However, a high energy of dispersion, i.e.

particulate from high velocity grinding, would have a recommended capture velocity of 500 to 2,000 fpm.

The contaminant's toxicity also plays an important role in the capture velocity's determination. Contaminants with low toxicity should follow the normal guidelines for effectively capturing the contaminant. However, contaminants with high toxicity (adverse health effects at low concentrations) should have safety factors (increased capture velocity, ventilation hood closer to point of generation, enclosures, etc.) built-in to the ventilation design to ensure effective capture. Extra precautions should also be taken to factor in the effects of cross drafts and surrounding traffic to evaluate potential impacts on the ventilation system's ability to effectively capture the contaminant. The toxicity considerations should be based on occupational exposure limits, carcinogenicity, target organs, biological uptake, and the known epidemiological study's strengths and limitations (Goodfellow and Tähti 2001). In the case of highly toxic contaminants, an enclosing hood should be considered to limit the contaminant's ability to escape into the workplace environment.

1.5.7 Capture Efficiency

A ventilation or LEV system's capture efficiency is the percentage of generated contaminant captured by the system. For example, if a process generates an airborne concentration of 100 milligrams per cubic meter (mg/m3) without any ventilation. After a LEV system is installed, the airborne concentration is measured at 10 mg/m3. The LEV system capture efficiency would be 90%.

Advances in technology, such as tracer gas methods, have allowed for better capture efficiency calculations. A tracer gas method is the release of a known gas (not used at the facility) at a known location and concentration. Real-time instrumentation placed throughout the study area, along with study area dimensions, can determine the concentration that is released into the study area instead of being captured by the ventilation system.

1.5.8 Transport Velocity

Transport velocity, also known as conveying velocity, is the minimum duct velocity required in order to keep material in the duct airstream and not settle out within the duct**.** A number of factors impact the transport velocity needed with each system. Ventilation designers should work closing with facility operations to identify the type of process and materials released for duct transport. Vapors and gasses require a much lower transport velocity (generally 1,000 to 2,000 fpm) while heavy or moist dusts require at least 4,500 fpm (ACGIH 2016). The ACGIH Industrial Ventilation Manual

reviews common contaminants and their respective transport velocities and Table 1.1 is adapted from Table 5-1 in the manual (ACGIH 2016).

Particle size and moisture content can greatly vary the needed transport velocity. A very fine dust, such as cotton, would require a much higher transport velocity if the dust contained a high moisture content than it would if it were dry. The additional moisture would add weight to the particles, increase their likelihood to agglomerate and to stick to duct walls if contacted.

The same can be said for rock dust which was evaluated in the last two specific aims of this dissertation. Fine rock dust from grinding requires a lower transport velocity (4,000 to 4,500 fpm) than rock dust from chipping operations which create larger, and more dense particles or chips (4,500 fpm or greater).

This research study aimed to evaluate novel ventilation systems that covered a wide range of transport velocities from vapors/gas to heavy or moist dusts. This ensured that system parameters noted would reflect conditions typically observed in the workplace.

1.6 System Loss

System loss is the total ventilation system loss due to entry loss, duct friction loss, dynamic loss, fan performance, air cleaning media or device, and exhaust system. For the purposes of this research and within each specific aim, we are assuming that fan performance and air cleaning media/device are the performing the same for all LEV systems and novel systems evaluated.

1.6.1 Coefficient of Entry

The coefficient of entry (Ce) is a measure of a hood's efficiency in converting static pressure to velocity pressure. The metric is a relationship between the theoretical flow compared to the actual flow measurement. Ce has also been called the Hood Flow Coefficient (ACGIH 2016). A hood with a 100% actual flow compared to theoretical would have a Ce of 1.00, the most efficient hood possible. Ce determinations approaching zero indicate less and less efficient hood designs. Equation 4 illustrates how Ce is calculated**.**

$$\boldsymbol{Ce} = \sqrt{\left(\frac{\boldsymbol{VP}}{\boldsymbol{SPh}}\right)} \qquad \text{Equation 4}$$

1.6.2 Friction Losses

Friction loss, also known as wall loss, occurs when the ventilated air comes in contact with the inner duct walls. The subsequent friction between the ventilated air and the wall causes the air to slow close to the wall, while the air in the center of the duct continues unimpeded. This uneven air distribution within a duct is why calculating duct velocities requires taking multiple VP measurements on a duct cross-section. This process is called a pitot traverse and is discussed in more detail earlier n this chapter.

The magnitude of friction loss is influenced by velocity, duct diameter, air density, air viscosity, and duct surface roughness (also known as absolute surface roughness). With velocity, duct diameter, air density, and air viscosity being often pre-determined,

the selection of a duct and the surface roughness can be a design feature to lessen the impact of potential friction losses.

The D'Arcy-Weisbach equation is a friction coefficient equation (Equation 5) that estimates the friction loss for a specified duct diameter and length with a design VP and friction coefficient. Equation 5 can be used to estimate friction loss, in "w.g., prior to construction (Ai and Mak 2013).

$h_f = f\,(L/d)VP$ Equation 5

h_f = friction losses in a duct, "w.g.

f= friction coefficient (dimensionless)

L = duct length, ft

d = duct diameter, ft

VP = velocity pressure, "w.g.

Once the D'Arcy-Weisbach friction coefficient is calculated and a relative roughness is determined, a Moody chart can be used to determine the Reynolds number, a measure of flow turbulence by the relationship between inertial and viscous forces (De Pauw et al. 2014).

Other references have tables with estimated duct losses by the length and construction of the duct. (ACGIH table 9-4 on page 9-42 with losses by length for sheet metal and plastic duct). Table 1.3 gives the surface roughness for common ventilation ductwork.

1.6.5 Dynamic Loss

Dynamic loss, also known as turbulent loss, is caused when the air movement changes due to physical changes in the ventilation system, i.e. elbows, openings, bends. While dynamic losses occur in every ventilation system, their impact can be diminished with proper design.

1.6.7 Crossdraft

A crossdraft is air movement due to an external factor in any direction other than the intended air movement of a designed ventilation system (Conroy 2000). Most common types of crossdrafts include the use of personal fans at a work station, air movement from machinery or equipment such as forklifts, conveyor belts or even other surrounding ventilation systems (Dunn et al. 2014; Hirst et al. 2014; Lo et al. 2015). Cross drafts can create situations in which the contaminant is never brought into the LEV hood or is captured but air turbulences created by the crossdraft pull the contaminant back out of the LEV hood (Flynn 1995; Altemose, Flynn, and Sprankle 1998; Flynn and Miller 1991; Kim and Flynn 1991).

If the crossdraft is constant, capture hood and capture velocity design can account for the crossdraft influences. Assuming that we want to have a certain capture velocity (Vc) at a certain distance (x), then we can calculate a total velocity, Vx, for a given crossdraft velocity (Vd) using equation 5 (Burgess, Ellenbecker, and Treitman 2004) .

$$Vx = Vc(x) + Vd(x) \qquad \text{Equation 6}$$

If crossdrafts are inconsistent, then the ACGIH guidelines (Table 5.1) provide a range of capture velocities for different dispersions of contaminant (ACGIH 2016). Designers are encouraged to use the upper end of the capture velocity range when crossdrafts are inconsistent.

1.6.8 Improper Positioning

LEV system have either fixed or flexible hoods. Fixed hoods are permanently installed and cannot be easily adjusted by the operator. Fixed hoods are most often installed in areas with consistent workflow and product type. Improper positioning issues are thought to be reduced by fixed LEV systems. However, improper training and use can still lead to improper positioning due to the point of contaminant generation being too far away from the LEV hood. Examples of a fixed LEV system include a biosafety cabinet, paint spray booth, and robotic welding lines.

Flexible hood LEV systems allow for the operator to move the LEV hood depending upon the task needs. Flexible hood LEV systems are often installed for areas in which the station is used for multiple tasks or products that vary in production rate and size. Flexible hood LEV systems are thought to be more susceptible to improper positioning issues due to variance in work practices and placement of the hood. If used properly, flexible LEV systems may offer a better capture efficiency than a fixed system because it can be moved closer to the contaminant point of generation and positioned

to take advantage of any contaminant inertia (e.g. above a hot process or behind a saw blade's discharge point) in order to facilitate capture.

1.6.9 Density Factor

In the past, most industrial ventilation research and design assumed that the air within a facility or ventilation system was considered to be standard air. Standard air is defined 100% dry air at 70°Farheinheit (°F) at sea level. The density of standard air is 0.075 pounds per cubic foot (lbs/ft^3). However, most industrial ventilation systems do not operate at these standard conditions. Therefore, the air density would be different and could potentially impact the ventilation system performance.

Density factor (df) is the "ratio of the actual air density to density of standard air" (ACGIH 2016). Multiplying standard air density by the density factor produces the actual air density. The actual air density or df should be accounted for when designing or evaluating the ventilation system instead of assuming standard air density. The density factor is a product of four environmental components: (1) Elevation; (2) Pressure; (3) Temperature; and (4) Moisture. Equation 6 illustrates the overall density factor calculation.

$$df = (df_e)\ (df_p)\ (df_T)\ (df_m) \qquad \text{Equation 7}$$

where df = overall density factor

df_e = Elevation density factor

df_p = Pressure density factor

df_T = Temperature density factor

df_m = Moisture density factor

Each of these density factor components must be measured and calculated in order to determine the actual air density. Appendix C in the ACGIH Industrial Ventilation Manual fully describes the calculation and application of density factors (ACGIH 2016). A previous rule of thumb longstanding in the ventilation design community is that as long as environmental parameters are less than 5% of the standard conditions, the density factors are not needed (Burgess, Ellenbecker, and Treitman 2004). However, others suggest that density factors should be used in all calculations regardless of variation from standard conditions (ACGIH 2016; United States. Occupational Safety and Health Administration. 1999; Goodfellow and Tähti 2001).

1.6.10 Mixing factors

Industrial ventilation does not assume that air is thoroughly mixed and concentrations within an environment are evenly distributed. In fact, certain scenarios, such as exposure control and LEV systems, rely on air being disproportionately mixed. Mixing factors (Km) are an approach to account for disproportionately mixed air. Mixing factors are an indication as to how well air is mixed and approaching uniformity.

1.7 Specific Aims

The following dissertation research investigated the effectiveness of novel ventilation designs at increasing capture velocities, measured novel design hood characteristics, and evaluated a concrete dowel drill local exhaust ventilation (LEV) and

system attachments for controlling respirable silica exposures during simulated workplace conditions. Specific Aim 1 data was obtained from experimental designs conducted at the University of Michigan School of Public Health (UM-SPH) wind tunnel. Specific Aim 2 research was conducted in the National Institute for Occupational Safety and Health (NIOSH) Engineering and Physical Hazards Branch (EPHB) ventilation laboratory. Specific Aim 3 used simulated workplace condition field data was collected at an outdoor NIOSH site specifically designed to conduct concrete dowel drill research.

The main objective of the dissertation research was to investigate the effectiveness of varying novel ventilation designs and their potential application in occupational settings to reduce workplace exposures to hazardous contaminants. The specific aims, hypotheses, and null hypotheses for this dissertation research were:

Specific Aim 1 (Chapter II)

- Determine the effectiveness of a novel ventilation design by comparing traditional fixed ventilation configurations to the same configurations after the integration of the novel design modification.
    - Hypothesis 1
        - The novel ventilation design will increase capture velocities as compared to the standard ventilation design without increasing overall energy requirements for the system.
    - Null Hypothesis 1
        - There is no difference between the novel ventilation design capture velocities and the traditional design capture velocities

Specific Aim 2 (Chapter III)

- Laboratory evaluation of manufacturer, commercially available, and novel design hoods for concrete dowel drill local exhaust ventilation system
    - Hypothesis 2
        - The NIOSH prototype hood will reduce face and inlet velocities when compared to the manufacturer's hood design
    - Null Hypotheses 2 and 3
        - The NIOSH prototype and manufacturer's hood have the same face velocities
        - The NIOSH prototype and manufacturer's hood have the same inlet velocities

Specific Aim 3 (Chapter IV)

- To optimize LEV hood and system configurations and perform field evaluations to investigate the effectiveness of novel designs during simulated workplace conditions
    - Hypothesis 3
        - The NIOSH prototype hood and system modifications will increase dowel drill efficiency while maintaining or exceeding previous system performance
    - Null Hypotheses 4, 5, and 6
        - The NIOSH prototype hood did not decrease face velocity compared to the manufacturer's hood
        - The pre-separator did not change filter loading and rear clean-out bucket weight
        - The smooth-bore hose gained the same amount of rock debris as the manufacturer's hose

Each Specific Aim is addressed in the following three chapters. Chapter V discusses the overarching conclusions derived from this dissertation research.

References

ACGIH 2016. Industrial ventilation: a manual of recommended practice. American Conference of Governmental and Industrial Hygenists: Cincinnati, OH.

ACGIH Committee on Industrial Ventilation 1991. Guide for testing ventilation systems. American Conference of Governmental Industrial Hygienists: Cincinnati, OH.

Ai, Z. T., and C. M. Mak. 2013. Pressure losses across multiple fittings in ventilation ducts, ScientificWorldJournal, 2013: 195763.

Altemose, B. A., M. R. Flynn, and J. Sprankle. 1998. Application of a tracer gas challenge with a human subject to investigate factors affecting the performance of laboratory fume hoods, Am Ind Hyg Assoc J, 59: 321-7.

Burgess, William A., Michael J. Ellenbecker, and Robert D. Treitman. 2004. Ventilation for control of the work environment. Wiley-Interscience: Hoboken, N.J.

DallaValle, J. M. 1944. Exhaust hoods. How to design for efficient removal of dust, fumes, vapors and gases. Heating and ventilating: New York.

DallaValle, J. M. 1952. Exhaust hoods. Industrial Press: New York.

Dallavalle, JMH. 1932. Studies in the Design of Local Exhaust Hoods, Trans ASME, 54: 370-75.

De Pauw, R., K. Choikhet, G. Desmet, and K. Broeckhoven. 2014. Occurrence of turbulent flow conditions in supercritical fluid chromatography, J Chromatogr A, 1361: 277-85.

Dunn, K. H., C. S. Tsai, S. R. Woskie, J. S. Bennett, A. Garcia, and M. J. Ellenbecker. 2014. Evaluation of leakage from fume hoods using tracer gas, tracer nanoparticles and nanopowder handling test methodologies, J Occup Environ Hyg, 11: D164-73.

Flynn, M. R. 1995. A review of wake effects on worker exposure, Annals of Occupational Hygiene, 39: 211-21.

Flynn, M. R., and C. T. Miller. 1991. Discrete vortex methods for the simulation of boundary layer separation effects on worker exposure, Ann Occup Hyg, 35: 35-50.

Flynn, M. R., and P. Susi. 2012. Local exhaust ventilation for the control of welding fumes in the construction industry--a literature review, Ann Occup Hyg, 56: 764-76.

Garrison, R. P. 1981. Centerline Velocity-Gradients for Plain and Flanged Local Exhaust Inlets, American Industrial Hygiene Association Journal, 42: 739-46.

Goodfellow, Howard D., and Esko Tähti. 2001. Industrial ventilation design guidebook. San Diego, California.

Hirst, D. V., K. H. Dunn, S. A. Shulman, D. R. Hammond, and N. Sestito. 2014. Evaluation of engineering controls for the mixing of flavorings containing diacetyl and other volatile ingredients, J Occup Environ Hyg, 11: 680-7.

Kim, T., and M. R. Flynn. 1991. Airflow pattern around a worker in a uniform freestream, Am Ind Hyg Assoc J, 52: 287-96.

Lo, L. M., C. S. Tsai, K. H. Dunn, D. Hammond, D. Marlow, J. Topmiller, and M. Ellenbecker. 2015. Performance of Particulate Containment at Nanotechnology Workplaces, J Nanopart Res, 17.

Meeker, J. D., P. Susi, and M. R. Flynn. 2007. Manganese and welding fume exposure and control in construction, J Occup Environ Hyg, 4: 943-51.

Popendorf, William. 2006. Industrial hygiene control of airborne chemical hazards. CRC/Taylor & Francis: Boca Raton, FL.

Shepherd, S., S. R. Woskie, C. Holcroft, and M. Ellenbecker. 2009. Reducing silica and dust exposures in construction during use of powered concrete-cutting hand tools: efficacy of local exhaust ventilation on hammer drills, J Occup Environ Hyg, 6: 42-51.

Silverman, L. 1942. Velocity Characteristics of Narrow Exhaust Slots, J Ind Hyg Tox, 20: 267-76.

Occupational Safety and Health Administration. 1999. OSHA technical manual. Washington, D.C.: Occupational Safety & Health Administration. https://www.osha.gov/dts/osta/otm/otm_toc.html

Wabeke, Roger L. 1998. Air contaminants and industrial hygiene ventilation : a handbook of practical calculations, problems, and solutions. Lewis Publishers: Boca Raton.

Chapter II

Evaluation of a Novel Ventilation Design for Increasing Capture Velocities in Traditional and Local Exhaust Ventilation

Abstract

Local exhaust ventilation is a commonly used engineering control that capture airborne contaminants, normally hazardous substances, which are generated in the form of dust, fume, mist, vapor, etc. Local exhaust ventilation is an essential tool for occupational safety and health professionals to reduce potential worker exposures. It can also be used to capture and recycle materials to decrease economic costs and increase production yields. Local exhaust ventilations systems have been utilized in a wide variety of industries from healthcare and research laboratories to the construction and mining industries.

The research investigated the effectiveness of novel ventilation designs at increasing capture velocities in a laboratory setting. Four novel ventilation designs were tested along with a traditional ventilation design. Each design (novel and traditional) was evaluated using four wind tunnel fan settings; two fan settings to recommended transport velocity guidelines for vapors/fumes and two fan settings to recommended transport velocity guidelines for dust and heavier materials. For each design and fan setting, capture velocity measurements were collected at nine distance locations from

the hood face to 24” in three inch increments.

The novel design capture velocities observed in this study both outperformed and underperformed when compared to the traditional ventilation design. However, the novel design only outperformed the traditional design when no flange was used on the hood. The lack of consistent performance across all testing scenarios did not allow for the construction of a mathematical model to predict capture velocities based upon ventilation parameters such as duct size, fan power, inner duct location, etc. While the novel design did not consistently outperform the traditional ventilation design, the need to further develop and test the novel design is needed based upon the potential shown in certain test scenarios where the novel design appeared to outperform the unflanged version of the traditional ventilation design.

2.1 Specific Aim One

Specific Aim One research investigated the effectiveness of novel ventilation designs at increasing capture velocities in a laboratory setting. Four novel ventilation designs were tested along with a traditional ventilation design. Each design (novel and traditional) was evaluated using four wind tunnel fan settings; two fan settings corresponding to recommended transport velocity guidelines for vapors/fumes and two fan settings corresponding to recommended transport velocity guidelines for dust and heavier materials. For each design and fan setting, capture velocity measurements were collected at nine centerline distance locations from the hood face up to 24” (in 3”

increments) in front of the hood. Experimental laboratory data was obtained utilizing the University of Michigan School of Public Health wind tunnel.

The main objective of the research was to investigate the effectiveness of the novel ventilation designs and their potential application in occupational settings in order to reduce potential workplace exposures to hazardous contaminants. Specific Aim One was defined as:

> Determine the effectiveness of each novel ventilation design by comparing various fixed ventilation configurations to the same configurations after the integration of the novel design

Hypothesis 1 was defined as:

> Each novel ventilation design will increase capture velocities as compared to the standard ventilation design without increasing overall energy requirements for the system.

Null Hypothesis 1 (Ho1) was defined as:

> There is no difference between each novel ventilation design capture velocity and the traditional design capture velocities

2.2 Introduction

From an occupational health and safety perspective, LEV systems are used for processes that require more ventilation near the worker or the process than general dilution ventilation can provide in order to reduce contaminant concentrations to maintain a safe working environment. LEV is positioned near the point of generation to minimize the area that is required to be controlled. This positioning decreases the influences of deleterious system factors (cross-drafts, uneven air distribution due to

equipment/workers, etc.) and also decreases the amount of air volume that needs to be removed. This lessens the economic impact of initial installation costs (increased fan costs, increased materials, etc.) and operating costs (heating/cooling, greater electricity consumption of larger fans, etc.).

A thorough search of the literature and various ventilation design manuals did not uncover a similar design or equations that would successfully predict the centerline velocity of the novel design (ACGIH 2016; Beamer, Topmiller, and Crouch 2004; Braconnier 1988; Burgess, Ellenbecker, and Treitman 2004; Dallavalle 1932; DallaValle 1944, 1952; Dunn et al. 2004; Flynn and Susi 2012; Garrison 1983; Ghorbani Shahna, Bahrami, and Farasati 2012; Goodfellow and Tähti 2001; Heinonen, Kulmala, and Saamanen 1996; Heinsohn 1991; Kulmala 1997; Martinez, Tubbs, and Ow 2001; Meeker, Susi, and Flynn 2007, 2010; Methner 2008, 2010; Old et al. 2008; Popendorf 2006; Shepherd et al. 2009; Silverman 1942; Wabeke 1998). The primary issue is that these equations predict centerline velocities generated by an LEV system with an unobstructed duct with uniform airflow distribution. The novel design had a small area of higher velocity in the centerline plus the uneven airflow distribution due to the smaller duct and the area of higher velocity.

The ultimate goal of this research project is to reduce potential occupational exposure through increased capture velocities of LEV systems. With that goal in mind, we investigated methods of increasing capture velocities in LEV systems. Table 2.1 lists the basic variables and test conditions to compare the traditional LEV to the novel designs.

Duct velocities were chosen by reviewing the ACGIH® and British Occupational Hygiene Society's (BOHS) recommended duct velocities for contaminants (ACGIH 2016; BOH 1987). ACGIH® recommends 1,000-2,000 fpm for vapors, gases, and smokes and 2,000-2,500 fpm for fumes and metal smoke (American Conference of Governmental Industrial Hygienists. Committee on Industrial Ventilation. 2010). The BOHS recommendations are 6-10 meters per second (m/s), or 1181-1969 fpm, for vapors, gases, and smokes and 7-10 m/s (1378-1969 fpm) for fumes which convert to be slightly lower but similar to ACGIH® recommendations (BOH 1987). Test conditions of 1,500 fpm and 2,000 fpm were chosen to simulate conditions for both categories of vapors, gases, and smokes as well as fumes and metal smokes. ACGIH® recommends that average industrial dust (includes sawdust, grinding materials, and other heavier particles) have a design velocity of 3,500-4,000 fpm (American Conference of Governmental Industrial Hygienists. Committee on Industrial Ventilation. 2010). The BOHS recommends 17.5-20 m/s (3,936 fpm) for the same category of average industrial dust (BOH 1987). Test conditions of 3,000 fpm and 4,000 fpm were chosen to simulate heavier particle transportation and higher transport velocity. By using these four test duct velocities, we are able to evaluate how the novel designs function under two common, industrial scenarios.

2.3 Traditional and Novel Designs

This study evaluated the capture velocities of one traditional and four novel design LEV systems. The traditional LEV system (Figure 2.1) consisted of the wind tunnel attached to a 5-foot section of 12" round aluminum duct that was evaluated both

with and without a 1.5 inch flange. The flange was affixed to the duct by duct tape and evaluated for leakage using smoke tubes.

The OSHA technical manual states that a maximum design capture distance is determined as 1.5 times the diameter (1.5 x D) or 18” for a 12” duct. For the purposes of this experiment, a capture distance of 6-9” was chosen for design purposes. Equation 1 was used to determine an acceptable effective flange width (EFW) with a 12” duct diameter and a 6-9” capture point range.

$$W = X - \left(\frac{1}{2}\right) D \qquad \text{Equation 1}$$

With the given capture distance range, an EFW would range from 1-3”. A 1.5” flanged hood (capture point = 7.5”) was available and selected because it was within the acceptable capture point and EFW range as well as the maximum capture distance requirement. Figure 2.2 illustrates the EFW selection process.

Novel Design 1 (ND1) was chosen for this study after a small pilot study identified it as the most promising novel design (Figure 2.3). The design consisted of the traditional LEV system with a 2” Thermaflex® flexible HVAC duct (secondary duct) branched 2 feet from the face and re-entered into the main duct at one foot from the face. Thermaflex® ductwork is an inner steel spring wire coated with flexible fiberglass cloth fabric and rated to 6,000 fpm and a wide range of temperatures (minus 20°F to 250°F). The inner duct intake was covered with tape to provide as smooth as an entry as possible. The secondary duct was then positioned in the main duct’s center by monofilament nylon cords. Figure 2.4 illustrates ND 1 with the flange attached for comparison.

Novel Design 2 (ND2) was the same design as ND1 but the 2” secondary duct was replaced with a 4” secondary duct. The secondary duct was then positioned in the main duct’s center by monofilament nylon cords.

Novel Design 3 (ND3) consisted of the traditional LEV system with a solid 2” disc suspended in the main duct’s center by monofilament nylon cords (Figure 2.5). This design evaluated the potential of vena contracta-like effects on capture velocities. Comparison of ND 1 and ND 3 evaluated the impact of an active flow in the main duct’s center versus vena contracta influences that may account for capture velocity effects.

Novel Design 4 (ND4) consisted of the traditional LEV system with a solid 4” disc suspended in the main duct’s center by monofilament nylon cords (Figure 2.6). This design evaluated the potential of vena contracta-like effects on capture velocities. Comparison of ND 2 and ND 4 evaluated the impact of an active flow in the main duct’s center versus vena contracta influences that may account for capture velocity effects.

2.3 Methods

Capture velocities for a traditional LEV system were compared to evaluate potential increases in capture velocities through novel design. All LEV systems consisted of a 5-foot section of 12” circular, aluminum duct connected to a wind tunnel. The wind tunnel is an Engineering Laboratory Design (Lake City, MN) open circuit Eiffel-design with a centaxial fan powered by a 3 horsepower, 1,800 revolutions per minute (rpm), 3 phase, induction motor housed within fabricated structural steel housing. The wind tunnel is capable of producing variable test velocity conditions. The wind tunnel

specifications indicate the tunnel is capable of producing velocities ranging from 2 to 78 feet per second (fps) or 120 to 4,680 cubic feet per minute (CFM).

All LEV systems were evaluated with a circular, aluminum flange (Flanged) and without the flange (Unflanged). The 12” circular flange had a 3” flange width (1 ½” flange width on each side). The flange was affixed to the duct by duct tape and evaluated for leakage using smoke tubes.

The wind tunnel was allowed to run for 10 minutes before any measurements were recorded. Face velocity measurements were taken to determine wind tunnel settings that corresponded to the two velocity categories for V_{LO} and two velocity categories for V_{HI}. Table 2.2 displays the wind tunnel fan speeds and the corresponding velocities as well as the representative category.

Capture velocities were measured directly in front of the center of the duct inlet at 3” increments from the face to 24” (N=9). Table 2.3 displays the position, distance from the hood face, and the duct diameter percentage the measurement was obtained. Capture velocity, temperature, and relative humidity were recorded using a calibrated TSI® Airflow™ Multi-Function Anemometer (TSI, Shoreview, Minnesota). Temperature and relative humidity were recorded prior to each testing configuration and experiment. A tripod held the anemometer to minimize airflow disruptions or eddies which may be caused by the human body[29].

Prior to each measurement, the anemometer was aligned perpendicular with the main duct’s center and the distance from the anemometer and the hood face was verified. Three measurements were collected at each distance while allowing the wind tunnel to run for 3 minutes in between each measurement. The arithmetic mean of the 3

measurements was recorded as the capture velocity for that trial. Three trials were collected on non-consecutive days. The average capture velocity for each combination of parameters was determined by the arithmetic mean of the three trials.

A pitot traverse was performed using a calibrated TSI® Airflow™ Multi-Function Anemometer (TSI, Shoreview, Minnesota) according to ASHRAE guidelines for circular ducts (ASHRAE 2009). A total of 12 measurement points along two orthogonal diameters (six per diameter) were evaluated. Static pressure (SP), velocity pressure (VP), and total pressure (TP) and flow rates (Q) measurements were collected for all test conditions. Average velocities were calculated using the VP and Q was calculated using the duct area. The pitot traverse was performed at approximately four duct diameters from the hood face but only 2 duct diameters from the branch entry location. This was the furthest location possible for pitot traverse due to the limited size of the main duct and the connection to the wind tunnel.

$$TP = VP + SP \qquad \textit{Equation 2}$$

Hood entry loss coefficients (Ce) were also calculated for all designs and fan speeds. Static pressure hood (SP_h) and VP measurements were taken using a calibrated TSI® Airflow™ Multi-Function Anemometer (TSI, Shoreview, Minnesota). C_e was calculated using equation 3. The absolute value of SP_h was used in all C_e calculations.

All statistical analysis was performed using Microsoft Excel® Office 2015 edition. Two-tail and one-tail t-test evaluated significant difference between traditional and novel

designs. We also calculated 95% confidence intervals for each capture velocity average.

$$Ce = \sqrt{\frac{VP}{|SPh|}} \qquad \textit{Equation 3}$$

2.4 Results

Overall average capture velocities did not improve through novel design when compared to the traditional LEV system. Table 2.4 displays the average capture velocities for all LEV systems (flanged and unflanged) tested and when all distance measurements where used to calculate capture velocities. ND1 outperformed the other three novel designs but was still considerably less effective than the traditional design for both unflanged (-18%) and flanged (-15%). Novel designs 2-4 were less effective than traditional designs for both unflanged (28-44% lower) and flanged (30-42% lower). Recorded average environmental test conditions included were temperature of 73°F and a relative humidity of 48% for all trials. Tables A1-A8 are the t-test results comparing all test scenarios to the traditional capture velocities.

Review of the individual distance measurements revealed that all novel designs performed substantially lower at face velocities to 3” but ND 1 (unflanged) outperformed the traditional LEV system in 78% (7 out of 9) distance measurements for V_{LO1} and 56% (5 out of 9) distance measurements for V_{LO2}. The substantially lower face velocity heavily influenced the arithmetic mean for the overall performance indicating no overall performance gains. Table 2.5 displays the average capture velocities for the traditional LEV system and the ND 1 LEV system at each measurement distance. For V_{LO1}, ND 1

(unflanged) outperforms the traditional LEV for each distance except the initial face velocity and at 21” from the face. However, ND 1 (unflanged) was again higher than the traditional LEV system at 24” from the hood face. For V_{LO2}, ND 1 (unflanged) was less effective in increasing capture velocities but the distance range was similar to those observed for V_{LO1}. The ND 1(unflanged) had greater average capture velocities than the traditional LEV system for distances 6-18” from the hood face.

Evaluation of all flanged scenarios did not illustrate the same effect. The flanged, traditional design outperformed all of the flanged, novel designs across all scenarios.

Table 2.6 displays the results for ND 1 (unflanged) for the V_{HI} categories. While still outperforming the traditional LEV system at some distances, the ND1 (unflanged) had diminished performance with higher fan speeds. The ND 1 (unflanged) only outperformed the traditional LEV system in 44% (4 out of 9) distance measurements for V_{HI3}. For high fan speeds, The ND 1 (unflanged) design best results were from 9-18” from the hood face which is a similar effective range as seen in the V_{LO} trials.

Due to the substantial difference in capture velocities at the hood face, average capture velocities were calculated for both distances of 6-24” from the hood (Table 2.7) and 15-24” from the hood (Table 2.8) for both unflanged and flanged. When accounting for the lower face velocities (6-24”), the ND 1 (unflanged) average capture velocity was greater than the traditional LEV system for V_{LO1}, V_{LO2}, and V_{HI3}. The ND 4 (unflanged) design outperformed at the V_{LO1} and V_{HI3} fan speeds.

However, even with taking the lack of face velocity into account no flanged novel design outperformed their flanged traditional LEV system counterpart. This was true for all velocity scenarios observed and in all trials.

A pitot traverse was used to determine the volumetric flow rate (Q) of each design. With regards to Q for unflanged scenarios, ND1 outperformed the traditional design for 3 of the 4 fan speed scenarios with only V_{HI4} underperforming. ND3 and ND4 outperformed the traditional design for 2 out of 4 fan speeds, V_{LO1}/V_{LO2} and V_{LO1}/V_{HI3} respectively. ND2 did outperform the traditional design in any unflanged scenario. Table 2.9 reports the velocity pressure, total pressure, and overall Q for the unflanged testing conditions.

While capture velocities for flanged novel designs did not show an increase over traditional designs, the overall Q was increased for ND1 (all four fan speeds), and for 50% of fan speeds for ND3 and ND4. ND2 did not increase Q for any fan speed or testing scenarios. Table 2.10 illustrates the velocity pressure, total pressure, and overall calculated Q for the flanged testing conditions.

The Ce was calculated for the traditional and all novel designs across all test conditions. Table 2.11 illustrates the unflanged average hood entry loss across the four fan speeds tested. Trial hood entry loss greater than ±5% of average hood entry loss are denoted. Table 2.12 illustrates the flanged average hood entry loss across the four fan speeds tested. Trial hood entry loss greater than ±5% of average hood entry loss are denoted.

2.5 Discussion

While some novel designs outperformed the traditional design in some testing scenarios, the novel design was not consistent enough across all testing scenarios to determine a mathematical model or ventilation equation. In addition, all flanged novel

designs did not outperform the traditional design which complicated interpretation of data. Typically, flanged ventilation designs increase capture velocity when compared to open hood designs. However, the novel designs tested did show the potential for improvements on traditional novel designs, especially when no flange is used. Further research is needed to improve upon the novel design to reduce losses and increase face velocity.

The largest concern for this study was loss of face velocity for the novel design. The novel designs' lack of face velocity directly lead to the novel designs not performing as well as the traditional design when evaluated for overall capture velocity. Only when evaluating capture velocities at distances away from the hood face did the novel design begin to outperform the traditional design. The loss of novel design face velocity could be due to a number of reasons such as friction loss, branch location in relation to fan, and other factors.

All novel design capture velocity gains observed during the unflanged testing scenarios were nullified when a flange was added to the hood. The addition of a flange dramatically changes the airflow into the hood, inducing greaterair movement from the front of the hood instead of from areas adjacent to the hood perimeter.

The Thermaflex® duct has a higher friction loss factor than galvanized steel because the Thermaflex® inner steel spring design is not as smooth as the galvanized duct wall. The Thermaflex® inner steel spring, even though coated to lessen wall losses, is still subject to greater friction and wall losses due the increases surface area of the wall and the rise and fall of air as it traverses the spring supported wall. The spring supported wall can be analogous to repeated speed bumps on a street. The air will lose

velocity as it rises and falls over the spring much like a car would lose velocity while navigating speed bumps on a street.

The Thermaflex® duct is also more susceptible to sag and bend losses due to the flexible nature of the product. The advantage of the Thermaflex® duct, to be flexible enough to accomplish acute turns and allow ease of manipulation, led to it being chosen as the novel design ductwork. However, the flexibility advantage could have been potentially nullified by increased bend and sag losses due to a lack of rigidity. The flexible ductwork was installed in such a manner to minimize sagging and reduce abrupt bends as much as possible.

Potential issues of cross drafts, room ventilation interferences, and obstacles in front of the duct disrupting air flow patterns were all minimized. All sources of cross drafts were removed from the immediate vicinity of the experiment. Room ventilation interferences, such as opening and closing doors, were accounted for by beginning any interrupted trial again five minutes after the interference occurred. All obstacles in front of the duct were also removed to the extent possible.

In future research, a hood or flanged hood could be added to the inner duct to potentially increase the inner duct's face velocity. An eductor could also be placed at the opening of the inner duct to evaluate effectiveness of increasing the novel design's face velocity.

The pitot traverses were performed at four duct diameters downstream from the hood but only two duct diameters upstream from the secondary duct branch location. The pitot traverse should be conducted at 4 duct diameters upstream from any disruptions in air flow (e.g., obstructions, opening, bends, and branches) (ACGIH 2016).

The close proximity of the pitot traverse to the secondary branch location may not have allowed enough distance for the air stream to settle into a uniform air distribution pattern. However, the traverse was used to collect multiple point measurements along two axis and should be minimally affected by the less than preferred distance from an obstruction.

Determining the hood loss coefficients was also influenced by the lack of duct length available downstream from the hood. The OSHA Technical Manual suggests that the hood static pressure be observed at 4-6 duct diameters downstream of the hood opening in a straight section of ductwork which was not possible with this experiment design (United States. Occupational Safety and Health Administration. 1999). The static hood pressure was collected at approximately four duct diameters downstream but was less than 2 duct diameters from the secondary branch location which may have influenced the static hood pressures observed and thus influenced the hood loss coefficient calculations.

2.6 Conclusion

The novel design capture velocities observed in this study both outperformed and underperformed when compared to the traditional ventilation design depending on the testing scenario. The novel design only outperformed the traditional design when no flange was used on the hood. The lack of consistent performance across all testing scenarios did not allow for the construction of a mathematical model or equation to predict capture velocities based upon ventilation parameters such as duct size, fan power, inner duct location, etc. While the novel design did not consistently outperform the traditional ventilation design, the need to further develop and test the novel design is

needed based upon the potential shown in certain test scenarios were the novel design appeared to outperform the unflanged traditional ventilation design.

References

ACGIH. 2016. Industrial ventilation: a manual of recommended practice. American Conference of Governmental and Industrial Hygenists: Cincinnati, OH.

ACGIH. Committee on Industrial Ventilation. 2010. Industrial ventilation: a manual of recommended practice. American Conference of Governmental and Industrial Hygenists: Cincinnati, OH.

ASHRAE 2009. 2009 ASHRAE handbook fundamentals. Atlanta, GA.

Beamer, B. R., J. L. Topmiller, and K. G. Crouch. 2004. Development of evaluation procedures for local exhaust ventilation for United States postal service mail-processing equipment. J Occup Environ Hyg, 1: 423-9.

BOH. 1987. Controlling airborne contaminants in the workplace Science Reviews; H and H Scientific Consultants: UK Leeds, UK.

Braconnier, R. 1988. Bibliographic Review of Velocity-Fields in the Vicinity of Local Exhaust Hood Openings. American Industrial Hygiene Association Journal, 49: 185-98.

Burgess, William A., Michael J. Ellenbecker, and Robert D. Treitman. 2004. Ventilation for control of the work environment. Wiley-Interscience: Hoboken, N.J.

DallaValle, J.M. 1944. Exhaust hoods. How to design for efficient removal of dust, fumes, vapors and gases. Heating and ventilating: New York.

DallaValle, J.M. 1952. Exhaust hoods Industrial Press: New York.

Dallavalle, J.M. 1932. Studies in the Design of Local Exhaust Hoods. Trans ASME, 54: 370-75.

Dunn, K. H., S. A. Shulman, A. B. Cecala, and D. E. Venturin. 2004. Evaluation of a local exhaust ventilation system for controlling refractory ceramic fibers during disc sanding., J Occup Environ Hyg, 1: D107-11.

Flynn, M. R., and P. Susi. 2012. Local exhaust ventilation for the control of welding fumes in the construction industry--a literature review. Ann Occup Hyg, 56: 764-76.

Garrison, R. P. 1983. Velocity Calculation for Local Exhaust Inlets - Empirical Design Equations., American Industrial Hygiene Association Journal. 44: 937-40.

Ghorbani Shahna, F., A. Bahrami, and F. Farasati. 2012. Application of local exhaust ventilation system and integrated collectors for control of air pollutants in mining company. Ind Health, 50: 450-7.

Goodfellow, Howard D., and Esko Tähti. 2001. Industrial ventilation design guidebook. San Diego, California.

Heinonen, K., I. Kulmala, and A. Saamanen. 1996. Local ventilation for powder handling - Combination of local supply and exhaust air. American Industrial Hygiene Association Journal, 57: 356-64.

Heinsohn, Robert Jennings. 1991. Industrial ventilation: engineering principles. Wiley: New York.

Kulmala, Ilpo. 1997. Air Flow Field near a Welding Exhaust Hood, Applied occupational and environmental hygiene, 12: 101-04.

Martinez, K., R. L. Tubbs, and P. Ow. 2001. Use of local exhaust ventilation to control aerosol exposures resulting from the use of a reciprocating saw during autopsy. Appl Occup Environ Hyg, 16: 709-17.

Meeker, J. D., P. Susi, and M. R. Flynn. 2007. Manganese and welding fume exposure and control in construction. J Occup Environ Hyg, 4: 943-51.

Meeker, J. D., Susi, P., and M. R. Flynn. 2010. Hexavalent chromium exposure and control in welding tasks. J Occup Environ Hyg, 7: 607-15.

Methner, M. M. 2008. Engineering case reports. Effectiveness of local exhaust ventilation (LEV) in controlling engineered nanomaterial emissions during reactor cleanout operations. J Occup Environ Hyg, 5: D63-9.

Methner, M. 2010. Effectiveness of a custom-fitted flange and local exhaust ventilation (LEV) system in controlling the release of nanoscale metal oxide particulates during reactor cleanout operations. Int J Occup Environ Health, 16: 475-87.

Old, L., K. H. Dunn, A. Garcia, and A. Echt. 2008. Engineering case reports: evaluation of a local exhaust ventilation system for controlling exposures during liquid flavoring production. J Occup Environ Hyg, 5: D103-10.

Popendorf, William. 2006. Industrial hygiene control of airborne chemical hazards CRC/Taylor & Francis: Boca Raton, FL.

Shepherd, S., S. R. Woskie, C. Holcroft, and M. Ellenbecker. 2009. Reducing silica and dust exposures in construction during use of powered concrete-cutting hand tools: efficacy of local exhaust ventilation on hammer drills. J Occup Environ Hyg, 6: 42-51.

Silverman, L. 1942. Velocity Characteristics of Narrow Exhaust Slots. J Ind Hyg Tox, 20: 267-76.

United States. Occupational Safety and Health Administration. 1999. OSHA technical manual. In Ted 1-0 15a. Washington, D.C.: Occupational Safety & Health Administration,

Wabeke, Roger L. 1998. Air contaminants and industrial hygiene ventilation : a handbook of practical calculations, problems, and solutions. Lewis Publishers: Boca Raton.

CHAPTER III
Evaluation and Design Optimization of Concrete Dowel Drilling Local Exhaust Ventilation Hoods

Abstract

Dowel drilling of concrete can lead to respirable crystalline silica overexposures unless otherwise controlled. Previous research indicated that engineering controls, such as local exhaust ventilation, can effectively control exposures. However, the current local exhaust ventilation system is prone to clogging, dust cake on the filter, and other deleterious conditions that quickly reduce the control's efficacy.

The research investigated the design efficiency of four enclosed hoods and two simple hoods for potential application on a dowel drill local exhaust ventilation system to reduce previously identified system issues. The evaluated enclosed hoods included two hood designs (NIOSH V1 and NIOSH V2) that are novel designs that were designed specifically for the dowel drill, the manufacturer's hood, and a commercially available hood. The NIOSH hood and the manufacturer's hood were also evaluated as simple hoods. NIOSH V1 and V2 have the same simple hood design.

Each hood was evaluated in a laboratory setting to determine the hood coefficient of entry, hood static pressure, duct transport velocity, hood inlet velocity, and

hood face velocity. These hood parameters were evaluated at nine trial velocities ranging from 500 to 4,500 feet per minute in 500 feet per minute increments.

Both NIOSH hood designs (NIOSH V1 and NIOSH V2) had a more efficient coefficient of hood entry loss, increased transport velocities, and had lower hood static pressure measurements when compared to the manufacturer's hood design and the commercially available hood design. When comparing NIOSH V1 and V2 for potential use on the dowel drill local exhaust ventilation system, the NIOSH V2 design was chosen due to the preferable coefficient of hood entry loss, increased duct transport velocities, and lower hood static pressure.

3.1 Introduction

Crystalline silica often refers to a larger mineral group comprised of silicon and oxygen. The three major forms of crystalline silica are quartz (most common), cristobalite, and tridymite (United States. Branch of Industrial Minerals. 1992). Crystalline silica can be found in a number of commonly used construction materials such as concrete, brick, etc. Construction tasks often require tuck-pointing, drilling, abrasive blasting, road milling, concrete cutting, sawing, and other activities that free the crystalline silica allowing it to enter into the worker's respiratory zone. A number of studies have found potential overexposures to crystalline silica associated with these construction tasks (Glindmeyer and Hammad 1988, Thorpe, Ritchie et al. 1999, Nash and Williams 2000, Akbar-Khanzadeh and Brillhart 2002, Linch 2002, Woskie, Kalil et al. 2002, Rappaport, Goldberg et al. 2003, Akbar-Khanzadeh, Milz et al. 2010). Most recently, occupational exposure to crystalline silica has become of increasing concern in

the hydraulic fracturing industry (Chalupka 2012, Esswein, Breitenstein et al. 2013, Witter, Tenney et al. 2014, Walters, Jacobson et al. 2015, Alexander, Esswein et al. 2016)

Inhalation of crystalline silica can lead to silicosis, a fibrotic lung disease. Silicosis is an irreversible (even after the exposure has been removed) pulmonary lung disease with normal latency periods of 10-15 years exposure prior to onset and manifests as either simple chronic silicosis, accelerated silicosis, or acute silicosis (Sander 1968, Reiser 1985, Rice and Stayner 1995). Symptoms include persistent cough, shortness of breath, respiratory failure which may lead to a lung transplant or death (Health 2015).

Respirable crystalline silica (aerodynamically small enough to reach the gas-exchange region of the lungs) refers to particles less than 10 micrometers (µm) and is of particular interest when investigating exposure-disease relationships (Merchant 1987). The respirable crystalline silica NIOSH Recommended Exposure Limit is 0.05 mg/m^3 for up to a 10 hour time weighted average (TWA) for a 40 hour work week (NIOSH 2002). OSHA recently released an updated respirable crystalline silica standard that lowered the permissible exposure limit to 0.05 mg/m^3 as an 8 hour TWA (OSHA 2016).

In 2004, Valianta et al. identified highway repair as a new silicosis threat after reviewing data from the NIOSH Sentinel Event Notification System for Occupational Risks (SENSOR) and 1999 crystalline silica exposures during road construction activities (Valiante, Schill et al. 2004).The article only reported two silica samples collected during “Drilling dowels” activities but both were above the OSHA PEL (Valiante, Schill et al. 2004). During construction of large paved area, dowels are

inserted between concrete slabs to distribute loading amongst multiple slabs especially during use of heavy equipment (Park, Jang et al. 2008). The installed steel dowel aids in transferring shear from one concrete slab (heavily loaded) to the adjacent concrete slab (Bush and Mannava 2000). This increases the service life of the concrete slabs and the maximum load capacity (Bush and Mannava 2000).

3.2. Previous NIOSH Dowel Pin Drill Research

Silica exposures and other health hazards associated with dowel drills have been investigated by the Engineering and Physical Hazards Branch (EPHB) of NIOSH (Echt, Sieber et al. 2003, Echt 2008, Echt 2011, Echt 2011, Echt 2011, Echt 2011, Echt 2012, Echt 2012, Echt 2013). During controlled field testing, the manufacturer's dust control system was determined to reduce potential exposures to respirable dust reductions by 86-92%.

NIOSH followed the controlled field studies by conducting three site visits to evaluate field efficiency of manufacturer-installed LEV dust control systems and to evaluate respirable silica exposures during workplace conditions (Echt 2011, Echt 2011, Echt 2012). Under these real world conditions, the LEV reduced the respirable dust by 80% but the crystalline silica exposures were still 3 to 8 times higher than the NIOSH REL (Echt 2012). A NIOSH Workplace Solutions document outlines research, control information, and recommendations for reducing worker exposures during dowel drilling in concrete (NIOSH 2015).

NIOSH investigators noted that the LEV dust control system had issues with overloading which would dramatically reduce (1) the dust control system's collection efficiency and (2) the operating time between dust collection maintenance tasks. The current dowel drill dust collection design, while effective in reducing silica exposures, needs improvement to prolong operation time between dust collection maintenance tasks. The constant clogging of the dust collection system and subsequent emptying of the collection receptacle and removing clogs could potentially add to silica exposures. NIOSH research indicated that dramatic reductions in total and respirable dust concentrations could be achieved with the LEV dust control system along with proper operation and maintenance (Echt 2013). However, multiple factors exist that limit the productivity and functionality of the LEV dust control system, as designed, allowing for redesign opportunities to increase capture efficiency, operating time between maintenance tasks, and reduce filter/debris cleanout exposures.

Chapter III describes the hood optimization and laboratory evaluation of multiple hood configurations. Chapter IV describes the system optimization to aid in preventing system clogging and prolonging operating time between maintenance stoppages.

3.2.1 Minnich Dowel Pin Drill

Chapters III and IV evaluated a Minnich A-1C Single Drill, On Slab Unit with a dust collection system (Model A-1C, Minnich Manufacturing Company, Mansfield, OH). For the purposes of this dissertation, the Minnich Single Drill, On Slab Unit will be referred to as the dowel drill. The pneumatic driven dowel drill used H-thread steels and

bits to drill 1 1/3” horizontal holes into concrete pavement at a 14” depth. Steel bits can range from 5/8” to 2 ½” diameters with cutting speeds varying from 15 to 30 seconds. The 700 pound unit has a maximum drill depth of 18” ranging from 2 ½” to 12 ¾” below the slab grade. Figure 3.1 is a photograph of the Minnich A-1C Single Drill, On Slab Unit. The Minnich dust collection system consists of an enclosing hood, flexible rubber ducting hose, eductor, canister filter and a 5-gallon collection bucket.

3.3 LEV Hood Descriptions

Four enclosed hoods were evaluated as well as two simple hoods. Two of the enclosed hoods are commercially available and were evaluated without modifications. Two enclosed hoods were NIOSH prototypes designed to lower inlet velocity, allowing larger particles to settle out of the dust collection system at the hood instead of entering the dust collection system. Removing these large particles prior to entering the dust collection system would reduce duct-clogging potential and extend operating time between maintenance activities. Two of the enclosed hoods were two piece designs which allowed for physical separation from the enclosure housing leaving the simple hood to be evaluated individually. These two simple hoods (Minnich and NIOSH prototype) were evaluated in the laboratory to isolate and analyze design features as a more traditional hood.

3.3.1 Minnich Enclosed Hood

The evaluated Minnich enclosed hood was the stock hood provided if users purchased the optional dust collection system. The enclosed hood consists of a 4 ½” inch diameter steel hood face with two rubber inlays connected to a steel housing. A 2" inlet opening leads to a 2” steel pipe approximately six inches long. The airstream encounters a 60° turn before entering the flexible hose connecting the hood to the vacuum source. Figure 3.2 displays the Minnich enclosed hood with steel casing that attaches to the drill frame.

3.3.2 NIOSH Prototype Hood

The NIOSH prototype hood design consists of a three dimensional (3-D) printed hood designed to attach to the existing Minnich dust collection housing. The NIOSH prototype hood consists of a 3 ½” x 2” oval inlet that gradually tapers from a three and one-half-inch transition to a two-inch circular neck. Figure 3.3 details the NIOSH prototype specifications.

The NIOSH prototype hood was designed in SolidWorks® 2011 and printed using a Dimension uPrint Plus 3D printer at NIOSH. After printing, the hood was measured to ensure that correct specifications were acquired. Figure 3.4 contains the computer generated illustration of the NIOSH prototype alongside the printed hood.

3.3.3 NIOSH Prototype Version 2 Hood

During initial testing, it was observed that the NIOSH V1 prototype hood was not aligning properly with the Minnich housing. Further inspection revealed that the rubber

inlays inside the Minnich housing had only a 2” inlet opening. The abrupt expansion from the 2” rubber inlays into the 3 ½” NIOSH prototype hood face caused an unexpected system loss. While the goal of the NIOSH prototype is to reduce the initial inlet velocity, the expansion system loss may lead to excessive dust particles dropping out of the airstream at the expansion. These dust particles may accumulate on the dust collection side of the rubber inlay. They would not easily fall out of the hood when repositioning the dowel drill and may potentially add an additional clogging point in the dust collection system. Therefore, a second NIOSH prototype, version 2 (NIOSH V2) was created using the same 3D printing process as described above. The NIOSH V2 design included the same simple hood as the previous design but expanded the rubber inlay inlet opening to match the 3 ½” hood opening. The new housing design sought to eliminate the system loss due to the rapid expansion from the 2” rubber inlay opening into the 3 ½” NIOSH simple hood face. Figure 3.5 illustrated the widened rubber inlay inlets to match the NIOSH simple hood face.

3.3.4 Dust Control Enclosed Hood

The Dustcontrol® enclosed hood #6001 (also known as a shroud) is a 4” tall and 6” wide circular, rubber hood. The hood has a 1 ¼” diameter opening in the top for inserting the steel bit through the hood and into the substrate. A 1 ¼” inlet leads to a 2” connection extension with an internally threaded tubing to connect to a vacuum source.

The hood was previously evaluated as a part of a dust collection system used in lateral concrete drilling using a pneumatic rock drill (Cooper, Susi et al. 2012). The hood

was chosen for laboratory testing based on its use in similar operations, such as lateral concrete drilling, and to assess adaptability to the dowel drill.

3.3.5 Simple Hood Comparison

Two enclosed hoods (Minnich and NIOSH prototype) are two piece hoods that can be physically separated into a simple hood. Each hood was removed from the enclosed housing and evaluated in the laboratory as a simple hood. Figure 3.7 is a photograph of both the Minnich and NIOSH prototype simple hoods.

The NIOSH V2 simple hood was not tested during the simple hood evaluation. NIOSH V2 has the same simple hood as the original NIOSH prototype design but with a differently designed housing.

3.4 Air Density Factor

Environmental conditions were measured to calculate the air density factor and determine the actual cubic feet per minute (acfm) flowrates (ACGIH 2016). The following equation is used to determine the air density factor:

$$df = (df_e)\ (df_p)\ (df_T)\ (df_m) \qquad \text{Equation 1}$$

where df = overall density factor

df_e = Elevation density factor

df_p = Pressure density factor

df_T = Temperature density factor

df_m = Moisture density factor

3.5 Specific Aim 2

The research for Specific Aim 2 investigated LEV hood characteristics and their potential impact on a concrete dowel drill LEV system. The laboratory evaluation of four LEV hoods (manufacturer, commercially available, and two novel design hoods) aimed to determine the most effective LEV hood for a concrete dowel drill local exhaust ventilation system. Specific Aim 2 was defined as the Laboratory evaluation of manufacturer, commercially available, and novel design hoods for concrete dowel drill local exhaust ventilation system.

Hypothesis 2 was defined as:

The NIOSH prototype hood (V1 and V2) will reduce face and inlet velocities when compared to the manufacturer's hood design

Null Hypotheses 2 and 3 (Ho2 and Ho3) were defined as:

Ho2: The NIOSH prototype and manufacturer's hood have the same face velocities

Ho3: The NIOSH prototype and manufacturer's hood have the same inlet velocities

Ho4: The NIOSH prototype and the commercially available hood will perform the same

3.6 Methods

This study aims to evaluate the dowel drill dust collection hood as available from the manufacturer and the proposed redesigns or substitutes. The hood evaluations were performed at the National Institute for Occupational Safety and Health (NIOSH) Engineering and Physical Hazard Branch's (EPHB) ventilation laboratory in Cincinnati, Ohio.

Four enclosed hoods were selected for laboratory evaluation: (1) Minnich; (2) NIOSH prototype; (3) NIOSH prototype version two or the NIOSH V2; and (4) Dustcontrol® enclosed hood (part number 6001). Each enclosed hood was evaluated for hood coefficient of entry; hood loss; face velocity; inlet velocity; and static pressure curves. Two enclosed hoods (Minnich and NIOSH Prototype) were analyzed by removing the enclosing housing and evaluating the simple hoods individually.

The same laboratory design and protocol was used for each hood evaluated. A laboratory protocol was established to ensure that each trial was consistent to minimize variations. Each hood was evaluated during three trials and the arithmetic average metrics were reported. If a trial exceeded 5% variance of the other trials, a fourth trial was conducted.

The laboratory design consisted of the hood being attached to a six foot long, two inch diameter, smooth wall PVC pipe by a two inch by two inch rubber coupling. The length of the PVC pipe was considerably more (more than three times) than the hood diameter that allowed for uniform airflow distribution. The coupling was tightened on

both the hood and PVC to ensure a secure connection. The other end of the PVC pipe was connected to a two inch Y-connector leading to a ShopVac® Contractor Wet/Dry Vacuum Model 90LN650C with a 6.5 horsepower motor (Williamsport, PA) and a Dustcontrol® DC3700C single phase, two stage fan spot extractor (Norsborg, Sweden). The ShopVac® Contractor vacuum was attached to a Metheson Scientific variable autotransformer (120 volts). The variable autotransformer allowed for variable flowrates within the PVC pipe.

Air was drawn through the PVC pipe at the following trial velocities: 500; 1,000; 1,500; 2,000; 2,500; 3,000; 3,500; 4,000; and 4,500 fpm. The trial velocities were verified by a four point pitot traverse using a TSI™ Velocicalc® Air Velocity Meter Model 9565 (Shoreview, MN) that was calibrated in July, 2015 (within the one year manufacturer's recommendation). The pitot traverse verifying the duct transport velocities was taken in the middle of the PVC pipe (more than eight duct diameters from the hood connection and the Y-connection to the vacuums)to minimize turbulence. Table 3.1 contains the trial velocity number and the corresponding duct transport velocity. When the desired duct transport velocity was achieved and verified by the pitot traverse, the variable autotransformer setting was marked. The duct flowrate (Q) is calculated by multiplying the velocity (fpm) and the area of the two inch duct in square feet (0.022).

Only the ShopVac® vacuum was used for duct transport velocities 500 to 3,500 fpm. For 4,000 and 4,500 fpm velocities, the Dustcontrol® DC3700C was operated in conjunction with the ShopVac® vacuum. When the desired duct transport velocity was achieved and verified by the pitot traverse, the variable autotransformer setting was

marked. The variable autotransformer marked settings allowed for consistent vacuum settings throughout the laboratory evaluation of each hood. Figure 3.8 is a photograph of the laboratory design with labeled laboratory equipment.

3.6.1 Hood Static Pressure

The hood static pressure (SPh) was measured with a TSI™ Velocicalc® Air Velocity Meter Model 9565 (Shoreview, MN) with a static pressure probe. The SPh measurement was collected as close to the hood connection to the PVC pipe as possible. The SPh was recorded for each hood at each of the trial velocity settings.

The laboratory evaluation provides a relationship between air flow and the hood static pressure which can be used in the field to estimate the flow rates by measuring hood static pressure with a manometer or static pressure tap. This method is often known as the Throat Suction method (Burgess, Ellenbecker et al. 2004, ACGIH 2016). A static pressure curve was created for each hood across all trial velocity settings.

3.6.2 Hood Coefficient of Entry

A laboratory design was constructed to evaluate the hood coefficient (Ce) for each enclosing or simple hood. By measuring Q and SPh, we can determine the Ce by the equation given below:

$$Ce = \frac{\mathrm{Q}}{4005\ (\mathrm{Ad})\sqrt{SPh}}$$ Equation 2

Ce = Coefficient of entry

Q = Airflow (cfm)

SPh = Hood static pressure (inches of water)

Ad = Cross-sectional area of duct (square feet)

Ce calculations were performed in Microsoft® Excel® and are reported as unitless values.

3.6.3 Hood Inlet Velocity

The hood inlet velocity (a.k.a. duct take-off velocity) was measured as close as possible at the opening within the hood leading into the PVC pipe. Using a TSI™ Velocicalc® Air Velocity Meter Model 9565 (Shoreview, MN) with a hot wire anemometer attachment, the hot wire anemometer was placed flush against the inlet. The hot wire anemometer was positioned so the open face was fully open to the inlet air stream and located in the middle of the inlet. Figure 3.9 is a photograph of the hood inlet velocity measurement location.

3.6.4 Hood Face Velocity

The hood face velocity was measured as close as possible at the hood face opening. On the dowel drill, the hood face is that part of the LEV hood which will go up

against the vertical concrete slab during drilling. Using a TSI™ Velocicalc® Air Velocity Meter Model 9565 (Shoreview, MN) with a hot wire anemometer attachment, the hot wire anemometer was placed flush against the hood face. The hot wire anemometer was positioned so that the anemometer's face was fully open to the incoming airstream. Measurements were collected in the middle of the hood face. Figure 3.10 is a photograph of the hood inlet velocity measurement location for the Dustcontrol® hood.

3.6.5 Duct Transport Velocity

Duct transport velocity measurements were collected in the middle of the PVC pipe (more than eight duct diameters from both the hood connection and the Y-connection to the vacuums) to minimize turbulence and allow for full development of the flow field. Measurements were collected using a TSI™ Velocicalc® Air Velocity Meter Model 9565 (Shoreview, MN) with a pitot tube using a 4-point traverse.

All statistical analysis was performed using Microsoft Excel® Office 2015 edition. Two-tail and one-tail t-test evaluated significant difference between manufacturer's hood and the novel designs and commercially available hood. Descriptive statistics were developed for each metric.

3.7 Results

Environmental conditions were measured to calculate the air density factor in order to determine the actual cubic feet per minute (acfm) flowrates (ACGIH 2016). The average laboratory environmental conditions were as follows: average temperature of

73 degrees Fahrenheit, relative humidity of 24.9%, and barometric pressure of 29.46 inches of mercury (in Hg). The elevation of the laboratory in Cincinnati, OH is 482 feet above sea level. The density factor was found to be 1.00 for the average environmental conditions observed.

The hood static pressure was measured for each simple and enclosed hood across a range of trial velocities. Table 3.2 contains the hood static pressure for each hood and trial velocity. For the simple hoods, the NIOSH hood had a lower hood static pressure range (0.03 to 2.64 “w.g.) than the Minnich hood (range 0.04 to 3.76 “w.g.) for each trial velocity. For the enclosed hoods, the hood static pressures for the NIOSH V1, NIOSH V2, and Dustcontrol® hoods were lower than the Minnich hood static pressure for 89% of the trial velocities. Due to the wider opening connecting the NIOSH simple hood design and the rubber inlay, the NIOSH V2 hood static pressure did not increase as dramatically as NIOSH V1 indicating that the NIOSH V2 hood design was more efficient at the higher velocity trials. The Minnich hood static pressure was equal to or lower than the other 3 hoods for only the 500 fpm velocity trial. This is the lowest trial velocity tested and the concrete dowel drill LEV system typically operates at greater than 3,000 fpm.

The hood coefficient of entry was also measured for each simple and enclosed hood across a range of trial velocities. Table 3.3 displays all the results for each hood and trial velocity. For the simple hood comparison, the NIOSH hood had an average hood coefficient of entry of 0.81 compared to 0.64 for the Minnich hood. The average hood coefficient of entry for the enclosed hoods were as follows: NIOSH (0.64), NIOSH V2 (0.64), Minnich (0.59) and Dustcontrol® (0.58). The hood coefficient of entry is a

measure of efficiency with more efficient hoods approaching 1 and less efficient hoods approaching zero.

For the simple hood, the NIOSH V1 hood inlet velocities were lower than the Minnich hood for all trial velocities (Figure 3.11). For the enclosed hoods, the NIOSH V1 and Minnich hood inlet velocities were similar except for the 4,000 and 4,500 fpm trials when the NIOSH V1 velocity was much lower than the Minnich. The NIOSH V2 hood inlet velocities were considerably lower than the Minnich hood for all trials while the Dustcontrol® was higher than the Minnich for all trials. All hood inlet velocity results are displayed in Table 3.4 by hood and trial velocity setting.

The NIOSH V1 ranked first when comparing highest hood face velocities in 7 out of 9 trial velocities tested (78%) and finished second in the other two trials (1,500 and 3,000 fpm trials). The NIOSH V2 design ranked first or second in 6 out of 9 trials (66.7%) and was third in the other three trials (500, 1,000, and 4,500 fpm). The Minnich hood ranked second or third in every trial velocity measured. The Dustcontrol® hood had the lowest hood face velocity of all hoods measured for each trial velocity. Table 3.5 shows all hood face velocity results for each trial velocity. Figure 3.12 illustrates the inconsistent results across all hoods and trial velocities. Simple hood were not evaluated for hood face velocities.

The NIOSH V2 hood design had the highest transport velocity in 7 out of 9 trial velocities tested (78%) and finished second (4,500 fpm trial) and third (4,000 fpm trial) in the other two trials. The NIOSH V1 hood design struggled in the lower trial velocities but was a strong performer when trial velocities were greater than 2,000 fpm. In these

higher transport velocity trials, the NIOSH V1 ranked either first or second for all trials with having the highest transport velocities in the 4,000 and 4,500 fpm trials. The Minnich hood finished third or fourth in all trials except for ranking second in the 1,000 fpm trial. The DustControl® finished second in 3 out of 9 trials (33%), third in 4 out of 9 trials (44%), and fourth in 2 out of 9 trials (22%). Table 3.6 shows all hood transport velocities for all trial velocities measured.

3.8 Discussion

Chapter III discusses the laboratory evaluation of four LEV hood designs for potential application on a dowel drill. The evaluation examined a number of LEV hood design parameters including Ce, transport velocity, hood face velocity, and hood inlet velocity. The four main LEV hood designs are enclosed hood types but simple hoods were also evaluated when possible. Evaluating the simple hoods allowed for the further comparison of individual components of the LEV hood than the enclosed hoods alone. This study evaluated the potential impact of LEV hood designs on a dowel drill LEV system in a controlled environment with a lower economic cost than real-world testing scenarios.

While the NIOSH V1 and NIOSH V2 hood designs performed well, they did not outperform the Minnich and DustControl® hoods in all parameters and trials. This indicates that future research should be conducted in order to further develop more efficient hoods. However, across the full evaluation spectrum, the NIOSH V1 and NIOSH V2 designs are improvements over the manufacturer's hood and the commercially available hood tested here.

While the laboratory evaluation examined a number of parameters, this evaluation did not simulate conditions that are encountered during real-world working conditions. For example, the environmental conditions in the laboratory do not simulate the wide range of temperature, relative humidity, barometric pressure, and elevation conditions that may be encountered. Therefore the density factor applications and airflow characteristics may have varying results than those found here.

The vacuum source used in the laboratory evaluation and the dowel drill source are different. The dowel drill vacuum may create transport velocities higher than those replicated in the laboratory environment. As we observed in our laboratory results, the flowrate can affect changes in the LEV system.

The laboratory evaluation also did not use the same duct material or simulate the ductwork turns observed in the manufacturer's LEV system. However, except for the changes in transport velocity the duct material and turns should not impact the hood efficiency measurements obtained in this study.

During real-world drilling, the dowel drill hood face will "jump" back and forth during the pneumatic drilling of the concrete. This jumping back and forth may create a cross-draft type interference with LEV rock dust collection. This study was unable to recreate or simulate the jumping back and forth and was therefore unable to evaluate the potential impact on the evaluated hood designs.

3.9 Conclusion

This study evaluated the potential impact of four enclosed LEV hood designs (including two simple hood designs) on the dowel drill LEV system. The NIOSH designs were more efficient for both the simple hood and enclosed hood evaluations. The NIOSH designs also increased transport velocities versus the manufacturer hood for a majority of the trial velocities including the 4,000 and 4,500 fpm duct trial velocities which are the required minimum duct transport velocities for rock dust. Based upon these results, the NIOSH designs would have a beneficial effect on the dowel drill LEV system leading to reduced clogging and maintenance issues previously observed in the literature. Based upon the lower hood static pressure at the higher trial velocities, equal Ce, and similar transport velocities the NIOSH V2 design was chosen for Aim 3, the simulated work conditions evaluation.

References

ACGIH (2016). Industrial ventilation: a manual of recommended practice. Cincinnati, OH, American Conference of Governmental and Industrial Hygenists.

Akbar-Khanzadeh, F. and R. L. Brillhart (2002). Respirable crystalline silica dust exposure during concrete finishing (grinding) using hand-held grinders in the construction industry. Ann Occup Hyg 46(3): 341-346.

Akbar-Khanzadeh, F., S. A. Milz, C. D. Wagner, M. S. Bisesi, A. L. Ames, S. Khuder, P. Susi and M. Akbar-Khanzadeh (2010). Effectiveness of dust control methods for crystalline silica and respirable suspended particulate matter exposure during manual concrete surface grinding. J Occup Environ Hyg 7(12): 700-711.

Alexander, B. M., E. J. Esswein, M. G. Gressel, J. L. Kratzer, H. Amy Feng, B. King, A. L. Miller and E. Cauda (2016). The Development and Testing of a Prototype Mini-Baghouse to Control the Release of Respirable Crystalline Silica from Sand Movers. J Occup Environ Hyg: 0.

Burgess, W. A., M. J. Ellenbecker and R. D. Treitman (2004). Ventilation for control of the work environment. Hoboken, N.J., Wiley-Interscience.

Bush, T. D. and S. M. Mannava (2000). Measuring the deflected shape of a dowel bar embedded in concrete. Experimental Techniques 24(3): 33-36.

Chalupka, S. (2012). Occupational silica exposure in hydraulic fracturing. Workplace Health Saf 60(10): 460.

Cooper, M. R., P. Susi and D. Rempel (2012). Evaluation and control of respirable silica exposure during lateral drilling of concrete. J Occup Environ Hyg 9(2): D35-41.

Echt, A. (2012). Respirable dust exposures of workers dowel drilling concrete pavement and evaluation of control measures. Ph.D. Dissertation, University of Kentucky.

Echt, A., K. Sieber, E. Jones, D. Schill, D. Lefkowitz, J. Sugar and K. Hoffner (2003). Control of respirable dust and crystalline silica from breaking concrete with a jackhammer. Appl Occup Environ Hyg 18(7): 491-495.

Echt, A. H., D; Kovein, R (2011). Control Technology for Dowel Drilling in Concrete at the Springfield-Branson National Airport. NIOSH. Cincinnati, OH.

Echt, A. K., R; Lambright, J (2012). Control Technology for Dowel Drilling in Concrete at the Hartsfield-Jackson Atlanta International Airport. Cincinnati, OH.

Echt, A. M., K; Farwick, D; Feng H. (2008). In-Depth Survey: Preliminary Evaluation of Dust Emissions Control Technology for Dowel-Pin Drilling at Minnich Manufacturing. NIOSH. Cincinnati, OH.

Echt, A. M., K; Feng, H; Farwick, D (2011). Control Technology for Dowel-Pin Drilling in Concrete Pavement at EZ Drill. NIOSH. Cincinnati, OH.

Echt, A. M., K; Feng, H; Farwick, D (2011). Control Technology for Dowel-Pin Drilling in Concrete Pavement at Minnich Manufacturing. NIOSH. Cincinnati, OH.

Echt, A. M., K; Kovein (2011). Control Technology for Dowel Drilling in Concrete at Columbus Municipal Airport. NIOSH. Cincinnati, OH.

Echt, A. M., K; Kovein (2013). Control Technology for Dowel Drilling in Concrete at Laborers International Union of North America Local 172. NIOSH. Cincinnati, OH.

Esswein, E. J., M. Breitenstein, J. Snawder, M. Kiefer and W. K. Sieber (2013). Occupational exposures to respirable crystalline silica during hydraulic fracturing. J Occup Environ Hyg 10(7): 347-356.

Glindmeyer, H. W. and Y. Y. Hammad (1988). Contributing factors to sandblasters' silicosis: inadequate respiratory protection equipment and standards. J Occup Med 30(12): 917-921.

Health, U. S. D. o. H. a. H. S. N. I. o. (2015, 2013). Silicosis. Retrieved March 26, 2015, from http://www.nlm.nih.gov/medlineplus/ency/article/000134.htm.

Linch, K. D. (2002). Respirable concrete dust--silicosis hazard in the construction industry. Appl Occup Environ Hyg 17(3): 209-221.

Merchant, J.A., Boehlecke, B.A., Taylor, G (1987). Occupational respiratory diseases. United States Department of Health and Human Services, Centers for Disease Control and Prevention. Washington, D.C.

Nash, N. T. and D. R. Williams (2000). Occupational exposure to crystalline silica during tuckpointing and the use of engineering controls. Appl Occup Environ Hyg 15(1): 8-10.

NIOSH (2002). NIOSH hazard review: health effects of occupational exposure to respirable crystalline silica. P. H. S. Department of Health and Human Services, Centers for Disease Control and Prevention, National Institute for Occupational Safety and Health. Cincinnati, OH: U.S.

NIOSH (2015). Reducing hazardous dust exposure when dowel drilling in concrete. By Echt A, Whalen. National Institute for Occupational Safety and Health. Cincinnati, OH.

OSHA (2016). Occupational Exposure to Respirable Crystalline Silica. OSHA. Washington, D.C. 81 FR 16285: 16285-16890.

Park, C., C. Jang, S. Lee and J. Won (2008). Microstructural investigation of Long-Term Degradation Mechanisms in GFRP Dowel Bars of Jointed Concrete Pavement. Journal of Applied Polymer Science.

Rappaport, S. M., M. Goldberg, P. Susi and R. F. Herrick (2003). Excessive exposure to silica in the US construction industry. Ann Occup Hyg 47(2): 111-122.

Reiser, K. (1985). Occupational medicine: silicosis and cancer risk. West J Med 143(4): 509.

Rice, F. L. and L. T. Stayner (1995). Assessment of silicosis risk for occupational exposure to crystalline silica. Scand J Work Environ Health 21 Suppl 2: 87-90.

Sander, O. A. (1968). Silicosis, the preventable occupational lung disease. Bull Natl Tuberc Assoc 54(2): 7-9.

Thorpe, A., A. S. Ritchie, M. J. Gibson and R. C. Brown (1999). Measurements of the effectiveness of dust control on cut-off saws used in the construction industry. Ann Occup Hyg 43(7): 443-456.

United States. Branch of Industrial Minerals. (1992). Crystalline silica primer. Washington, D.C.?, U.S. Dept. of the Interior, U.S. Bureau of Mines.

Valiante, D. J., D. P. Schill, K. D. Rosenman and E. Socie (2004). Highway repair: a new silicosis threat. Am J Public Health 94(5): 876-880.

Walters, K., J. Jacobson, Z. Kroening and C. Pierce (2015). PM 2.5 Airborne Particulates Near Frac Sand Operations. J Environ Health 78(4): 8-12.

Witter, R. Z., L. Tenney, S. Clark and L. S. Newman (2014). Occupational exposures in the oil and gas extraction industry: State of the science and research recommendations. Am J Ind Med 57(7): 847-856.

Woskie, S. R., A. Kalil, D. Bello and M. A. Virji (2002). Exposures to quartz, diesel, dust, and welding fumes during heavy and highway construction. AIHA J (Fairfax, Va) 63(4): 447-457.

CHAPTER IV

Simulated Workplace Evaluation of a Concrete Dowel Drill Local Exhaust Ventilation System

Abstract

This study evaluated potential changes to a dowel drill LEV system to reduce previously identified performance and operation problems associated with duct clogging and filtration system maintenance. Proposed changes included replacing the manufacturer's hood with a NIOSH prototype, replacing the corrugated duct hose with smooth bore hose, and the addition of a cyclone prior to the horizontal duct run and filtration system. Six total test scenarios consisting of two trials with 10 drilled holes per trial were evaluated in simulated work conditions.

The NIOSH prototype hood and smooth bore hose reduced material within the hose by as much as 6 times per 10 holes drilled, compared to the manufacturer's configuration. We observed a greater than 95% reduction in collected dust reaching the filtration system due to the cyclone addition. Exposure characterizations through particle count measurements were inconsistent due to changing environmental conditions and wind.

Recommended, minimal cost substitutions and additions to the dowel drill LEV system can have a positive impact on LEV performance, prolonging service time between maintenance, increasing filter life, and maintaining transport velocities to reduce respirable crystalline exposures.

4.1 Introduction

Chapter III discussed in detail the issues related to the dowel drill LEV system. The laboratory evaluation identified the most efficient LEV hood. Chapter IV aims to evaluate this LEV hood along with other system changes to optimize the entire LEV system and evaluate those changes in simulated work conditions.

Previous research confirmed the LEV system was effective in reducing respirable crystalline silica exposure in both simulated and actual workplace conditions (Echt and Mead 2016a; Echt et al. 2016; Echt et al. 2003; Echt 2011b; Echt 2012b; Echt 2008; Echt 2011a; Echt 2011d, 2011c, 2013). However, the previous research also identified major deficiencies in the LEV system's effectiveness during long time periods of operation due to duct clogging and filter caking. These deficiencies lead to increased maintenance breaks and poor LEV system performance after only minutes of operation.

4.1.1Minnich Dowel Pin Drill

The dowel drill evaluated was a Minnich A-1C Single Drill, On Slab Unit with a dust collection system (Model A-1C, Minnich Manufacturing Company, Mansfield, OH). For the purposes of this dissertation, the Minnich Single Drill, On Slab Unit will be

referred to as the dowel drill. The pneumatic driven dowel drill used H-thread steels and bits to drill 1 1/3” horizontal holes into concrete pavement at a 14” depth. Steel bits can range from 5/8” to 2 ½” diameters with cutting speeds varying from 15 to 30 seconds. The 700 pound unit has a maximum drill depth of 18” ranging from 2 ½” to 12 ¾” below the slab grade. Figure 3.1 is a photograph of the Minnich A-1C Single Drill, On Slab Unit.

The basic work cycle for dowel drill is the same regardless of which LEV version is operated. The drill operator positions the drill to align the drill bit and LEV system face as close to the concrete substrate as possible. The hole is drilled typically in under 60 seconds but is dependent upon the concrete density, drill bit condition, pneumatic pressure, and other parameters. After completing the hole, the drill bit is removed from the hole. The drill operator releases the brake and repositions the drill to the next hole. The process is repeated until the desired number of holes is drilled.

The Minnich LEV dust collection system consists of an enclosing hood, flexible rubber ducting hose, eductor, cartridge filter and a 5-gallon collection bucket. The drill bit is enclosed by the LEV hood which is attached to a 2” corrugated, flexible hose. The flexible hose was also corrugated on its inner surface. The other end of the flexible hose was connected to a dust collector system comprised of a pneumatic eductor, pleated urethane filter cartridge (60 square meters filter area), and a cleanout bucket. The eductor is a canister dust collector that relies on a venturi style system with each canister accommodating up to two rock drills (only one rock drill was used in this study). The pleated filter cartridge was rated as a 13 for minimum efficiency reporting value, commonly known as the MERV rating. The cleanout bucket was a 5-gallon translucent

bucket. Figure 3.1 is a photograph of the current manufacturer's LEV system and dowel drill design.

In the field, maintenance is limited. However, when the LEV is clogged or not performing well troubleshooting activities have been observed. The filter is removed from the housing and excess dust is removed via rolling and taping on the ground as well as using compressed air. The layer of dust accumulation on the filter, or caking of the filter, increases filter resistance (ACGIH 2016). The LEV cleanout bucket is removed and debris is scattered in the vicinity of the drill. The LEV hose is also removed and shook to remove clogs and excess debris.

Prior research characterizing respirable crystalline silica exposures associated with dowel drills have been investigated by NIOSH (Echt 2012a; Echt et al. 2003; Echt 2011b; Echt 2012b; Echt 2008; Echt 2011a; Echt 2011d, 2011c, 2013). During controlled field testing, the manufacturer's dust control system was determined to reduce potential exposures to respirable dust reductions by 86-92%.

During field evaluations, NIOSH investigators noted that the LEV dust control system had issues with overloading which would dramatically reduce (1) the dust control system's collection efficiency and (2) the operating time between dust collection maintenance tasks. A recent NIOSH study found a 33% reduction in airflow rates at the dust collector after a 2 day study with intermittent drilling and that airflow was not fully recovered after filter cleaning (Echt and Mead 2016b). NIOSH research indicated that reductions in total and respirable dust concentration exposures could be achieved with the LEV dust control system with proper operation and maintenance (Echt 2013). However, multiple factors exists that limit the productivity and functionality of the LEV

dust control system as designed allowing for redesign opportunities to increase capture efficiency, operating time between maintenance tasks, and reduce filter/debris cleanout exposures.

4.2 Potential System Changes

A wide range of potential system changes were considered during the initial evaluation of the dowel drill LEV system. The selected changes were identified based upon low economic cost to implement along with the greatest potential impact on system performance. All changes are commercially available, except the NIOSH prototype hood designs, which can easily be replicated by the drill manufacturer.

4.2.1 Flexible Ductwork

The current LEV dust control system is fitted with a 2” corrugated (inside and out) flexible hose. This type of ducting has one of the highest friction loss per foot of material ratings. The magnitude of friction loss is influenced by velocity, duct diameter, air density, air viscosity, and duct surface roughness (also known as absolute surface roughness). Friction loss increases the static pressure needed to create the minimal transport velocity of 4,000 fpm. It also is more susceptible to clogging due to decreasing airflow near the duct wall that allow rock dust to fall out of the airstream and build-up on the outer walls. Chapter I section I.6.2 discusses how friction loss impacts LEV systems. Other reference have tables with estimated duct losses by the length and construction of the duct (ACGIH 2016; Burgess, Ellenbecker, and Treitman 2004). Table 4.1 gives the surface roughness for common ventilation ductwork.

The optimal use of this corrugated flexible ductwork is for short distances in which maximum flexibility is required. When this type of duct is used for long distances it will sag in areas where it is not supported. Due to the flexibility of the hose, a greater length of hose is often used due to this sagging leading to additional friction loss and exacerbating the wall build-up issue. However, the dowel drill LEV dust control system does not require the use of this type of hose and thus, it may be replaced.

A clear, smooth bore rigid flexible duct was chosen to replace the current corrugated hose. The smooth bore design has a more efficient surface roughness value and is less susceptible to wall build-up (ACGIH 2016). The hose rigidity also allows for shorter hose lengths and is less susceptible to sagging even after prolonged use. The use of a clear hose allows for clogging identification without taking the hose off the LEV control system.

4.2.2 Cyclone

Cyclones, or pre-separators, are widely used dust collection devices that rely on cyclonic air movement to remove particles from the airstream (Leith and Mehta 1973; Bahrami et al. 2009; Cheremisinoff 1993; Heumann 1997; Schifftner 2002). Cyclones are inexpensive, durable, and consistent dust removal mechanisms with predictable, long-lasting performance as long as they are properly selected (Heumann 1997; Schifftner 2002). Cyclones are often used prior to more efficient dust collector as a pre-cleaner in order to prolong the more efficient dust collector’s life span (Heumann 1997; Leith and Mehta 1973; Schifftner 2002).

While the pressure drop across a cyclone is low to moderate when compared to other dust collection systems, it is inherent to the cyclone design and can only be minimized through proper selection and design. Leith and Mehta list the five reasons for pressure drop in a cyclone as below (Leith and Mehta 1973):

1. *"Loss due to expansion of the gas when it enters the cyclone chamber.*
2. *Loss as kinetic energy of rotation in the cyclone chamber.*
3. *Losses due to wall friction in the cyclone chamber.*
4. *Any additional frictional losses in the exit duct, resulting from the swirling flow above and beyond those incurred by straight flow.*
5. *Any regain of the rotational kinetic energy as pressure energy."*

An Oneida Industrial Steel Dust Deputy® (Oneida Air Systems Syracuse, NY Item #AXD001002) was selected for pre-separating rock dust from the airstream prior to both the horizontal section of the duct and the pleated filter cartridge. The industrial version is designed for highly abrasive material such as rock dust. The cyclone manufacturer claims that air exiting the cyclone has over 99% of debris removed (Systems 2016).

The Dust Deputy® has a 2" diameter inlet and outlet which matches the manufacturer's hose diameter and the proposed smooth-bore hose. The Dust Deputy® is also fitted with a tight sealing 5-gallon bucket that collects dust as it falls out of the airstream within the cyclone. Emptying the cyclone collection bucket is also much faster than performing filter maintenance for the eductor system.

4.2.3 NIOSH Redesigned Hood

Chapter III describes the laboratory evaluation of the proposed LEV system hoods and the manufacturer's hood. Based upon the laboratory evaluation, the NIOSH

V2 hood was originally selected for the simulated work conditions. However, after fitting the NIOSH V2 hood to the dowel drill and running a small number of test holes it became clear that the NIOSH V2 would not withstand the amount of drilling needed. The NIOSH V2 hood plastic model was printed on a 3D printer and considered a prototype. The NIOSH V2 model consisted of a secondary 3D printed component that widened the opening from the LEV hood into the LEV duct. This secondary component was attached directly to the drill face and began to crack under the high demands of drilling.

The NIOSH V1 prototype did not have the secondary component and attached to the drill away from the high impact area. After a small number of test holes, NIOSH V1 did not show any signs or stress or critical failure. Therefore, we used NIOSH V1 for the simulated work conditions. Chapter III discusses the differences between NIOSH V1 and NIOSH V2. However, their overall performance was similar in the laboratory evaluation.

4.3 Potential Exposures

While the research utilized simulated workplace conditions, potential exposure to hazardous dust and physical agents were considered prior to field work. In order to reduce potential occupational exposures to the participants during the study, the NIOSH health and safety staff were consulted. Administrative controls (such as powering down the compressor when not used and having the drill assist personnel stand away from the drill) were instituted to minimize potential exposures and personal protective equipment (described below) was worn.

4.3.1 Silica

Respirable crystalline silica exposures during dowel drilling is well-defined in the literature. Even though the potential exposures were considered to be low with limited operation time and outdoor conditions, respiratory protection was required during drill operation. Both the drill operator and drill support person wore a quantitatively fit-tested 3M™ Powerflow™ full-facepiece powered air purifying respirator with a P-100 cartridge. Both participants were enrolled in the NIOSH respiratory protection program and were medically cleared for respirator use.

4.3.2 Noise

Potential noise exposure is due to both the nature of the pneumatic drill and the air compressor generator needed to power the drill. The drill design requires the drill operator to stand close to the drill during drilling activities in order to manual manipulate the drill. No remote operation capabilities were available during the simulated work conditions.

During the simulated work conditions, the air supply hose length (20 feet) limited the positioning of the air compressor generator in relation to the drill. The testing facility configuration often forced the drill operator to stand between the drill and the air compressor generator. Figure 4.1 illustrates the proximity of the drill operator to the dowel drill and air compressor.

Both the drill operator and drill support person wore both ear muffs and ear plugs during drill operation. No noise exposure data was available to estimate potential noise exposures prior to the simulated work trials.

Specific Aim 3

To optimize LEV hood and system configurations and perform field evaluation to investigate the effectiveness of novel designs during simulated workplace conditions

Hypothesis 3

The NIOSH prototype hood and system modifications will increase dowel drill operation times while maintaining or exceeding previous system performance

Null Hypotheses

Ho5: The NIOSH prototype hood did not decrease face velocity compared to the manufacturer's hood

Ho6: The pre-separator did not change filter loading and rear clean-out bucket weight

Ho7: The smooth-bore hose gained the same amount of rock debris as the manufacturer's hose

Ho8: The drill operating time will be the same regardless of modification configuration

4.4 Methods

This study aimed to evaluate the dowel drill as available from the manufacturer and the proposed redesigns. The evaluation was conducted at the NIOSH T-9 facility in Cincinnati, Ohio. The NIOSH T-9 facility has a raised concrete platform with one side

that allows for four 11” x 20” x 36” concrete blocks to be placed alongside the concrete platform (Figure 4.2). After the exposed concrete substrate has been drilled, the concrete blocks are either rotated or replaced for additional drilling.

Test scenarios were based upon permutations of hood (manufacturer or NIOSH prototype), hose (manufacturer and smooth-bore), and cyclone (with and without). Table 4.2 shows the testing scenarios for each configuration. Testing was conducted on two consecutive Fridays at the end of January and the beginning of February 2016. No drilling occurred when temperatures were below 40 degrees Fahrenheit to ensure measurement equipment was within environmental parameters.

Each test scenario consisted of two trials in which 10 holes were drilled. The drill operator was a NIOSH Industrial Hygiene Technician with limited training on operation and maintenance of the dowel drill. The drill operator, type of drill bit, and work cycle was the same for all test scenarios.

Face and inlet velocities were measured both prior to and immediately following each 10-hole trial. These velocities were measured using TSI^{TM} Velocicalc® Air Velocity Meter Model 9565 (Shoreview, MN) with a hot wire anemometer attachment or pitot tube. Hood static pressure along with static and velocity pressure measurements were collected at various points in the LEV system depending on the test scenario.

The cleanout bucket weight (under manufacturer’s eductor and cyclone when used) was measured before and after each 10 hole trial on a Accuteck® heavy duty digital metal industry shipping postal scale with a weight capacity of up to 440 pounds (lbs) and 0.05 lbs increments. Hose weight measurements were collected by placing the

hose into a large container that was previously tared to zero on the Accuteck® scale. Hose weight measurements were also collected before and after each 10-hole trial. Analysis of cleanout bucket weight is a novel approach to evaluating the effectiveness of the ventilation system.

Particle counts were measured by utilizing general area and personal breathing zone monitors. The general area particle count concentrations were monitored by two DustTrak DRX 8533 aerosol monitors located near the drill and approximately 5 feet from the drill. The DustTrak DRX monitors operated on a 3 liter per minute flowrate and data logged every 1 second. Data was downloaded using manufacturer provided software TrakPro. Each DustTrak DRX monitor was factory calibrated by ISO 12103-1, A1 Arizona test dust and contained a calibration certificate. Each DustTrak DRX was zeroed using the manufacturer provided zero filer prior to data collection.

Personal breathing zone particle counts were measured using a TSI SidePak^{TM} personal aerosol monitor model AM510 with a 10 millimeter nylon Dorr-Oliver cyclone with a flowrate of 1.7 liters per minute to sample for respirable fraction aerosol with a 50% cut point at 4 micrometers. Particle count data was logged every 1 second. Data was downloaded using manufacturer provided software TrakPro. The Dorr-Oliver cyclone was cleaned prior to sampling including removing debris from the grit pot.

After the first day of testing, it was noted that noise exposures, especially to the drill operator, may be excessive. A review of the literature did not find any noise level estimates. While both the drill operator and drill assist personnel wore ear muffs and ear plugs, noise dosimetry was conducted on the drill operator during the second day of

drilling. On the second day, the drill operator wore a Larson Davis 706RC integrating noise dosimeter for approximately 7 hours. Noise exposures were intermittent due to the nature of changing configurations between trial scenarios.

All statistical analysis was performed using Microsoft Excel® Office 2015 edition. Two-tail and one-tail t-test evaluated significant difference between manufacturer's LEV design and each novel designs configuration. Descriptive statistics were developed for each metric.

4.5 Results

Measurements were compared to the original manufacturer's LEV configuration (test scenario 1) which included the manufacturer's hood and hose. The environmental conditions during the simulated work conditions were within the working parameters of the monitoring equipment. During drilling operations, the temperature ranged from 40 to 43 degrees Fahrenheit and relative humidity ranged from 65 to 74%. Wind speed throughout the sampling periods had an average of 7 miles per hour (mph) and with gust up to 24 mph.

Face and inlet velocities were measured both before and after each trial and the arithmetic average is reported. The highest average face velocities were trial scenario 2 (manufacturer's hood with a smoothbore hose) and trial scenario 4 (manufacturer's hood, smoothbore hose, and cyclone) at 998 and 774 fpm respectively. The three NIOSH hood test scenarios had the next highest face velocities and the manufacturer's hood test scenario 1 had the lowest face velocity.

Ranking the inlet velocities from highest to lowest found the same pattern as with the face velocity measurements. The highest average inlet velocities were trial scenario 2 (manufacturer's hood with a smoothbore hose) and trial scenario 4 (manufacturer's hood, smoothbore hose, and cyclone) at 4,296 and 3504 fpm respectively. The original manufacturer's LEV system had the lowest inlet velocity of 1,719 fpm. Table 4.3 shows the face and inlet velocity measurement for all test scenarios.

Test scenarios 1, 2, 6, and 7 did not use the cyclone so only the manufacturer's cleanout bucket was measured. For test scenarios 4 and 5 that used the cyclone, both the manufacturer's cleanout bucket and the cyclone cleanout bucket were measured. Test scenario 1 (manufacturer hood) and test scenario 7 (NIOSH prototype) both used only the manufacturer's hose. The total dust collected for test scenario 7 (3.53 lbs) was nearly 3.7 times more dust collected than test scenario 1 (0.95 lbs).

Test scenarios 2 and 6 compared the two hoods when replacing the manufacturer's hose with a smooth-bore hose. Test scenario 2 collected almost one pound more on average than the NIOSH prototype test scenario 6.

Test scenarios 4 (manufacturer hood) and 5 (NIOSH prototype) compared the hoods when both the smooth-bore hose and cyclone were added. The NIOSH prototype hood (test scenario 5) collected 1.5 times more dust than the manufacturer's hood (test scenario 4). The cyclone's specifications report over a 99% dust removal after installation. For test scenario #4, we observed a 95.8 % reduction and for test scenario #5 we observed a 99.2% reduction in dust removal. Table 4.4 contains all the cleanout bucket results for each test scenario.

Hose weight was measured for all test scenarios that did not include the cyclone. The original manufacturer's LEV system collected the highest hose weight (0.3 lbs) average per 10 holes drilled. The NIOSH prototype hood and smooth-bore hose weight was 6 times lower (0.05) per 10 holes drilled. Table 4.5 has all the results for each test scenario that with hose weight measurements.

General area particle counts were measured both near the drill and on the opposite side of the drill approximately five feet away. Average particulate matter (PM) below 1 micron (PM_1), $PM_{2.5}$, respirable, PM_{10}, and total concentrations are given in Table 4.6. Test scenario 2 (manufacturer's hood and smooth-bore hose) had the highest average total aerosol concentration for the general area monitor located closest to the drill (3.51 milligrams/m^3). Figures 4.3 and 4.4 graphically illustrate the average area aerosol concentrations for the monitor nearest the drill and on the opposite side of the drilling platform respectively.

Drill operator respirable personal breathing zone aerosol information is unavailable for test scenarios 1 and 2 due to equipment failure. The monitor exceeded the data storage capacity for the drill operator in test scenario 7 and for the drill assist personnel in test scenario 6 and 7. Due to the equipment failure and data storage issues, little information can be gained from the respirable personal breathing zone aerosol sampling. Table 4.7 contains all the available information.

The time-weighted average (TWA) noise exposure was monitored on the second day of testing. A seven hour sample period was monitored. The TWA noise exposure was 99 dBA when evaluated using the NIOSH recommended exposure limit (REL).

Using the NIOSH REL, the dose (percent) was 2,519 which indicates overexposure. Based upon the measured noise exposures, the use of hearing protection and other exposure reduction methods should be used to reduce noise exposure. Double hearing protection, such as earmuffs worn over top of earplugs, should be used for maximum noise reduction.

Table 4.8 contains the noise exposure measurements when using the NIOSH REL, OSHA permissible exposure limit (PEL), and OSHA Action Level. Figure 4.5 illustrates the time history graph of noise exposures (averaged at 5 second intervals) throughout the monitoring period.

4.4 Discussion

The research evaluated the potential impact of changes to a dowel drill LEV system. Impacts were measured during simulated work conditions in changing environmental conditions. Different meteorological conditions can lead to variable results than observed here. Wind direction and speed, including gusts, could have significant impact on measurements, particularly the particle count observations.

Multiple dowel drill models are available from the manufacturer. These models may include multiple drill head and dust collection systems. This study only evaluated a single drill head and a single dust collection system. The number of trials per condition was small (N=2). Based upon the observed results, future research can focus on understanding the potential impact of the most effective combination observed here.

The drill operator had minimal training on drill operation but performed two test drilling sessions prior to the study. Results may differ with more experienced operators as they will most likely perform the same task in a more systematic and efficient manner.

Initial test drilling indicated that the plastic prototype NIOSH V2 hood would not withstand the rigorous drilling and was replaced with the NIOSH V1 hood. Even though NIOSH V1 and V2 hoods performed similar in the laboratory evaluation, NIOSH V2 was selected to have the greatest potential impact. Development of a steel or other durable material prototype NIOSH V2 hood would enable further research to be conducted.

The NIOSH V2 prototype demonstrated different inlet and face velocities in the laboratory evaluation but was unable to be used during the simulated work conditions. It can be assumed that the NIOSH V2 prototype may have also performed differently with regards to inlet and face velocities during the simulated work conditions.

The cleanout bucket and hose weight were measured for each 10-hole trial. This assumes that each hole drilled creates the same amount and particle size distribution of rock dust that is available for capture. Meteorological conditions can also vary the dust amount captured by creating cross-drafts that move material away from the LEV's capture zone.

Particle count measurements were inconsistent and influenced by environmental conditions. Due to the variable conditions, it is difficult to determine trends or differentiate measurement variations from changes to the LEV system or due to variable

environmental conditions. Future research efforts should aim to minimize the potential impact of environmental conditions by the use of barriers or enclosures.

Based on the measured sound levels, hearing protection should be worn during drilling operations. Due to the transient nature of drilling activities, the installation of permanent noise reduction barriers is not feasible. Increasing the distance between the air compressor and the drill may also reduce noise exposure. Remote control operation of the drill would also allow for increased distance between the operator and the noise generating devices.

It is important to note that measured drilling operations were intermittent during the day and not as constant as those observed during construction activities. Collection of noise dosimetry data over the course of one day with intermittent exposure is a major limitation for extrapolating the exposure to other workplaces. Therefore, further noise exposure characterization is needed.

4.5 Conclusion

This study evaluated potential changes to a dowel drill LEV system to reduce previously identified performance and operation problems associated with duct clogging and filtration system maintenance. Changes such as using the NIOSH prototype hood, substituting a smooth bore hose, and the addition of a cyclone decreased indicators of clogging and prevented more rock dust material from reaching the filtration system. The NIOSH prototype hood and smooth bore hose reduce material within the hose by as much as 6 times relative to the manufacturer's configuration per 10 holes drilled. We

observed a greater than 95% reduction in collected dust reaching the filtration system by the cyclone addition. Recommended, minimal cost changes to the dowel drill LEV system can have an impact on LEV performance prolonging service time between maintenance, increasing filter life, and maintaining transport velocities to reduce respirable crystalline exposures.

References

ACGIH. 2016. Industrial ventilation: a manual of recommended practice. American Conference of Governmental and Industrial Hygenists: Cincinnati, OH.

Bahrami, A., F. Ghorbani, H. Mahjub, F. Golbabei, and M. Aliabadi. 2009. Application of traditional cyclone with spray scrubber to remove airborne silica particles emitted from stone-crushing factories. Ind Health, 47: 436-42.

Burgess, William A., Michael J. Ellenbecker, and Robert D. Treitman. 2004. Ventilation for control of the work environment. Wiley-Interscience: Hoboken, N.J.

Cheremisinoff, Paul N. 1993. Air pollution control and design for industry. M. Dekker: New York.

Echt, A. 2012a. Respirable dust exposures of workers dowel drilling concrete pavement and evaluation of control measures. Dissertation, University of Kentucky.

Echt, A., and K. Mead. 2016a. Evaluation of a Dust Control for a Small Slab-Riding Dowel Drill for Concrete Pavement. Ann Occup Hyg, 60: 519-24.

Echt, A. S., W. T. Sanderson, K. R. Mead, H. Amy Feng, D. R. Farwick. 2016. Effective Dust Control Systems on Concrete Dowel Drilling Machinery. J Occup Environ Hyg: Apr 13:0 [Epub ahead of print].

Echt, A., K. Sieber, E. Jones, D. Schill, D. Lefkowitz, J. Sugar, and K. Hoffner. 2003. Control of respirable dust and crystalline silica from breaking concrete with a jackhammer. Appl Occup Environ Hyg, 18: 491-5.

Echt, A.; Mead, K; Feng, H; Farwick, D. 2011a. Control Technology for Dowel-Pin Drilling in Concrete Pavement at Minnich Manufacturing. In-depth survey report by NIOSH, 35. Cincinnati, OH.

Echt, A; Hirst, D; Kovein, R. 2011b. Control Technology for Dowel Drilling in Concrete at the Springfield-Branson National Airport. In-depth survey report by NIOSH, 46. Cincinnati, OH.

Echt, A; Kovein, R; Lambright, J. 2012b. Control Technology for Dowel Drilling in Concrete at the Hartsfield-Jackson Atlanta International Airport. In-depth survey report by Department of Health and Human Services Centers for Disease Control and Prevention National Institute for Occupational Safety and Health. Cincinnati, OH.

Echt, A; Mead, K; Farwick, D; Feng H. 2008. In-Depth Survey: Preliminary Evaluation of Dust Emissions Control Technology for Dowel-Pin Drilling at Minnich Manufacturing. In-depth survey report by NIOSH, 29. Cincinnati, OH.

Echt, A; Mead, K; Feng, H; Farwick, D. 2011c. Control Technology for Dowel-Pin Drilling in Concrete Pavement at EZ Drill. In-depth survey report by NIOSH, 35. Cincinnati, OH.

Echt, A; Mead, K; Kovein. 2011d. Control Technology for Dowel Drilling in Concrete at Columbus Municipal Airport. In-depth survey report by NIOSH, 33. Cincinnati, OH.

Echt A, Mead K, Kovein R. 2013. Control Technology for Dowel Drilling in Concrete at Laborers International Union of North America Local 172. In-depth survey report by NIOSH, 28. Cincinnati, OH.

Heumann, William L. 1997. Industrial air pollution control systems (McGraw-Hill: New York).

Leith, David, and Dilip Mehta. 1973. Cyclone Performance and Design. Atmospheric Environment Pergamon, 7: 527-49.

Schifftner, Kenneth C. 2002. Air pollution control equipment selection guide (Lewis Publishers: Boca Raton, Fla.).

Systems, Oneida Air. 2016. Industrial Steel Dust Deputy DIY Cyclone Separator. Accessed May 3. http://www.oneida-air.com/category.asp?Id={CC6B6F2A-E3D7-4F18-A53C-B5C357DFE131}.

CHAPTER V

Conclusion

5.1 Summary of the research

The present research evaluated novel designs in local exhaust ventilation (LEV) for a concrete dowel drill. In occupational safety and health practice, LEV is a commonly used engineering control to reduce or capture airborne contaminants, normally hazardous substances, which are generated in the form of dust, fume, mist, vapor, etc. In the hierarchy of occupational safety and health controls, engineering controls, such as LEV, are one of the most preferred methods of reducing exposures only after elimination or substitution of a less hazardous material or practice. It can also be used to capture and recycle materials to decrease economic costs and increase production yields. LEV systems have been utilized in a wide variety of industries from healthcare and research laboratories to the construction and mining industries.

A comparison between traditional LEV hood designs and a novel approach was examined in Chapter II. The traditional hood design outperformed the novel approach when examining average capture velocities from all distances. However, when examining individual capture velocities for individual distance measurements the novel design outperformed the traditional designs in a small number of trials. For example, the novel design performed best in unflanged distances further than one duct diameter away from the hood face. Further examination of the individual capture velocity measurement showed that the novel design struggled to achieve elevated velocities

near the hood face. The novel design's inconsistent performance also does not allow for modeling to predict future ventilation designs that may want to incorporate the novel design. This study was the first to explore placing a small, high speed duct inside of a larger lower speed duct to artificially increase capture velocity without increasing fan power and electrical consumption. However, the small duct never obtained a higher speed (at the face) than the main duct.

Chapters III and IV moved towards designing and evaluating concrete dowel drilling LEV systems to reduce potential respirable crystalline silica. On March 24, 2016, the Occupational Safety and Health Administration (OSHA) released revisions to the respirable crystalline silica permissible exposure limit (PEL) (OSHA 2016a, 2016b). The final rule also stated that engineering controls (such as the dowel drill LEV system evaluated in Chapters III and IV) shall be utilized to reduce exposures by June 23, 2021 (OSHA 2016b).

Chapter III described a laboratory evaluation of four LEV hood designs including two NIOSH prototypes, the dowel drill manufacturer's hood, and a commercially available hood that had been previously studied as an option for controlling rock dust from pneumatic rock drills. The current laboratory evaluation found that both NIOSH prototypes hood to be markedly more efficient in terms of coefficient of entry, a measure of hood efficiency. The NIOSH prototype designs reduced sharp airflow turns and created a smoother transition from the hood face to the LEV ductwork. The more efficient hood designs also increased transport velocities which should decrease clogging during drilling operations, a previously identified problem with the current manufacturer's LEV system.

Chapter IV describes LEV system changes based upon the laboratory hood evaluation in Chapter III and new proposed changes to the current manufacturer's LEV system. Chapter III identified NIOSH V2 as the most promising hood design. However, the 3D-printed plastic prototype was not durable enough for the rigors of the simulated workplace drilling. NIOSH V2 contained an extension that allowed for better airflow from the hood into the LEV ductwork. NIOSH V1, which tested similarly to NIOSH V2, does not contain the extension and the durability tested much better than NIOSH V2 during test drills. Therefore, NOISH V1 was substituted for NIOSH V2 during the simulated work conditions. Novel metrics (hood face velocity, hood inlet velocity, hose weight, and cleanout weight) for LEV performance were also evaluated during this study.

The NIOSH prototype hood, smoothbore hose, and cyclone combination was the best performing test scenario for hose and cleanout weight. The NIOSH prototype was designed to lower face and inlet velocities in order for larger particles to fall out of the airstream to further reduce clogging in the duct and prevent filter cake build-up. The NIOSH prototype did lower inlet and face velocities while maintaining overall capture velocity performance. The impact of the smoothbore hose and cyclone significantly impacted the performance of the LEV system and potentially increasing the amount of time between maintenance activities.

5.2 Research limitations and further research needs

The novel LEV hood design discussed in Chapter II evaluated the novel design against traditional hood designs. However, the results were inconsistent and do not

allow for modeling to predict future design performance. Duct materials with lower surface roughness factors (galvanized metal, aluminum, etc.) should be used in future research to increase inner duct velocities. Smoother duct transitions and elbow connections would also reduce friction loss and improve velocity results. The ratio between outer and inner duct and impact on airflow and capture velocities would also be of research interest for optimization.

At the conclusion of the first round of the traditional and novel design evaluation the University of Michigan wind tunnel was dismantled and moved to provide additional space for unrelated research. The dismantling prevented any further trials or subsequent evaluations of changes to the novel design in the same laboratory setting as previously evaluated.

The present dowel drill LEV system work, while useful for its comparative intent, may be limited by the laboratory evaluation and simulated work conditions and how they related to actual workplace conditions and usage. Work practices, equipment condition, maintenance, and environmental conditions can all play a large role in the performance of the dowel drill LEV system. The controlled laboratory environmental and limited testing during simulated work conditions will not replicate all conditions encountered during workplace operation.

The laboratory evaluation discussed in Chapter III used a different vacuum source than is used by the dowel drill LEV system. While the desired transport velocities were generated, the dowel drill eductor system is capable of creating transport velocities higher than evaluated in Chapter III.

The laboratory evaluation was also unable to simulate the dowel drill “jumping” away from the concrete substrate during drilling. The large force needed to pneumatically drill the hole would push the drill bit and subsequently the LEV hood away from the concrete surface. This “jumping” could create turbulent airflow and allow for cross-draft manipulation due to any cross winds.

The current study also only used the NIOSH V1 prototype hood during simulated work conditions even though the laboratory evaluation indicated the NIOSH V2 prototype hood may perform better in the LEV system. Future research should include a durable NIOSH V2 prototype model constructed with the lowest surface roughness coefficient possible.

Chapter IV utilized a commercially available cyclone as a pre-separator in the dowel drill LEV system. A customized cyclone could be designed in order to maximize particle collection and overall efficiency of the LEV system.

Due to an inexperienced operator, variations in trial time, short trials (10 holes drilled), and uncontrollable environmental conditions, results may differ in other studies. Future research should include experienced operators using the equipment with proposed dowel drill LEV system changes for extended periods of time to further evaluate the efficacy of the control.

5.3 Impact/ Innovation

Ventilation and LEV are commonly used engineering controls to capture airborne contaminants, normally hazardous substances, which are generated in the form of dust,

fume, mist, or vapor. Ventilation and LEV are essential tools for occupational safety and health professionals to reduce potential worker exposures. It can also be used to capture and recycle materials to decrease economic costs and increase production yields. Various ventilation and LEV systems have been utilized in a wide variety of industries from healthcare and research laboratories to the construction and mining industries.

Chapter II describes a novel LEV hood design that is not previously described in the literature. The design aimed at increasing capture velocity, and therefore system efficiency, without increasing fan power or electrical consumption. While the novel design did not have overwhelming success, the research indicated that further research should be conducted to modify the novel design in order to achieve the stated goals above.

Chapters III and IV describe efforts to improve the LEV system of a concrete dowel drill to increase the system's efficiency and performance. While the recommended changes are not novel in terms of use in other ventilation controls, their application to the current dowel drill LEV system design is new. These increases in system efficiency and performance will lead to reduction in respirable crystalline silica exposures. In the United States alone, the new OSHA PEL final ruling on respirable crystalline silica estimates that 2.3 million workers and approximately 676,000 in construction, general industry, and maritime workplaces will be impacted (OSHA 2016b). The final rule specifically mandates engineering controls such as ventilation and LEV systems to effectively control respirable crystalline silica exposures. This reflects

the hierarchy of control approach that recognizes that silica exposures cannot be substituted out of these workplaces and the next best approach is engineering controls.

Economically, the recommended changes are a small fraction of the overall dowel drill cost. The dowel drill was purchased by NIOSH for approximately $14,000 in 2012. In 2016, the recommended changes would cost approximately $200 per unit (smooth bore hose and commercially available cyclone). The $200 increase represents a 1.4% increase in per unit cost (without taking into the consideration of the current corrugated hose cost).

5.4 Moving forward

Significant changes to the dowel drill LEV system are recommended based upon the results of the present study. Future research should evaluate any changes made to the LEV system to ensure that respirable crystalline silica are still controlled to acceptable concentrations. Future research should also address the limitations discussed here.

For occupational safety and health, the hierarchy of controls dictates that elimination or substitution be the first step in addressing exposures with adverse health or environmental effects. However, respirable crystalline silica is inherent in many construction processes, including concrete dowel drilling, and therefore cannot be substituted or eliminated. The next hierarchy of control is engineering controls. Engineering controls have a long and successful history in controlling occupational exposure, but only when successfully designed, installed, operated, and maintained.

References

OSHA. 2016a. Occupational Exposure to Respirable Crystalline Silica. OSHA, 16285-890. Washington, D.C.

OSHA. 2016b. OSHA's Final Rule to Protect Workers from Exposure to Respirable Crystalline Silica. Accessed May 5, 2016. https://www.osha.gov/silica/.

Figures

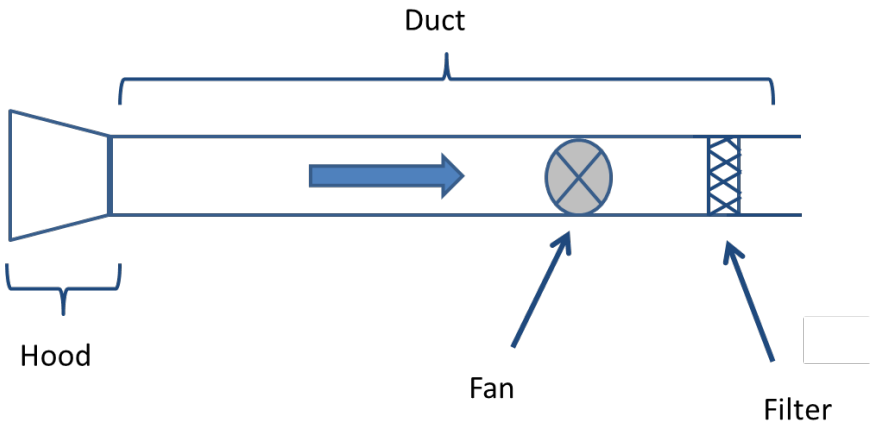

Figure 1.1 Basic four components of LEV system

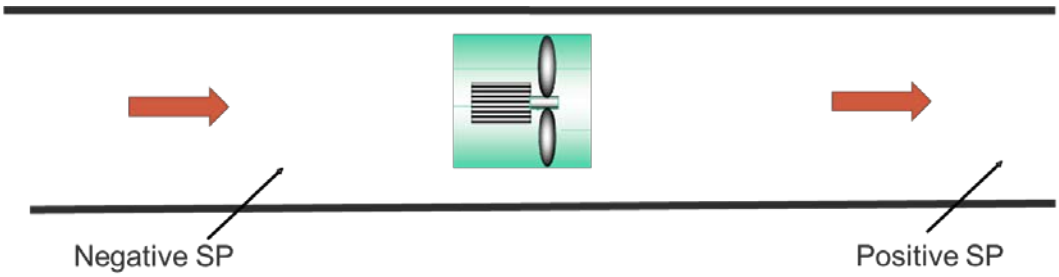

Figure 1.2 Relationship between static pressure, fan, and measurement location

Figure 2.1 Unflanged traditional LEV inlet design (Traditional)

FIGURE III:3-6. EFFECTIVE FLANGE WIDTH (W)

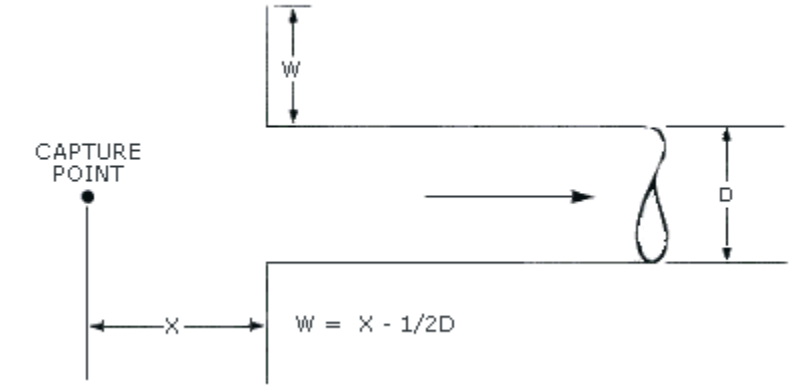

Figure 2.2 Effective flange width figure from OSHA Technical Manual Section III: Chapter 3

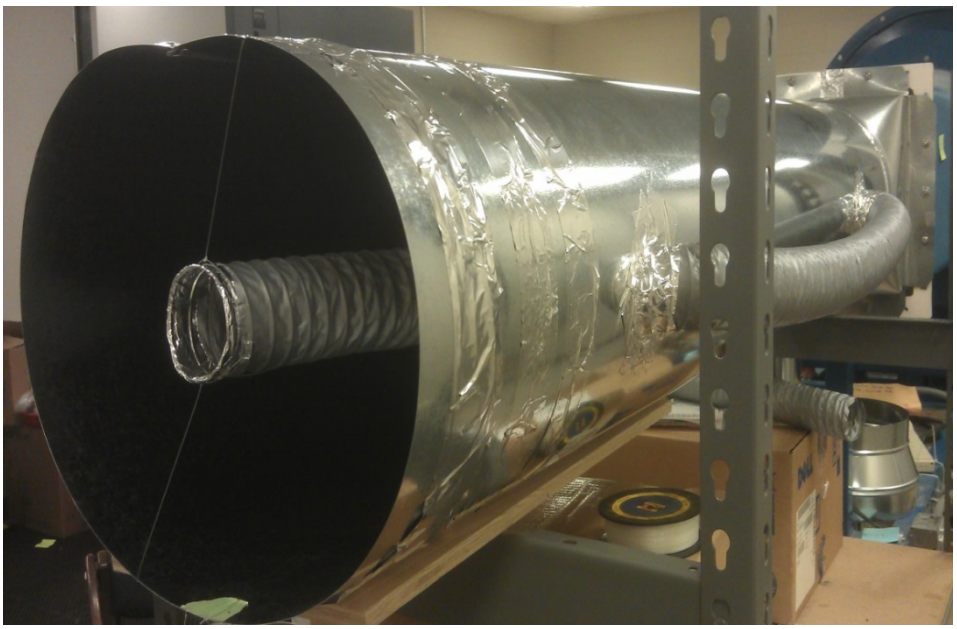

Figure 2.3 Unflanged novel design 1 (ND1)

Figure 2.4 Flanged novel design 1 (ND1)

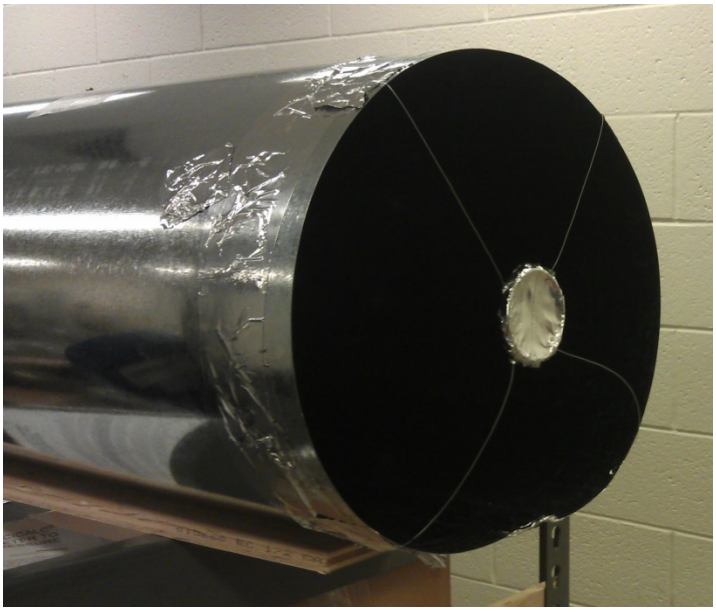

Figure 2.5 Unflanged novel design 3 (ND3)

Figure 2.6 Flanged novel design 4 (ND4)

Figure 3.1 Minnich A-1C Single Drill, On Slab Unit with optional dust collection system

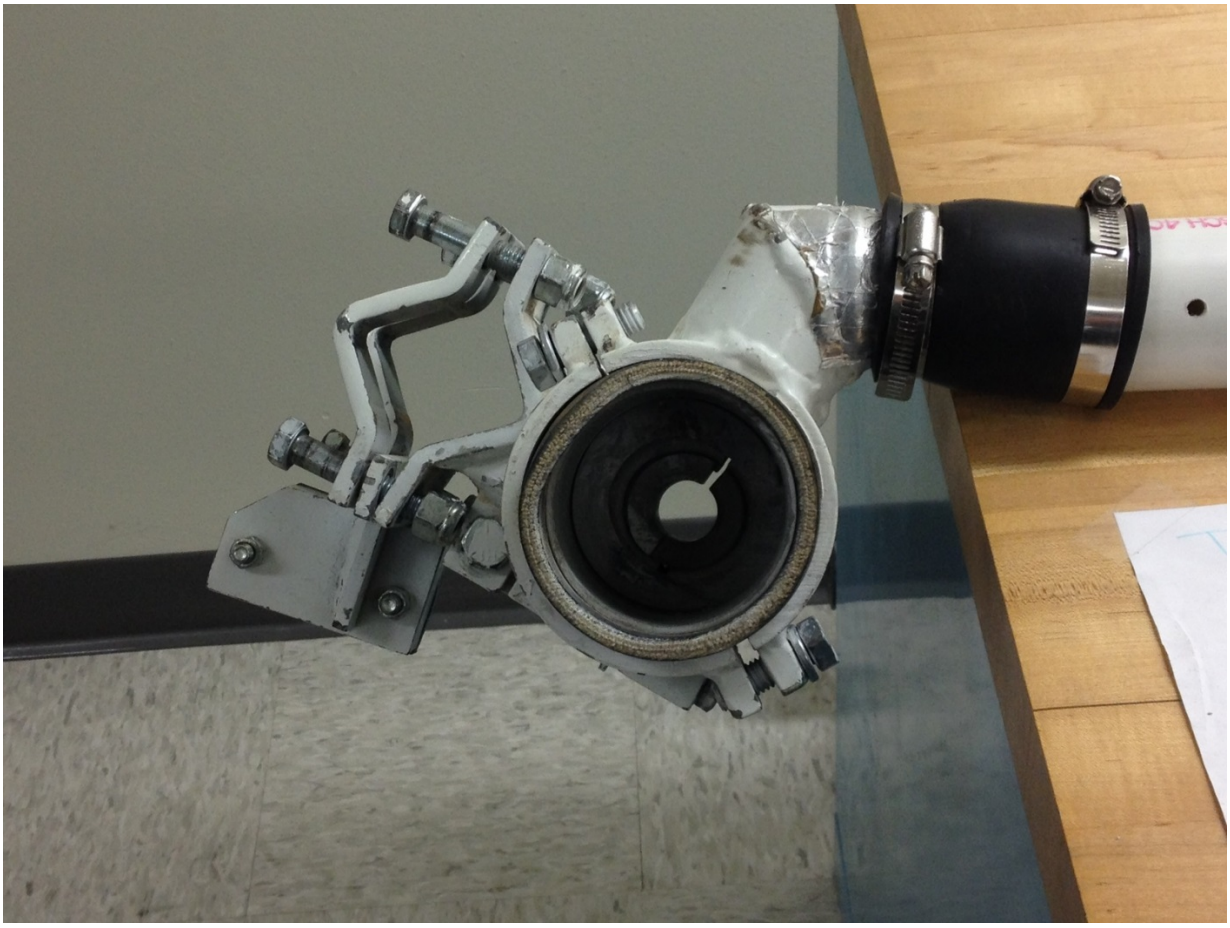

Figure 3.2 Manufacturer hood

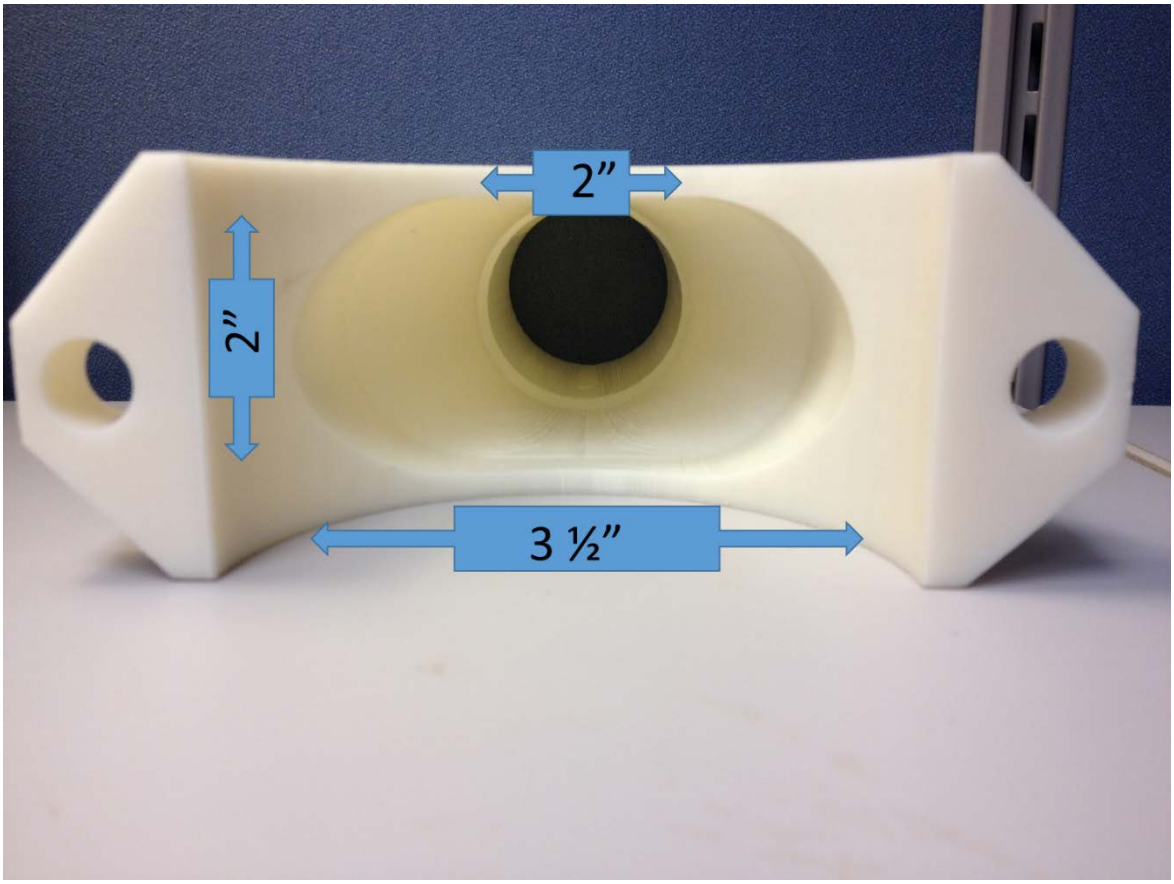

Figure 3.3 NIOSH prototype dimensions

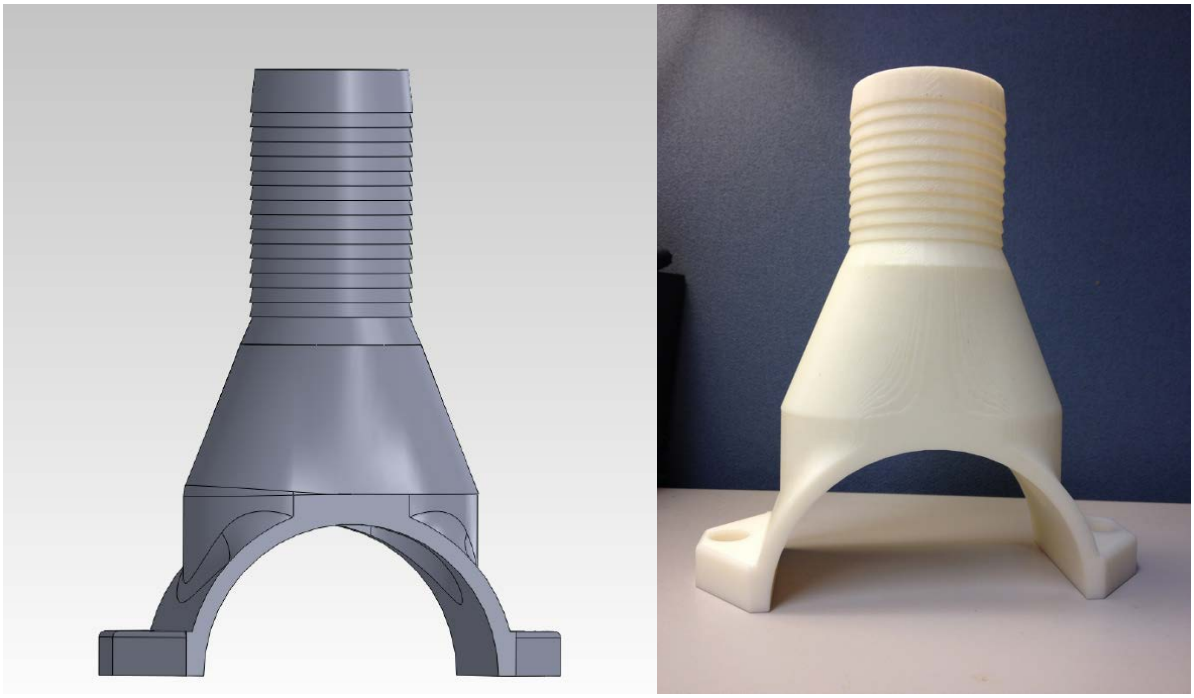

Figure 3.4 The NIOSH simple hood 3-D software model (left) and the printed model (right)

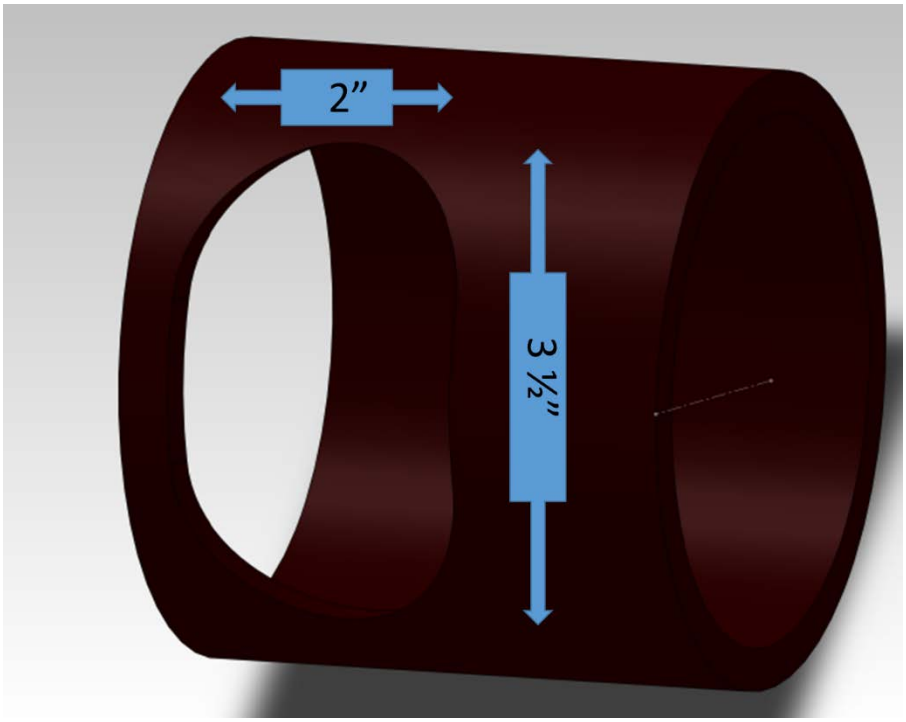

Figure 3.5 The 3-D software model with widened “rubber” inlay

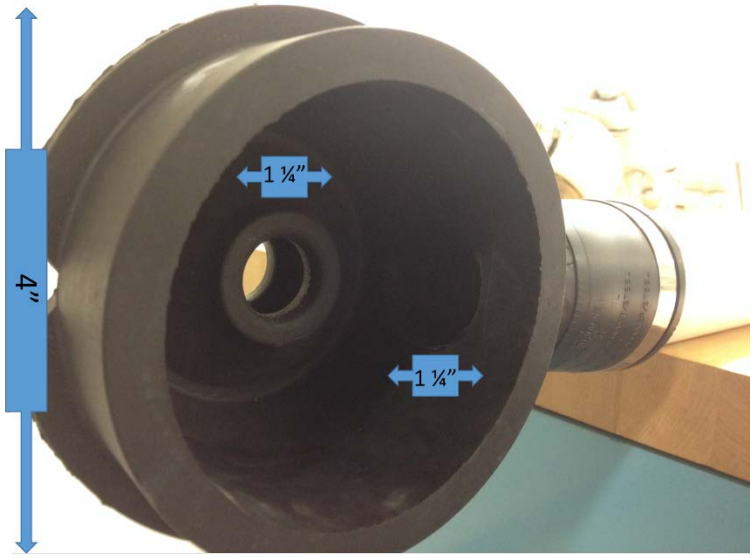

Figure 3.6 DustControl® pneumatic rock drill hood dimensions

Figure 3.7 Minnich and NIOSH prototype simple hoods after removal from enclosing housing

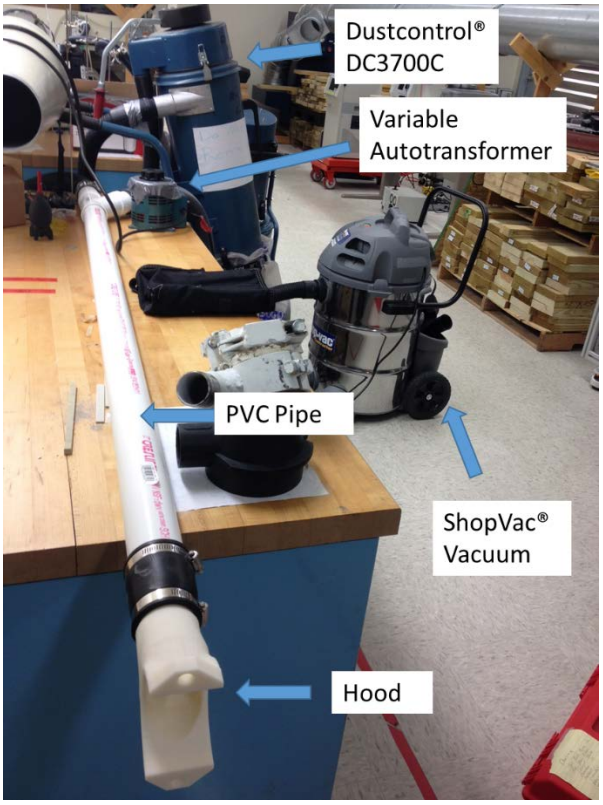

Figure 3.8 Laboratory setup for evaluation of hood performance

Figure 3.9 Inlet velocity measurement location on the DustControl® pneumatic rock drill hood

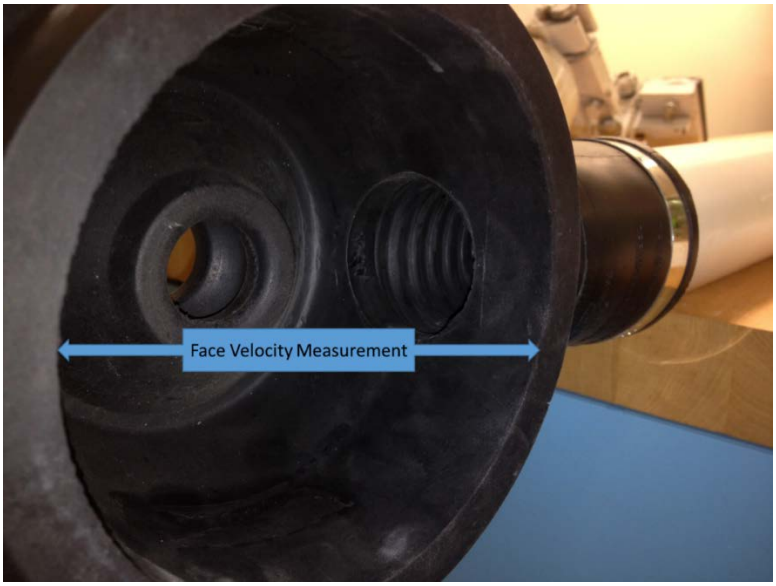

Figure 3.10 Face velocity measurement location on the DustControl® pneumatic rock drill hood

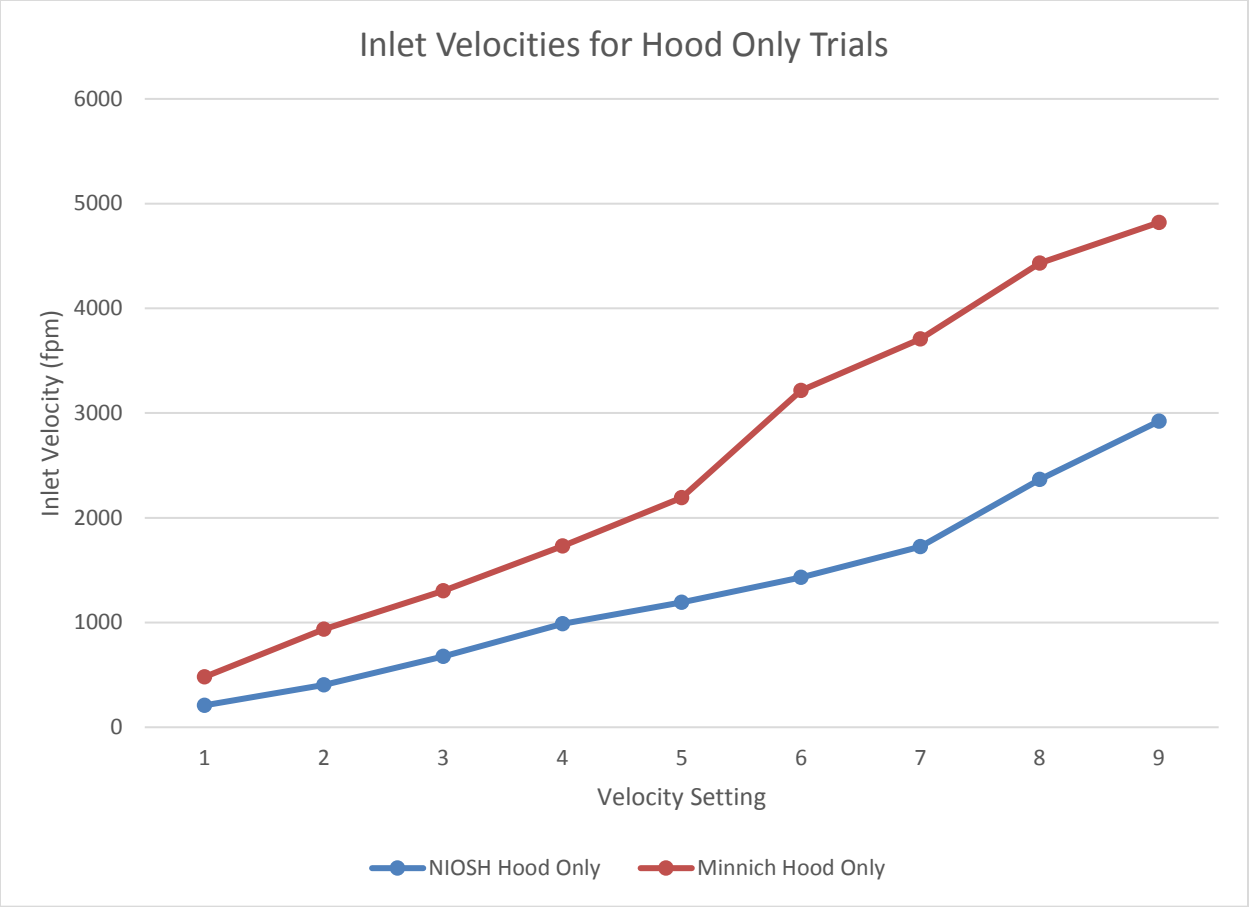

Figure 3.11 Inlet velocities for hood only trials

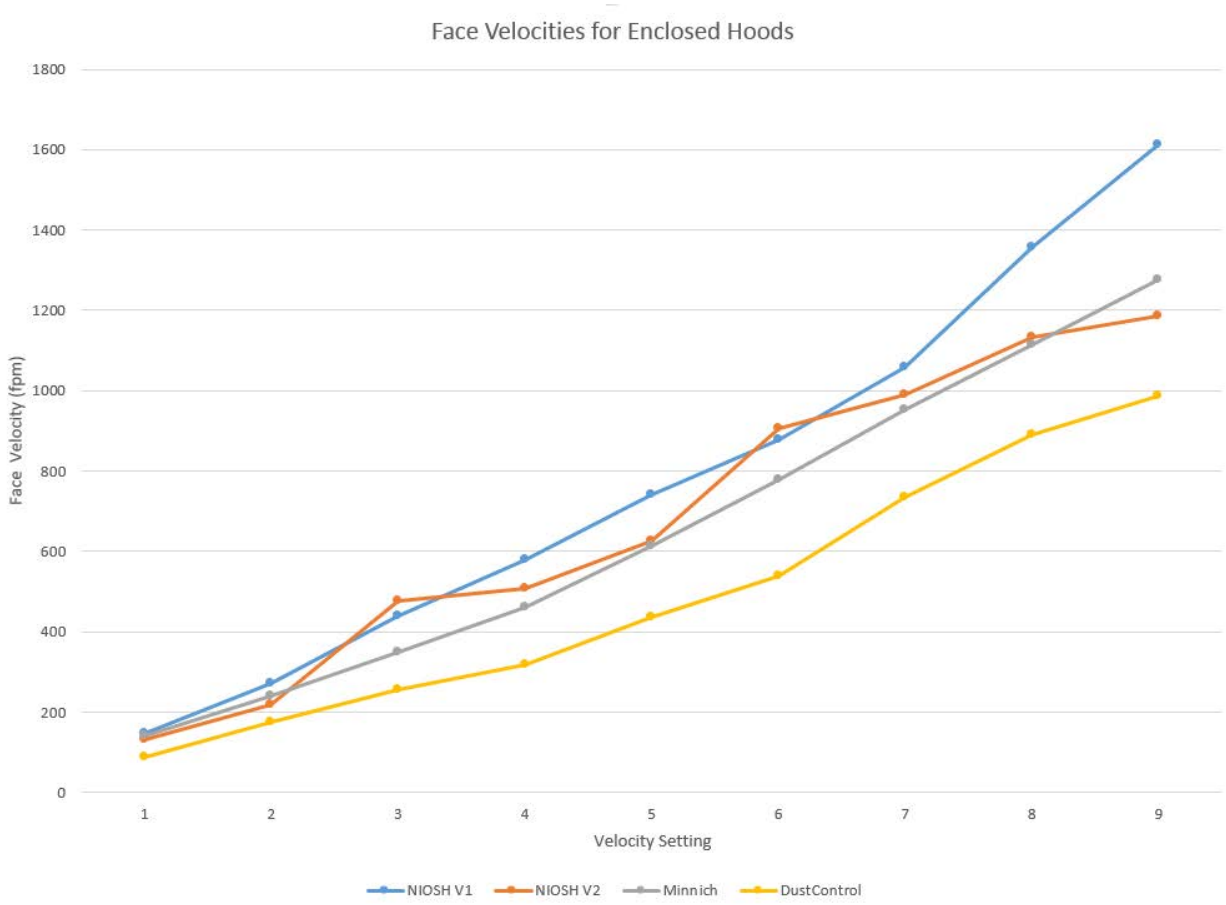

Figure 3.12 Face velocities for enclosed hood trials

Figure 4.1 Proximity of the drill operator to the dowel drill and the air compressor

Figure 4.2 Raised concrete platform with removable concrete slabs

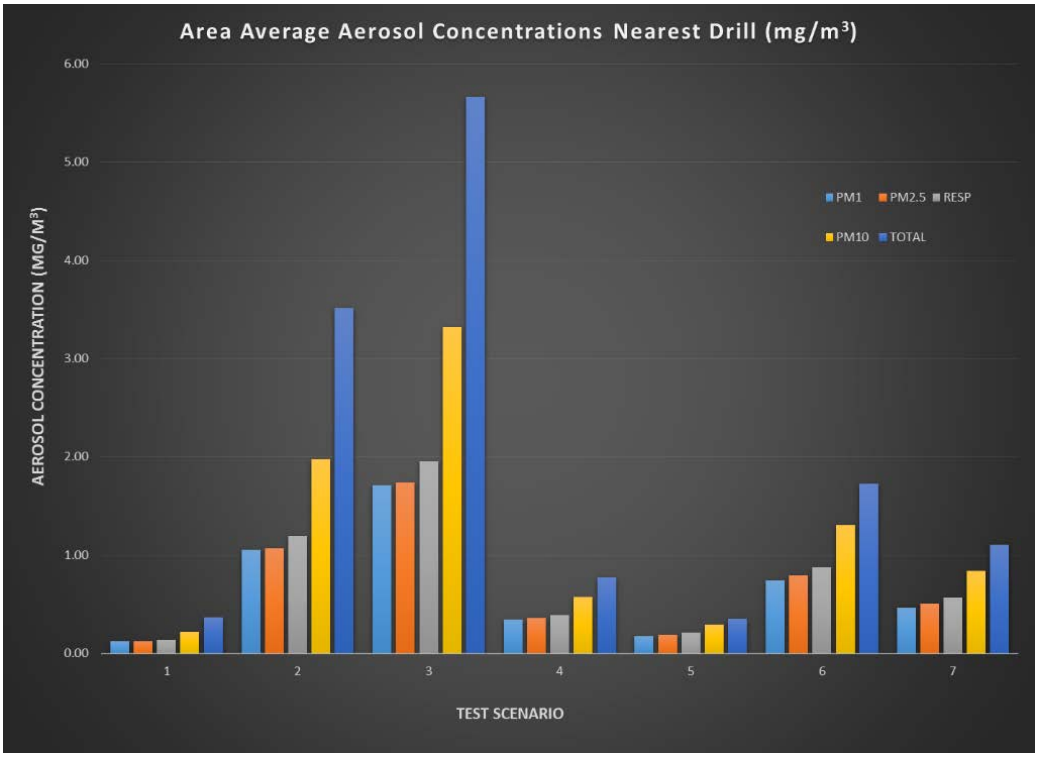

Figure 4.3 Area average aerosol concentrations nearest drill

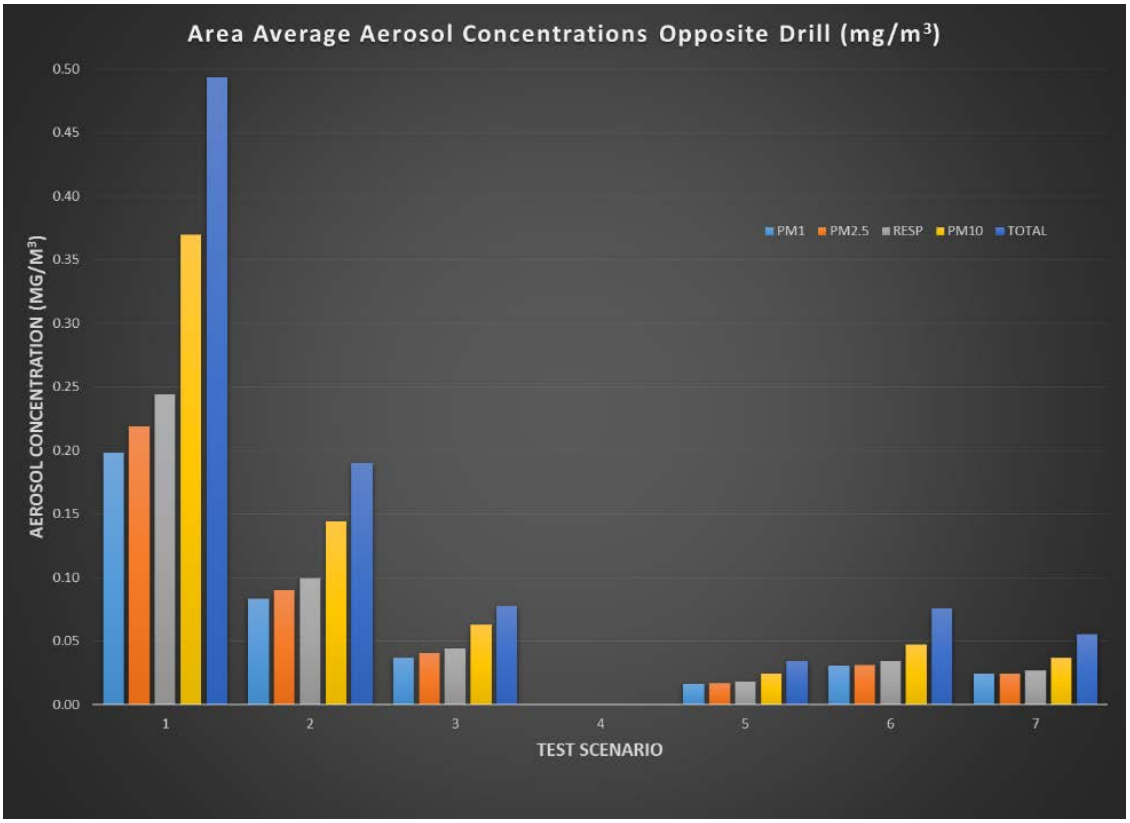

Figure 4.4 Area average aerosol concentrations opposite drill

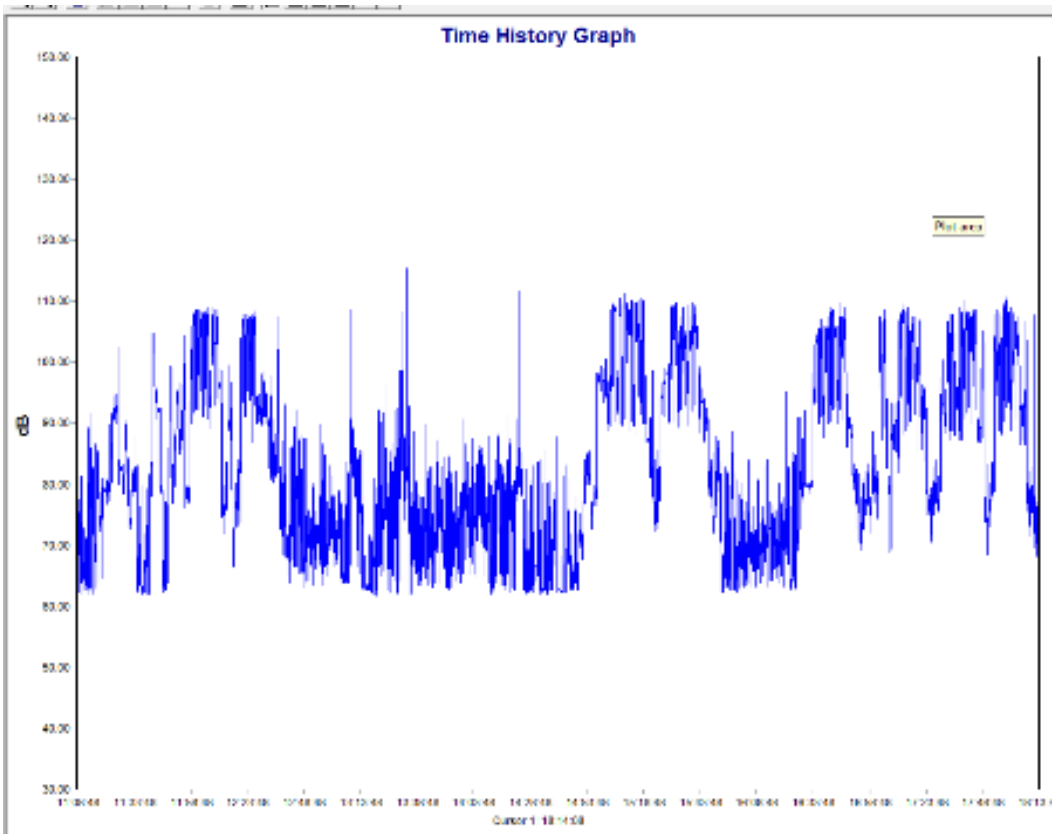

Figure 4.5 Noise dosimeter for Day 2 drilling

Tables

Table 1.1 Pitot traverse example (calculated df = 1)

		Horizontal Insertion		Vertical Insertion	
Traverse Point	Fraction Duct Diameter	VP (“w.g.)	V (fpm)	VP (“w.g.)	V (fpm)
1	0.043	0.10	1266	0.11	1328
2	0.290	0.13	1444	0.15	1551
3	0.710	0.15	1551	0.16	1602
4	0.957	0.12	1387	0.11	1328
	Average		1412		1452

Duct Diameter: 4 inches
Area (ft^2): 0.0873 ft^2
Average velocity (fpm): 1,432
Q (cfm): 125

Table 1.2 Common industrial contaminants and required transport velocity for industrial ventilation

Contaminant	Transport Velocity (fpm)
Vapors/Gas	1,000 – 2,000
Fumes	2,000 – 2,500
Fine Dust	2,500 – 3,000
Dry Dust	3,000 – 3,500
Industrial Dust	3,500 – 4,000
Heavy Dusts	4,000 – 4,500
Heavy or Moist Dusts	4,500 or greater

Table adapted from ACGIH Industrial Ventilation Manual Table 5-1 (ACGIH 2016)

Table 1.3 Surface roughness design values for selected ducts

Duct Material	Surface Roughness (k) per feet
Galvanized Metal	0.00055
Aluminum	0.00015
Flexible duct (wire exposed)	0.01005
Flexible duct (covered wire)	0.00301

Table 2.1 Specific Aim 1 Variables and Test Conditions for Fixed LEV

Variable	Test Conditions
12” Round Duct	Unflanged Flanged
Design	Traditional Novel Designs 1-4
Duct Face Velocity	Vapors, Gases, Fumes (V_{LO}) • 1,500 fpm (V_{LO1}) • 2,000 fpm (V_{LO2}) Average Industrial Dust (V_{HI}) • 3,000 fpm (V_{HI3}) • 4,000 fpm (V_{HI4})
Centerline Capture Velocity Measurements	9 Total Measurements Face to 24” (3” increments)

Table 2.2 Wind Tunnel Fan Speed Setting and Corresponding Velocity

Fan Speed (Hz)	Face Velocity (fpm)	Category
31.0	1,500	V_{LO1}
36.6	2,000	V_{LO2}
48.0	3,000	V_{HI3}
58.5	4,000	V_{HI4}

Table 2.3 Centerline Velocity Measurement Position, Distance, and Duct Diameter Percentage

Position	Measurement distance from hood face (in.)	Duct Diameter Percentage
1	0	0
2	3	25
3	6	50
4	9	75
5	12	100
6	15	125
7	18	150
8	21	175
9	24	200

Table 2.4 Average Capture Velocity from Face-24". All velocities are in feet per minute (fpm)

FS	Traditional		ND1		ND2		ND3		ND4	
	Unflanged	Flanged	Unflanged	Flanged	Unflanged	Flanged	Unflanged	Flanged	Unflanged	Flanged
V_{LO1}	331	374	285	307	244	246	180	255	224	244
V_{LO2}	443	490	363	417	313	321	235	264	297	337
V_{HI3}	670	716	544	618	471	491	379	390	482	512
V_{HI4}	887	953	715	813	650	661	530	521	656	711

Table 2.5 Measured Centerline Capture Velocity for Low Fan Speeds*

		Traditional						ND1 Unflanged					
FS	D	AVG	Min	Max	SD	95 CI Lower	95 CI Upper	AVG	Min	Max	SD	95 CI Lower	95 CI Upper
V_{LO1}	Face	1512	1500	1520	8.5	1502	1521	871	870	872	0.9	870	872
	3	682	675	690	6.2	675	689	742	739	746	2.9	739	745
	6	343	340	346	2.5	341	346	379	375	383	3.3	375	382
	9	169	168	170	0.9	168	170	236	230	243	5.3	230	242
	12	110	105	115	4.1	105	115	144	142	146	1.7	142	146
	15	76	72	81	3.9	71	80	81	78	85	3.1	77	84
	18	41	38	45	2.9	38	44	56	54	59	2.2	54	58
	21	32	29	36	2.9	29	35	23	21	25	1.7	21	25
	24	13	11	14	1.2	11	14	36	32	39	2.9	33	39
V_{LO2}	Face	2002	1998	2006	3.3	1998	2006	1141	1138	1144	2.5	1138	1143
	3	968	962	972	4.5	963	973	967	964	969	2.1	964	969
	6	441	438	446	3.4	437	445	472	470	474	1.7	470	474
	9	224	222	226	1.7	222	226	272	269	274	2.2	270	274
	12	129	126	131	2.2	127	131	175	172	179	2.9	172	179
	15	102	95	107	5.0	96	107	103	102	105	1.2	102	105
	18	55	53	56	1.4	53	57	98	96	100	1.7	96	100
	21	41	36	44	3.4	37	45	29	28	31	1.2	28	31
	24	20	17	23	2.5	18	23	13	11	14	1.2	11	14

*Highlighted capture velocities indicate where the ND system outperformed the traditional LEV system

D = Measurement distance from hood face

AVG = mean capture velocity (fpm)

Min = Minimum capture velocity (fpm)

Max = Maximum capture velocity (fpm)

SD = Standard deviation

95 CI = Upper and lower 95% confidence intervals

Table 2.6 Measured Centerline Capture Velocity for High*

		Traditional						ND 1 Unflanged					
FS	D	AVG	Min	Max	SD	95 CI Lower	95 CI Upper	AVG	Min	Max	SD	95 CI Lower	95 CI Upper
V_{HI3}	Face	3001	2993	3010	7.0	2993	3009	1891	1888	1893	2.4	1889	1894
	3	1590	1579	1607	12.4	1576	1604	1465	1461	1468	3.1	1462	1469
	6	665	661	670	3.7	661	669	656	652	658	2.8	653	659
	9	314	300	328	11.4	301	327	335	332	337	2.1	332	337
	12	185	176	190	6.2	178	192	209	207	211	1.7	207	211
	15	127	121	131	4.2	122	131	178	172	184	4.9	173	184
	18	70	67	74	2.9	67	73	86	85	87	0.8	85	87
	21	51	48	54	2.4	48	54	50	45	55	4.1	45	54
	24	28	24	30	2.6	25	31	28	24	31	2.9	25	31
V_{HI4}	Face	4006	3996	4014	7.5	3998	4014	2693	2684	2699	6.5	2686	2700
	3	1964	1960	1972	5.4	1958	1970	1835	1834	1835	0.5	1834	1835
	6	885	884	886	0.8	884	886	801	796	804	3.6	797	805
	9	442	435	450	6.2	435	449	426	424	427	1.2	424	427
	12	255	246	264	7.4	247	264	266	263	271	3.6	262	270
	15	182	180	184	1.7	180	184	166	164	169	2.1	164	169
	18	115	111	119	3.3	112	119	120	118	122	1.7	118	122
	21	83	79	86	2.9	79	86	71	68	75	2.9	68	74
	24	52	49	58	4.0	48	57	54	52	55	1.2	52	55

*Highlighted capture velocities indicate where the ND system outperformed the traditional LEV system

FS = Fan speed

D = Measurement distance from hood face

AVG = mean capture velocity (fpm)

Min = Minimum capture velocity (fpm)

Max = Maximum capture velocity (fpm)

SD = Standard deviation

95 CI = Upper and lower 95% confidence intervals

Table 2.7 Average Capture Velocity from 6-24". All velocities are in feet per minute (fpm)*

FS	Traditional		ND1		ND2		ND3		ND4	
	Unflanged	Flanged	Unflanged	Flanged	Unflanged	Flanged	Unflanged	Flanged	Unflanged	Flanged
V_{LO1}	112.0	133.7	136.5	118.0	107.3	117.8	104.4	125.7	115.9	129.1
V_{LO2}	144.6	177.6	166.1	158.6	137.9	153.9	133.2	157.3	141.1	164.2
V_{HI3}	205.7	248.2	220.2	226.3	194.8	226.0	192.7	224.0	216.2	241.7
V_{HI4}	287.7	343.2	271.9	307.0	263.9	298.5	262.3	304.6	287.1	321.4

*Highlighted capture velocities indicate where the ND system outperformed the traditional LEV hood design

Table 2.8 Average Capture Velocity from 15-24". All velocities are in feet per minute (fpm)*

FS	Traditional		ND1		ND2		ND3		ND4	
	Unflanged	Flanged	Unflanged	Flanged	Unflanged	Flanged	Unflanged	Flanged	Unflanged	Flanged
V_{LO1}	40.3	47.7	49.0	39.5	36.6	35.6	29.1	46.8	35.2	37.8
V_{LO2}	54.4	61.1	60.9	48.3	44.1	51.3	40.3	61.8	38.0	48.1
V_{HI3}	68.8	77.0	85.5	71.2	59.8	75.5	54.3	74.2	64.8	75.1
V_{HI4}	108.0	120.8	102.7	110.3	90.5	105.0	89.5	116.5	95.7	107.8

*Highlighted capture velocities indicate where the ND system outperformed the traditional LEV system

Table 2.9 Pitot Traverse Measurements and Calculated Flowrates Unflanged*

Fan Speed	Traditional			ND1			ND2			ND3			ND4		
	VP	TP	Q	VP	TP	Q	VP	TP	Q	VP	TP	Q	VP	TP	Q
V_{LO1}	0.11	-0.10	1047	0.12	-0.10	1067	0.08	-0.15	903	0.12	-0.11	1068	0.12	-0.10	1074
V_{LO2}	0.18	-0.19	1318	0.18	-0.18	1345	0.17	-0.22	1268	0.18	-0.20	1322	0.16	-0.20	1243
V_{HI3}	0.41	-0.42	1992	0.45	-0.39	2093	0.33	-0.51	1785	0.39	-0.48	1973	0.42	-0.40	2045
V_{HI4}	0.79	-0.60	2787	0.68	-0.74	2576	0.56	-0.91	2323	0.60	-0.80	2441	0.67	-0.72	2568

*Highlighted capture velocities indicate where the ND system outperformed the traditional LEV system

VP = Velocity Pressure (”w.g.)
TP = Total Pressure (”w.g.)
Q = Flowrate (cubic feet per minute)

Table 2.10 Pitot Traverse Measurements and Calculated Flowrates Flanged*

Fan Speed	Traditional			ND1			ND2			ND3			ND4		
	VP	TP	Q	VP	TP	Q	VP	TP	Q	VP	TP	Q	VP	TP	Q
V_{LO1}	0.13	-0.06	1119	0.14	-0.06	1153	0.10	-0.11	989	0.24	-0.04	1373	0.11	-0.07	1060
V_{LO2}	0.20	-0.13	1414	0.22	-0.13	1485	0.17	-0.19	1267	0.22	-0.14	1481	0.21	-0.13	1434
V_{HI3}	0.51	-0.23	2223	0.54	-0.22	2315	0.37	-0.43	1901	0.43	-0.36	2044	0.50	-0.25	2216
V_{HI4}	0.85	-0.41	2884	0.87	-0.43	2916	0.65	-0.70	2521	0.74	-0.59	2696	0.87	-0.40	2930

*Highlighted capture velocities indicate where the ND system outperformed the traditional LEV system

VP = Velocity Pressure (”w.g.)
TP = Total Pressure (”w.g.)
Q = Flowrate (cubic feet per minute)

Table 2.11 Hood entry loss (Ce) for all unflanged designs and fan speeds

Design	Fan Speed	Static Pressure Hood*†	Velocity Pressure*	Hood Entry Loss (Ce)	Average Hood Entry Loss
TRADITIONAL	V_{LO1}	0.22	0.11	0.72	0.71
	V_{LO2}	0.38	0.18	0.68	
	V_{HI3}	0.85	0.41	0.69	
	V_{HI4}	1.43	0.79	0.75	
ND1	V_{LO1}	0.22	0.12	0.74	0.73
	V_{LO2}	0.36	0.18	0.74	
	V_{HI3}	0.85	0.45	0.70	
	V_{HI4}	1.44	0.68	0.73	
ND2	V_{LO1}	0.24	0.08	0.58‡	0.62
	V_{LO2}	0.40	0.17	0.65	
	V_{HI3}	0.85	0.33	0.62	
	V_{HI4}	1.52	0.56	0.61	
ND3	V_{LO1}	0.23	0.12	0.72‡	0.68
	V_{LO2}	0.39	0.18	0.68	
	V_{HI3}	0.88	0.39	0.67	
	V_{HI4}	1.40	0.60	0.65	
ND4	V_{LO1}	0.22	0.12	0.74‡	0.69
	V_{LO2}	0.38	0.16	0.65‡	
	V_{HI3}	0.86	0.42	0.70	
	V_{HI4}	1.45	0.67	0.68	

*Units are inches of water (”w.g.)

† Absolute value

‡ Trial hood entry loss greater than ±5% of average hood entry loss

Table 2.12 Hood entry loss (Ce) for all flanged designs and fan speeds

Design	Fan Speed	Static Pressure Hood*†	Velocity Pressure*	Hood Entry Loss (Ce)	Average Hood Entry Loss
Traditional	V_{LO1}	0.19	0.13	0.82	0.81
	V_{LO2}	0.35	0.20	0.77	
	V_{HI3}	0.74	0.51	0.83	
	V_{HI4}	1.26	0.85	0.82	
ND1	V_{LO1}	0.20	0.14	0.84	0.82
	V_{LO2}	0.35	0.22	0.79	
	V_{HI3}	0.77	0.54	0.84	
	V_{HI4}	1.31	0.87	0.82	
ND2	V_{LO1}	0.22	0.10	0.67	0.67
	V_{LO2}	0.38	0.17	0.67	
	V_{HI3}	0.85	0.37	0.66	
	V_{HI4}	1.43	0.65	0.67	
ND3	V_{LO1}	0.23	0.12	0.72‡	0.68
	V_{LO2}	0.39	0.18	0.68	
	V_{HI3}	0.88	0.39	0.67	
	V_{HI4}	1.40	0.60	0.65	
ND4	V_{LO1}	0.19	0.11	0.75	0.79
	V_{LO2}	0.35	0.21	0.78	
	V_{HI3}	0.75	0.50	0.81	
	V_{HI4}	1.28	0.87	0.82	

*Units are inches of water (“w.g.)

† Absolute value

‡ Trial hood entry loss greater than ±5% of average hood entry loss

Table 3.1 Trial velocity settings and corresponding duct transport velocity and duct flowrate

Trial Velocity Setting	Duct Transport Velocity fpm	Duct Flowrate (Q) ACFM
1	500	11
2	1,000	22
3	1,500	33
4	2,000	44
5	2,500	55
6	3,000	66
7	3,500	77
8	4,000	88
9	4,500	99

Table 3.2 Hood Static Pressure*

Trial Velocity (fpm)	Hood Only		Enclosed			
	NIOSH	Minnich	NIOSH	NIOSH V2	Minnich	Dustcontrol®
500	0.03	0.04	0.04	0.03	0.03	0.04
1000	0.08	0.12	0.12	0.08	0.14	0.15
1500	0.18	0.28	0.26	0.20	0.31	0.35
2000	0.34	0.51	0.49	0.38	0.59	0.63
2500	0.55	0.82	0.81	0.54	1.00	1.03
3000	0.84	1.31	1.23	1.21	1.52	1.57
3500	1.19	1.86	1.76	1.48	2.22	2.26
4000	2.09	2.95	3.33	1.86	3.68	3.56
4500	2.64	3.76	4.02	2.24	4.66	4.47

*All hood static pressure measurements are in inches of water gauge (“w.g.)

Table 3.3 Hood Coefficient of Entry

Trial	Hood Only		Enclosed			
Velocity (fpm)	NIOSH	Minnich	NIOSH V1	NIOSH V2	Minnich	Dustcontrol®
500	0.75	0.67	0.62	0.62	0.68	0.34
1000	0.88	0.74	0.72	0.72	0.67	0.64
1500	0.89	0.70	0.73	0.73	0.67	0.64
2000	0.86	0.52	0.53	0.53	0.49	0.47
2500	0.84	0.69	0.69	0.69	0.63	0.61
3000	0.82	0.65	0.68	0.68	0.61	0.60
3500	0.80	0.64	0.66	0.66	0.59	0.58
4000	0.69	0.58	0.55	0.55	0.52	0.53
4500	0.69	0.58	0.56	0.56	0.53	0.53
Average Ce	0.81	0.64	0.64	0.64	0.59	0.58

Table 3.4 Inlet Velocities (fpm) by trial velocity setting

Trial Velocity (fpm)	Hood Only		Enclosed			
	NIOSH	Minnich	NIOSH V1	NIOSH V2	Minnich	Dustcontrol®
500	209	480	524	280	517	670
1000	405	935	1085	488	1135	1336
1500	676	1302	1585	1081	1635	1955
2000	986	1730	2153	1087	2155	2562
2500	1192	2190	2651	1385	2949	3408
3000	1431	3215	3275	1938	3440	4244
3500	1725	3707	3850	2141	4240	4983
4000	2366	4430	5284	2413	6358	6736
4500	2922	4820	5913	2684	7029	7680

Table 3.5 Hood face velocity (fpm)

Duct Trial Velocity (fpm)	NIOSH V1	NIOSH V2	Minnich	Dustcontrol®
500	148	133	140	89
1000	271	220	242	176
1500	439	477	351	255
2000	579	507	461	319
2500	740	627	615	437
3000	877	905	780	538
3500	1060	989	954	736
4000	1357	1132	1114	891
4500	1612	1185	1276	987

Table 3.6 Transport Velocity (fpm)

Trial	Hood Only		Enclosed			
Velocity (fpm)	NIOSH V1	Minnich	NIOSH V1	NIOSH V2	Minnich	Dustcontrol®
500	465	457	155	491	434	461
1000	950	852	410	950	801	749
1500	1452	1236	1129	1402	1181	1284
2000	2004	1747	1727	1869	1608	1710
2500	2436	2256	2317	2444	2074	1981
3000	3040	2809	2871	3405	2462	2583
3500	3698	3301	3295	3695	3004	2971
4000	4842	4251	4476	4045	3989	4154
4500	5243	4725	4858	4693	4370	4550

Table 4.1 Surface roughness design values for selected ducts

Duct Material	Surface Roughness (k) per feet
Galvanized Metal	0.00055
Aluminum	0.00015
Flexible duct (wire exposed)	0.01005
Flexible duct (covered wire)	0.00301

Table 4.2 Trial Scenarios and settings

	Manufacturer's Hood			NIOSH Prototype Hood		
Trial Scenario	Manufacturer's Hose	Smooth, Clear Hose	Dust Deputy	Manufacturer's Hose	Smooth, Clear Hose	Dust Deputy
1	X					
2		X				
3*		X	X			
4		X	X			
5					X	X
6					X	
7				X		
*Testing scenario 3 was disregarded due to improper cyclone installation						

Table 4.3 Face and inlet velocity measurements by trial

	Test Scenario	Face Velocity (fpm)			Inlet Velocity (fpm)		
		Before	After	Overall Average	Before	After	Overall Average
Manufacturers Hood	1	360	411	386	1661	1776	1719
	2	988	1007	998	4263	4328	4296
	3						
	4	813	735	774	3558	3449	3504
NIOSH Prototype Hood	5	610	668	639	2465	2843	2654
	6	555	459	507	1923	1733	1828
	7	442	548	495	2290	2329	2310

Table 4.4 Clean-Out and Cyclone Bucket Weight

Hood	Test Scenario	Manufacturer's Cleanout Gain (lbs)	Pre-separator Cleanout Gain (lbs)	Total Dust Collected (lbs)
Manufacturer	1 (Manufacturer Hose)	0.95	N/A	0.95
	2 (Smooth-bore Hose)	3.80	N/A	3.80
	4 (Smooth-bore hose and pre-separator)	0.18	3.88	4.06
NIOSH Prototype	5 (Smooth-bore hose and pre-separator)	0.05	6.25	6.30
	6 (Smooth-bore Hose)	2.88	N/A	2.88
	7 (Manufacturer Hose)	3.53	N/A	3.53

Table 4.5 Average difference between hose weight prior to drilling trial and after drilling trial

	Manufacturer's Hood		NIOSH Prototype Hood	
Test Scenario	Manufacturer's Hose Weight	Smooth, Clear Hose Weight	Manufacturer's Hose Weight	Smooth, Clear Hose Weight
1	0.3			
2		0.23		
6				0.05
7			0.10	
*Trials 5-10 utilized the dust deputy which did not allow for hose removal without significantly changing the system between trials				

Table 4.6 Average Area Aerosol Concentrations (mg/m^3)

	PM_1		$PM_{2.5}$		Respirable		PM_{10}		Total	
Test Scenario*	Near Drill	Opposite Drill	Near Drill	Opposite Drill	Near Drill	Opposite Drill	Near Drill	Opposite Drill	Near Drill	Opposite Drill
1	0.12	0.20	0.12	0.22	0.14	0.24	0.22	0.37	0.37	0.49
2	1.05	0.08	1.07	0.09	1.20	0.10	1.97	0.14	3.51	0.19
4	0.34	N/A	0.36	N/A	0.39	N/A	0.58	N/A	0.77	N/A
5	0.17	0.02	0.19	0.02	0.21	0.02	0.29	0.02	0.35	0.03
6	0.74	0.03	0.80	0.03	0.88	0.03	1.30	0.05	1.73	0.08
7	0.47	0.02	0.51	0.02	0.57	0.03	0.84	0.04	1.11	0.06

*Test scenario 3 was not included due to an improperly installed cyclone.

Table 4.7 Respirable Personal Breathing Zone Average Aerosol Concentrations (mg/m^3)

Test Scenario	Drill Operator	Drill Assist
1	Equipment Failure	0.02
2	Equipment Failure	0.01
4	0.02	0.01
5	0.02	0.01
6	0.07	Data Storage Exceeded
7	Data Storage Exceeded	Data Storage Exceeded

Table 4.8 Noise measurement results and occupational exposure limit criterion

Noise Measurement Criterion	Occupational Exposure Limit	Noise Measurement Results	
		TWA (dBA)	Dose (percent)
OSHA Action Level	85	94.8	196
OSHA PEL	90	94.5	186
NIOSH REL	85	99.0	2519

Appendix

Table A1. Test VLO1 with the following assumptions and t-test parameters: two sample, unequal variances, 2-tail, and normal distribution.

VLO1	Traditional		ND1		ND1		ND2		ND2		ND3		ND3		ND4		ND4	
	Unfla	Flan	Unfla	t-test	Flan	t-test	Unfla	t-test	Flan	t-test	Unfla	t-test	Flan	t-test	Unfla	t-test	Flan	t-test
Face	1500	1630	872	0.0001§	1083	0.0000§	812	0.0000§	760	0.0000§	238	0.0000§	237	0.0000§	454	0.0001§	517	0.0000§
	1520	1618	870		1078		803		755		240		235		460		512	
	1515	1627	870		1079		806		751		234		238		458		509	
3	675	803	741	0.0015†	859	0.0005§	630	0.0035†	626	0.0000§	648	0.0090†	681	0.1604	748	0.0004§	781	0.0278*
	690	808	746		851		634		633		645		674		754		786	
	680	795	739		860		636		640		651		795		741		784	
6	340	414	378	0.00040‡	342	0.0001‡	333	0.0223*	366	0.0005§	348	0.3669	323	0.1626	373	0.0092†	410	0.9070
	346	411	375		346		337		369		346		326		367		409	
	344	406	383		343		335		365		343		406		361		413	
9	170	212	236	0.0025†	206	0.0241*	174	0.0332*	206	0.1429	165	0.1376	217	0.7928	178	0.1346	203	0.0639
	170	223	230		197		175		208		161		221		182		211	
	168	217	243		204		179		215		168		217		171		207	
12	115	117	142	0.0027†	120	0.2767	97	0.0127*	108	0.0131*	104	0.1793	122	0.1018	122	0.0129*	134	0.0306*
	110	114	145		118		94		105		102		125		130		143	
	105	121	146		127		90		104		107		121		127		129	
15	81	68	79	0.2291	64	1.0000	70	0.0660	49	0.0358*	62	0.0100	82	0.2458	62	0.0172*	53	0.00670†
	72	67	85		65		65		54		57		82		65		58	
	74	64	78		70		66		59		57		64		58		57	
18	45	53	55	0.0057†	46	0.0333*	36	0.1882	39	0.0027†	29	0.0211*	57	0.4786	47	0.0736	51	0.1865
	38	55	54		43		38		33		30		60		47		46	
	40	49	59		46		37		36		34		49		49		49	

Table A1 (continued). Test VLO1 with the following assumptions and t-test parameters: two sample, unequal variances, 2-tail, and normal distribution.

21	36	41	24	0.0329*	26	0.0036†	29	0.1076	28	0.0013†	19	0.0056†	39	0.1635	18	0.0157*	33	0.0475*
	31	44	21		28		26		25		17		37		23		29	
	29	39	25		26		25		24		12		39		22		37	
24	11	31	37	0.0030†	17	0.0099†	14	0.0739	33	0.3529	13	0.2567	13	0.1225	13	0.3235	13	0.0013†
	14	33	32		20		17		25		10		11		11		15	
	13	28	39		23		16		22		9		28		7		12	

*p-value ≤0.05, †p-value ≤0.01, ‡p-value ≤0.001, §p-value ≤0.0001

Table A2. Test VLO1 with the following assumptions and t-test parameters: two sample, unequal variances, 1-tail, and normal distribution.

VLO1	Traditional		ND1		ND1		ND2		ND2		ND3		ND3		ND4		ND4	
	Unfl	Flan	Unfl	t-test	Flan	t-test	Unfl	t-test	Flan	t-test	Unfl	t-test	Flan	t-test	Unfl	t-test	Flan	t-test
Face	1500	1630	872	0.0000§	1083	0.0000§	812	0.0000§	760	0.0000§	238	0.0000§	237	0.0000§	454	0.0000§	517	0.0000§
	1520	1618	870		1078		803		755		240		235		460		512	
	1515	1627	870		1079		806		751		234		238		458		509	
3	675	803	741	0.0007‡	859	0.0002‡	630	0.0018†	626	0.0000§	648	0.0045†	681	0.0802	748	0.0002‡	781	0.0139*
	690	808	746		851		634		633		645		674		754		786	
	680	795	739		860		636		640		651		795		741		784	
6	340	414	378	0.0002‡	342	0.0001§	333	0.0112*	366	0.0002‡	348	0.1835	323	0.0813	373	0.0046†	410	0.4535
	346	411	375		346		337		369		346		326		367		409	
	344	406	383		343		335		365		343		406		361		413	
9	170	212	236	0.0012†	206	0.0120*	174	0.0166*	206	0.0715	165	0.0688	217	0.3964	178	0.06730	203	0.0320*
	170	223	230		197		175		208		161		221		182		211	
	168	217	243		204		179		215		168		217		171		207	
12	115	117	142	0.0013†	120	0.1384	97	0.0063†	108	0.0065†	104	0.0897	122	0.0509	122	0.0064†	134	0.0153*
	110	114	145		118		94		105		102		125		130		143	
	105	121	146		127		90		104		107		121		127		129	
15	81	68	79	0.1146	64	0.5000	70	0.0330*	49	0.0179*	62	0.0050†	82	0.1229	62	0.0086†	53	0.0035†
	72	67	85		65		65		54		57		82		65		58	
	74	64	78		70		66		59		57		64		58		57	
18	45	53	55	0.0028†	46	0.0166*	36	0.0941	39	0.0014†	29	0.0105*	57	0.2393	47	0.0368*	51	0.0932
	38	55	54		43		38		33		30		60		47		46	
	40	49	59		46		37		36		34		49		49		49	
21	36	41	24	0.0165*	26	0.0018†	29	0.0538	28	0.0007‡	19	0.0028†	39	0.0818	18	0.0078†	33	0.0237*
	31	44	21		28		26		25		17		37		23		29	
	29	39	25		26		25		24		12		39		22		37	
24	11	31	37	0.0015†	17	0.0049†	14	0.0370*	33	0.1765	13	0.1284	13	0.0612	13	0.1617	13	0.0007‡
	14	33	32		20		17		25		10		11		11		15	
	13	28	39		23		16		22		9		28		7		12	

*p-value ≤0.05, †p-value ≤0.01, ‡p-value ≤0.001, §p-value ≤0.0001

Table A3. Test VLO2 with the following assumptions and t-test parameters: two sample, unequal variances, 2-tail, and normal distribution.

VLO2	Traditional		ND1		ND1		ND2		ND2		ND3		ND3		ND4		ND4	
	Unfl	Flan	Unfl	t-test	Flan	t-test	Unfl	t-test	Flan	t-test	Unfl	t-test	Flan	t-test	Unfl	t-test	Flan	t-test
Face	2006	2104	1140	0.0000§	1488	0.0031†	1053	0.0000§	997	0.0009‡	369	0.0000§	358	0.0004‡	709	0.0000§	836	0.0005
	1998	2013	1144		1490		1047		1005		364		362		705		824	
	2002	2119	1138		1485		1062		995		368		367		713		818	
3	972	1084	969	0.6683	1153	0.0002‡	794	0.0000§	813	0.0000§	821	0.0000§	909	0.0000§	981	0.34921	1045	0.0287
	971	1094	967		1152		803		817		822		905		978		1059	
	962	1086	964		1158		801		822		817		918		965		1068	
6	438	545	471	0.0016†	455	0.0000§	447	0.7758	479	0.0000§	440	0.2152	434	0.0000§	467	0.0016†	524	0.0024
	446	542	474		458		438		483		436		436		462		519	
	440	548	470		453		435		481		435		440		469		527	
9	226	294	273	0.0000§	283	0.0113*	219	0.1893	251	0.0004‡	206	0.0066†	273	0.0011†	230	0.4541	261	0.0196
	225	290	274		279		221		254		210		271		226		272	
	222	297	269		283		224		254		213		267		223		276	
12	130	164	172	0.0001§	175	0.0059†	125	0.5871	137	0.0113*	123	0.0840	142	0.0229*	145	0.0105*	165	0.2667
	131	161	175		181		125		139		127		147		147		165	
	126	155	179		184		132		138		123		151		139		162	
15	107	98	105	0.6872	96	0.0263*	72	0.0103*	80	0.0031†	65	0.0059†	110	0.1047	76	0.0068†	68	0.0005
	103	105	102		91		75		85		67		108		74		71	
	95	104	103		90		72		86		69		106		82		75	
18	56	74	96	0.0000§	50	0.0002‡	58	0.6174	56	0.0002‡	54	0.4968	68	0.0766	32	0.0396*	57	0.0274
	53	75	99		51		53		52		56		73		38		63	
	56	77	100		54		57		53		59		66		45		66	
21	36	37	29	0.0303*	23	0.0474*	30	0.0399*	30	0.0053†	22	0.0035†	49	0.0036†	25	0.0065†	41	0.0881
	42	39	31		28		29		32		21		51		16		44	
	44	41	28		33		29		28		17		47		15		42	
24	21	30	13	0.0313*	26	0.1007	19	0.3162	43	0.0500*	19	0.3293	24	0.0299*	16	0.2709	16	0.0035
	23	27	11		18		18		36		19		21		18		18	
	17	26	14		19		17		34		16		19		19		16	

*p-value ≤0.05, †p-value ≤0.01, ‡p-value ≤0.001, §p-value ≤0.0001

Table A4. Test VLO2 with the following assumptions and t-test parameters: two sample, unequal variances, 1-tail, and normal distribution.

VLO2	Traditional		ND1		ND1		ND2		ND2		ND3		ND3		ND4		ND4	
	Unfl	Flan	Unfl	t-test	Fla	t-test	Unfl	t-test	Flan	t-test	Unfl	t-test	Flan	t-test	Unfl	t-test	Flan	t-test
Face	2006	2104	1140	0.0000§	1488	0.0015†	1053	0.0000§	997	0.0004‡	369	0.0000§	358	0.0002‡	709	0.0000§	836	0.0003‡
	1998	2013	1144		1490		1047		1005		364		362		705		824	
	2002	2119	1138		1485		1062		995		368		367		713		818	
3	972	1084	969	0.3341	1153	0.0001‡	794	0.0000§	813	0.0000§	821	0.0000§	909	0.0000§	981	0.1746	1045	0.0144*
	971	1094	967		1152		803		817		822		905		978		1059	
	962	1086	964		1158		801		822		817		918		965		1068	
6	438	545	471	0.0008‡	455	0.0000§	447	0.3879	479	0.0000§	440	0.1076	434	0.0000§	467	0.0008‡	524	0.0012†
	446	542	474		458		438		483		436		436		462		519	
	440	548	470		453		435		481		435		440		469		527	
9	226	294	273	0.0000§	283	0.0056†	219	0.0947	251	0.0002‡	206	0.0033†	273	0.0005‡	230	0.2270	261	0.0098†
	225	290	274		279		221		254		210		271		226		272	
	222	297	269		283		224		254		213		267		223		276	
12	130	164	172	0.0000§	175	0.0030†	125	0.2936	137	0.0056†	123	0.0420*	142	0.0115*	145	0.0052†	165	0.1334
	131	161	175		181		125		139		127		147		147		165	
	126	155	179		184		132		138		123		151		139		162	
15	107	98	105	0.3436	96	0.0131*	72	0.0051†	80	0.0016†	65	0.0029†	110	0.0524	76	0.0034†	68	0.0003‡
	103	105	102		91		75		85		67		108		74		71	
	95	104	103		90		72		86		69		106		82		75	
18	56	74	96	0.0000§	50	0.0001§	58	0.3087	56	0.0001§	54	0.2484	68	0.0383*	32	0.0198*	57	0.0137*
	53	75	99		51		53		52		56		73		38		63	
	56	77	100		54		57		53		59		66		45		66	
21	36	37	29	0.0152*	23	0.0237*	30	0.0200*	30	0.0026†	22	0.0018†	49	0.0018†	25	0.0032†	41	0.0440*
	42	39	31		28		29		32		21		51		16		44	
	44	41	28		33		29		28		17		47		15		42	
24	21	30	13	0.0156*	26	0.0504	19	0.1581	43	0.0250*	19	0.1646	24	0.0149*	16	0.1354*	16	0.0018†
	23	27	11		18		18		36		19		21		18		18	
	17	26	14		19		17		34		16		19		19		16	

*p-value ≤0.05, †p-value ≤0.01, ‡p-value ≤0.001, §p-value ≤0.0001

Table A5. Test VHI1 with the following assumptions and t-test parameters: two sample, unequal variances, 2-tail, and normal distribution.

VHI1	Traditional		ND1		ND1		ND2		ND2		ND3		ND3		ND4		ND4	
	Unfl	Flan	Unfl	t-test	Flan	t-test	Unfl	t-test	Flan	t-test	Unfl	t-test	Flan	t-test	Unfl	t-test	Flan	t-test
Face	3000	3122	1893	0.0000§	2253	0.0000§	1663	0.0000§	1592	0.0000§	820	0.0000§	547	0.0000§	1318	0.0000§	1328	0.0000§
	3010	3127	1888		2258		1667		1594		822		558		1326		1341	
	2993	3119	1893		2250		1674		1587		816		570		1330		1308	
3	1607	1589	1461	0.0032†	1722	0.0000§	1210	0.0002‡	1253	0.0000§	1243	0.0004‡	1383	0.0000§	1501	0.0045†	1590	0.1877
	1579	1577	1467		1715		1207		1248		1240		1384		1494		1583	
	1583	1575	1468		1727		1201		1246		1236		1376		1492		1602	
6	665	782	652	0.0504	677	0.0002‡	624	0.0036†	714	0.0001§	650	0.0150*	664	0.0000§	718	0.0001§	748	0.0032†
	670	776	658		676		629		724		648		663		722		751	
	661	785	658		679		638		722		647		657		726		751	
9	300	427	332	0.1243	376	0.0003‡	312	0.6819	369	0.0002‡	305	0.5849	404	0.0068†	318	0.4466	405	0.0132*
	328	420	337		384		315		366		318		400		326		398	
	315	419	335		381		304		364		303		402		322		409	
12	190	224	207	0.0249*	242	0.0013†	184	0.8450	198	0.0005‡	178	0.1278	208	0.0025†	208	0.0162*	246	0.1229
	188	226	208		240		186		191		173		204		214		235	
	176	229	211		244		181		192		172		211		209		231	
15	128	123	184	0.0004‡	144	0.0227*	108	0.0098†	131	0.1634	97	0.0011†	141	0.0120*	133	0.0746	145	0.0514
	131	127	179		134		109		128		90		146		138		137	
	121	116	172		136		104		127		87		136		136		130	
18	74	76	87	0.0118*	69	0.0929	59	0.0316*	73	0.0343*	68	0.1242	64	0.0302*	54	0.0044†	101	0.0487*
	67	84	85		76		62		66		62		72		51		95	
	69	88	86		74		61		66		64		67		56		91	
21	51	58	49	0.7179	46	0.0030†	50	0.5880	44	0.0085†	41	0.0161*	55	0.0727	44	0.0887	40	0.0067†
	48	65	45		40		47		44		40		56		48		32	
	54	60	55		43		52		42		39		48		39		27	
24	30	42	24	0.9107	33	0.0048†	26	0.1129	64	0.0015†	23	0.0576	32	0.0330*	24	0.5276	35	0.0142*
	29	40	29		28		21		63		20		35		25		36	
	24	45	31		31		19		58		21		38		29		32	

*p-value ≤0.05, †p-value ≤0.01, ‡p-value ≤0.001, §p-value ≤0.0001

Table A6.Test VHI1 with the following assumptions and t-test parameters: two sample, unequal variances, 1-tail, and normal distribution.

VHI1	Traditional		ND1		ND1		ND2		ND2		ND3		ND3		ND4		ND4	
	Unfl	Flan	Unfl	t-test	Flan	t-test	Unfl	t-test	Flan	t-test	Unfl	t-test	Flan	t-test	Unfl	t-test	Flan	t-test
Face	3000	3122	1893	0.0000§	2253	0.0000§	1663	0.0000§	1592	0.0000§	820	0.0000§	547	0.0000§	1318	0.0000§	1328	0.0000§
	3010	3127	1888		2258		1667		1594		822		558		1326		1341	
	2993	3119	1893		2250		1674		1587		816		570		1330		1308	
3	1607	1589	1461	0.0016†	1722	0.0000§	1210	0.0001§	1253	0.0000§	1243	0.0002‡	1383	0.0000§	1501	0.0025†	1590	0.0939
	1579	1577	1467		1715		1207		1248		1240		1384		1494		1583	
	1583	1575	1468		1727		1201		1246		1236		1376		1492		1602	
6	665	782	652	0.0252*	677	0.0001§	624	0.0018†	714	0.0001§	650	0.0075†	664	0.0000§	718	0.0001§	748	0.0016†
	670	776	658		676		629		724		648		663		722		751	
	661	785	658		679		638		722		647		657		726		751	
9	300	427	332	0.0622	376	0.0001§	312	0.3409	369	0.0001§	305	0.2925	404	0.0034†	318	0.2233	405	0.0066†
	328	420	337		384		315		366		318		400		326		398	
	315	419	335		381		304		364		303		402		322		409	
12	190	224	207	0.0124*	242	0.0007‡	184	0.4225	198	0.0003‡	178	0.0639	208	0.0013†	208	0.0081†	246	0.0614
	188	226	208		240		186		191		173		204		214		235	
	176	229	211		244		181		192		172		211		209		231	
15	128	123	184	0.0002‡	144	0.0114*	108	0.0049†	131	0.0817	97	0.0005‡	141	0.0060†	133	0.0373*	145	0.0257*
	131	127	179		134		109		128		90		146		138		137	
	121	116	172		136		104		127		87		136		136		130	
18	74	76	87	0.0059†	69	0.0465*	59	0.0158*	73	0.0172*	68	0.0621	64	0.0151*	54	0.0022†	101	0.0243*
	67	84	85		76		62		66		62		72		51		95	
	69	88	86		74		61		66		64		67		56		91	
21	51	58	49	0.3589	46	0.0015†	50	0.2940	44	0.0042†	41	0.0081†	55	0.0364*	44	0.0444*	40	0.0033†
	48	65	45		40		47		44		40		56		48		32	
	54	60	55		43		52		42		39		48		39		27	
24	30	42	24	0.4554	33	0.0024†	26	0.0564	64	0.0008‡	23	0.0288*	32	0.0165*	24	0.2638	35	0.0071†
	29	40	29		28		21		63		20		35		25		36	
	24	45	31		31		19		58		21		38		29		32	

*p-value ≤0.05, †p-value ≤0.01, ‡p-value ≤0.001, §p-value ≤0.0001

Table A7. Test VHI2 with the following assumptions and t-test parameters: two sample, unequal variances, 2-tail, and normal distribution.

VHI2	Traditional		ND1		ND1		ND2		ND2		ND3		ND3		ND4		ND4	
	Unfl	Flan	Unfl	t-test	Flan	t-test	Unfl	t-test	Flan	t-test	Unfl	t-test	Flan	t-test	Unfl	t-test	Flan	t-test
Face	3996	4061	2684	0.0000§	2923	0.0000§	2408	0.0000§	2193	0.0000§	1304	0.0000§	724	0.0000§	1932	0.0000§	2098	0.0000§
	4008	4081	2696		2918		2413		2201		1313		731		1941		2121	
	4014	4075	2699		2933		2413		2203		1318		718		1922		2137	
3	1960	2034	1834	0.0008‡	2238	0.1592	1592	0.0000§	1652	0.0206*	1626	0.0000§	1837	0.0528	1954	0.4741	2040	0.4187
	1961	2036	1835		2244		1599		1662		1625		1825		1965		2032	
	1972	2229	1835		2243		1597		1660		1620		1830		1962		2031	
6	885	1056	796	0.0005‡	899	0.0000§	827	0.0000§	933	0.0000§	835	0.0001§	870	0.0000§	913	0.0154*	991	0.0005‡
	886	1051	803		891		831		925		831		864		907		998	
	884	1062	804		891		830		925		832		861		920		1005	
9	435	558	427	0.0631	510	0.0003‡	418	0.0116*	480	0.0000§	412	0.0142	521	0.0002‡	431	0.4035	538	0.0202*
	440	560	426		502		410		485		410		516		439		529	
	450	565	424		499		415		477		408		524		44		518	
12	246	302	271	0.1659	306	0.0684	243	0.0977	260	0.0004‡	237	0.0579	281	0.0024†	271	0.0350*	291	0.0610
	256	298	263		311		246		264		235		277		279		289	
	264	306	264		315		235		260		234		284		280		298	
15	180	199	169	0.0014†	197	0.1250	172	0.0062†	158	0.0001§	162	0.0059†	193	0.0257*	161	0.0166*	173	0.0096†
	181	203	166		198		166		157		153		184		165		168	
	184	201	164		190		167		152		160		186		153		159	
18	116	128	118	0.1976	125	0.0427*	93	0.0039†	110	0.0002‡	106	0.0215*	126	0.6954	105	0.0689	113	0.0255*
	119	131	119		123		81		112		95		131		107		106	
	111	128	122		119		87		113		98		133		93		117	
21	83	95	75	0.0160*	80	0.0030†	59	0.0019†	84	0.0155*	57	0.0014†	86	0.1362	62	0.0024†	78	0.2361
	86	91	70		76		63		85		62		90		63		89	
	79	90	68		74		60		82		63		89		67		90	
24	58	63	55	0.6922	51	0.0066†	51	0.1790	68	0.0822	37	0.0247*	62	0.6544	53	0.2486	66	0.1439
	50	63	52		44		45		74		38		61		61		63	
	49	58	54		46		42		65		43		58		58		71	

*p-value ≤0.05, †p-value ≤0.01, ‡p-value ≤0.001, §p-value ≤0.0001

Table A8. Test VHI2 with the following assumptions and t-test parameters: two sample, unequal variances, 1-tail, and normal distribution.

VHI2	Traditional		ND1		ND1		ND2		ND2		ND3		ND3		ND4		ND4	
	Unfl	Flan	Unfl	t-test	Flan	t-test	Unfl	t-test	Flan	t-test	Unfl	t-test	Flan	t-test	Unfl	t-test	Flan	t-test
Face	3996	4061	2684	0.0000§	2923	0.0000§	2408	0.0000§	2193	0.0000§	1304	0.0000§	724	0.0000§	1932	0.0000§	2098	0.0000§
	4008	4081	2696		2918		2413		2201		1313		731		1941		2121	
	4014	4075	2699		2933		2413		2203		1318		718		1922		2137	
3	1960	2034	1834	0.0004‡	2238	0.0796	1592	0.0000§	1652	0.0103*	1626	0.0000§	1837	0.0264*	1954	0.2370	2040	0.2094
	1961	2036	1835		2244		1599		1662		1625		1825		1965		2032	
	1972	2229	1835		2243		1597		1660		1620		1830		1962		2031	
6	885	1056	796	0.0003‡	899	0.0000§	827	0.0000§	933	0.0000§	835	0.0000§	870	0.0000§	913	0.0077†	991	0.0002‡
	886	1051	803		891		831		925		831		864		907		998	
	884	1062	804		891		830		925		832		861		920		1005	
9	435	558	427	0.0316*	510	0.0002‡	418	0.0058†	480	0.0000§	412	0.0071†	521	0.0001§	431	0.2018	538	0.0101*
	440	560	426		502		410		485		410		516		439		529	
	450	565	424		499		415		477		408		524		44		518	
12	246	302	271	0.0830	306	0.0342*	243	0.0488*	260	0.0002‡	237	0.0289*	281	0.0012†	271	0.0175*	291	0.0305*
	256	298	263		311		246		264		235		277		279		289	
	264	306	264		315		235		260		234		284		280		298	
15	180	199	169	0.0007‡	197	0.06250	172	0.0031†	158	0.0001§	162	0.0030†	193	0.0128*	161	0.0083†	173	0.0048†
	181	203	166		198		166		157		153		184		165		168	
	184	201	164		190		167		152		160		186		153		159	
18	116	128	118	0.0988	125	0.0214*	93	0.0020†	110	0.0001§	106	0.0107*	126	0.3477	105	0.0344*	113	0.0128*
	119	131	119		123		81		112		95		131		107		106	
	111	128	122		119		87		113		98		133		93		117	
21	83	95	75	0.0080†	80	0.0015†	59	0.0009‡	84	0.0078†	57	0.0007‡	86	0.0681	62	0.0012†	78	0.1180
	86	91	70		76		63		85		62		90		63		89	
	79	90	68		74		60		82		63		89		67		90	
24	58	63	55	0.3461	51	0.0033†	51	0.08950	68	0.0411*	37	0.0123*	62	0.32720	53	0.1243	66	0.0719
	50	63	52		44		45		74		38		61		61		63	
	49	58	54		46		42		65		43		58		58		71	

*p-value ≤0.05, †p-value ≤0.01, ‡p-value ≤0.001, §p-value ≤0.0001

Table A9. Inlet Velocity. T-test parameters: two sample, unequal variances, 2-tail, normal distribution

Trial	Minnich	NIOSH V1		Minnich	NIOSH V1		DustControl		NIOSH V2	
Velocity	Hood Only	Hood Only	t-test	Enclosed	Enclosed	t-test	Enclosed	t-test	Enclosed	t-test
500	480	209		517	524		670		280	
	495	203		518	521		679		292	
	487	201		506	513		675		283	
AVG	487	204	0.0000§	514	519	0.3265	675	0.0000§	285	0.0000§
1000	935	405		1135	1085		1336		488	
	941	403		1146	1079		1349		485	
	943	412		1124	1075		1332		480	
AVG	940	407	0.0000§	1135	1080	0.0053†	1339	0.0000§	484	0.0000§
1500	1302	676		1635	1585		1955		1081	
	1302	667		1628	1592		1947		1089	
	1305	668		1642	1594		1942		1072	
AVG	1303	670	0.0000§	1635	1590	0.0014†	1948	0.0000§	1081	0.0003‡
2000	1730	986		2155	2153		2562		1087	
	1745	993		2144	2148		2551		1078	
	1732	974		2149	1243		2567		1095	
AVG	1736	984	0.0000§	2149	1848	0.4241	2560	0.0000§	1087	0.0000§
2500	2190	1192		2949	2651		3408		1385	
	2178	1174		2956	2659		3415		1401	
	2183	1186		2937	2641		3398		1394	
AVG	2184	1184	0.0000§	2947	2650	0.0000§	3407	0.0000§	1393	0.0000§
3000	3215	1431		3440	3275		4244		1938	
	3206	1436		3440	3261		4235		1925	
	3209	1452		3431	3267		4239		1920	
AVG	3210	1440	0.0000§	3437	3268	0.0000§	4239	0.0000§	1928	0.0000§
3500	3707	1725		4240	3850		4983		2141	
	3715	1735		4218	3837		4996		2134	
	3702	1739		4242	3846		5001		2129	
AVG	3708	1733	0.0000§	4233	3844	0.0000§	4993	0.0000§	2135	0.0000§
4000	4430	2366		6358	5284		6736		2413	
	4445	2354		6337	5269		6729		2432	
	4423	2376		6331	5276		6719		2409	
AVG	4433	2365	0.0000§	6342	5276	0.0000§	6728	0.0000§	2418	0.0000§
4500	4820	2922		7029	5913		7680		2684	
	4839	2935		7038	5927		7698		2669	
	4831	2908		7031	5901		7672		2685	
AVG	4830	2922	0.0000§	7033	5914	0.0000§	7683	0.0000§	2679	0.0000§

*p-value ≤0.05, †p-value ≤0.01, ‡p-value ≤0.001, §p-value ≤0.0001

Table A10. Inlet Velocity. T-test parameters: two sample, unequal variances, 1-tail, normal distribution

Trial	Minnich	NIOSH V1		Minnich	NIOSH V1		DustControl		NIOSH V2	
Velocity	Hood Only	Hood Only	t-test	Enclosed	Enclosed	t-test	Enclosed	t-test	Enclosed	t-test
500	480	209		517	524		670		280	
	495	203		518	521		679		292	
	487	201		506	513		675		283	
AVG	487	204	0.0000§	514	519	0.1632	675	0.0000§	285	0.0000§
1000	935	405		1135	1085		1336		488	
	941	403		1146	1079		1349		485	
	943	412		1124	1075		1332		480	
AVG	940	407	0.0000§	1135	1080	0.0000§	1339	0.0000§	484	0.0000§
1500	1302	676		1635	1585		1955		1081	
	1302	667		1628	1592		1947		1089	
	1305	668		1642	1594		1942		1072	
AVG	1303	670	0.0000§	1635	1590	0.0000§	1948	0.0000§	1081	0.0000§
2000	1730	986		2155	2153		2562		1087	
	1745	993		2144	2148		2551		1078	
	1732	974		2149	1243		2567		1095	
AVG	1736	984	0.0000§	2149	1848	0.3730	2560	0.0000§	1087	0.0000§
2500	2190	1192		2949	2651		3408		1385	
	2178	1174		2956	2659		3415		1401	
	2183	1186		2937	2641		3398		1394	
AVG	2184	1184	0.0000§	2947	2650	0.0000§	3407	0.0000§	1393	0.0000§
3000	3215	1431		3440	3275		4244		1938	
	3206	1436		3440	3261		4235		1925	
	3209	1452		3431	3267		4239		1920	
AVG	3210	1440	0.0000§	3437	3268	0.0003‡	4239	0.0000§	1928	0.0000§
3500	3707	1725		4240	3850		4983		2141	
	3715	1735		4218	3837		4996		2134	
	3702	1739		4242	3846		5001		2129	
AVG	3708	1733	0.0000§	4233	3844	0.0000§	4993	0.0000§	2135	0.0000§
4000	4430	2366		6358	5284		6736		2413	
	4445	2354		6337	5269		6729		2432	
	4423	2376		6331	5276		6719		2409	
AVG	4433	2365	0.0000§	6342	5276	0.0000§	6728	0.0000§	2418	0.0000§
4500	4820	2922		7029	5913		7680		2684	
	4839	2935		7038	5927		7698		2669	
	4831	2908		7031	5901		7672		2685	
AVG	4830	2922	0.0000§	7033	5914	0.0000§	7683	0.0000§	2679	0.0000§

*p-value ≤0.05, †p-value ≤0.01, ‡p-value ≤0.001, §p-value ≤0.0001

Table A11. Face Velocity. T-test parameters: two sample, unequal variances, 2-tail, normal distribution

Trial	Minnich	NIOSH V1		DustControl		NIOSH V2	
Velocity	Enclosed	Enclosed	t-test		t-test		t-test
500	140	148		89		133	
	142	152		98		125	
	133	156	0.0197*	94	0.0003‡	129	0.0610
AVG	138.3	152		93.7		129	
1000	242	271		176		220	
	234	269		164		225	
	249	265	0.0150*	178	0.0004‡	227	0.0374*
AVG	241.7	268.3		172.7		224	
1500	351	442		255		477	
	349	439		247		483	
	360	445	0.0002‡	261	0.0000§	474	0.0000§
AVG	353.3	442		254.3		478	
2000	461	579		319		507	
	456	585		325		502	
	452	572	0.0000§	323	0.0000§	511	0.0002‡
AVG	456.3	578.7		322.3		506.7	
2500	615	740		437		627	
	621	751		441		635	
	624	743	0.0000§	435	0.0000§	624	0.1122
AVG	620	744.7		437.7		628.7	
3000	780	877		538		905	
	776	880		534		912	
	785	869	0.0000§	542	0.0000§	906	0.0000§
AVG	780.3	875.3		538		907.7	
3500	954	1060		736		989	
	959	1054		744		979	
	946	1064	0.0000§	739	0.0000§	985	0.0035†
AVG	953	1059.3		739.7		984.3	
4000	1114	1357		891		1132	
	1124	1351		893		1126	
	1124	1349	0.0000§	895	0.0000§	1135	0.0754
AVG	1120.667	1352.3		893		1131	
4500	1276	1612		987		1185	
	1284	1615		975		1194	
	1280	1608	0.0000§	969	0.0000§	1191	0.0000§
AVG	1280	1611.7		977		1190	

*p-value ≤0.05, †p-value ≤0.01, ‡p-value ≤0.001, §p-value ≤0.0001

Table A12. Face Velocity. T-test parameters: two sample, unequal variances, 1-tail, normal distribution

Trial	Minnich	NIOSH V1		DustControl		NIOSH V2	
Velocity	Enclosed	Enclosed	t-test	Enclosed	t-test	Enclosed	t-test
500	140	148		89		133	
	142	152		98		125	
	133	156	0.0098†	94	0.0001§	129	0.0305*
AVG	138	152		94		129	
1000	242	271		176		220	
	234	269		164		225	
	249	265	0.0075‡	178	0.0002‡	227	0.0187*
AVG	242	268		173		224	
1500	351	442		255		477	
	349	439		247		483	
	360	445	0.0001§	261	0.0000§	474	0.0000§
AVG	353	442		254		478	
2000	461	579		319		507	
	456	585		325		502	
	452	572	0.0000§	323	0.0000§	511	0.0001§
AVG	456	579		322		507	
2500	615	740		437		627	
	621	751		441		635	
	624	743	0.0000§	435	0.0000§	624	0.0561
AVG	620	745		438		629	
3000	780	877		538		905	
	776	880		534		912	
	785	869	0.0000§	542	0.0000§	906	0.0000§
AVG	780	875		538		908	
3500	954	1060		736		989	
	959	1054		744		979	
	946	1064	0.0000§	739	0.0000§	985	0.0017†
AVG	953	1059		740		984	
4000	1114	1357		891		1132	
	1124	1351		893		1126	
	1124	1349	0.0000§	895	0.0000§	1135	0.0377*
AVG	1121	1352		893		1131	
4500	1276	1612		987		1185	
	1284	1615		975		1194	
	1280	1608	0.0000§	969	0.0000§	1191	0.0000§
AVG	1280	1612		977		1190	

*p-value ≤0.05, †p-value ≤0.01, ‡p-value ≤0.001, §p-value ≤0.0001

Table A13. Coefficient of entry. T-test parameters: two sample, unequal variances, 2-tail, normal distribution

Trial	Minnich	NIOSH V1		Minnich	NIOSH V1		DustControl		NIOSH V2	
Velocity	Hood Only	Hood Only	t-test	Enclosed	Enclosed	t-test	Enclosed	t-test	Enclosed	
500	0.67	0.75		0.68	0.62		0.64		0.62	
	0.66	0.74		0.69	0.61		0.64		0.62	
	0.67	0.74	0.0001§	0.69	0.61	0.0001§	0.63	0.0005‡	0.63	0.0002‡
AVG	0.67	0.74		0.69	0.61					
1000	0.74	0.88		0.67	0.72		0.64		0.72	
	0.74	0.88		0.67	0.73		0.65		0.72	
	0.74	0.87	0.0006‡	0.67	0.73	0.0034†	0.63	0.0378*	0.72	0.0000§
AVG	0.74	0.88		0.67	0.73					
1500	0.72	0.89		0.67	0.73		0.64		0.73	
	0.71	0.88		0.68	0.73		0.64		0.71	
	0.72	0.88	0.0000§	0.67	0.73	0.0034†	0.64	0.0085†	0.73	0.0066†
AVG	0.72	0.88		0.67	0.73					
2000	0.52	0.86		0.49	0.53		0.47		0.53	
	0.52	0.88		0.51	0.53		0.49		0.52	
	0.53	0.88	0.0000§	0.50	0.53	0.0351*	0.48	0.0683	0.53	0.0214*
AVG	0.52	0.87		0.50	0.53					
2500	0.69	0.84		0.63	0.69		0.61		0.69	
	0.70	0.86		0.64	0.70		0.63		0.69	
	0.70	0.86	0.0003‡	0.64	0.70	0.0002‡	0.63	0.1413	0.66	0.0414*
AVG	0.70	0.85		0.64	0.70					
3000	0.65	0.82		0.61	0.68		0.60		0.68	
	0.66	0.83		0.62	0.69		0.61		0.65	
	0.66	0.83	0.0000§	0.62	0.69	0.0001§	0.63	0.7304	0.66	0.0159*
AVG	0.66	0.83		0.62	0.69					
3500	0.64	0.80		0.59	0.66		0.58		0.66	
	0.65	0.81		0.60	0.66		0.59		0.66	
	0.65	0.80	0.0000§	0.60	0.66	0.0028†	0.61	0.7822	0.67	0.0002‡
AVG	0.65	0.80		0.60	0.66					
4000	0.58	0.69		0.52	0.55		0.53		0.55	
	0.57	0.70		0.53	0.56		0.53		0.58	
	0.57	0.69	0.0000§	0.53	0.56	0.0031†	0.53	0.4522	0.55	0.0781
AVG	0.57	0.69		0.53	0.56					
4500	0.58	0.69		0.53	0.56		0.53		0.56	
	0.57	0.69		0.54	0.56		0.53		0.56	
	0.57	0.69	0.0008‡	0.53	0.55	0.0078†	0.52	0.2741	0.55	0.0079†
AVG	0.57	0.69		0.53	0.56					

*p-value ≤0.05, †p-value ≤0.01, ‡p-value ≤0.001, §p-value ≤0.0001

Table A14. Coefficient of entry. T-test parameters: two sample, unequal variances, 1-tail, normal distribution

Trial	Minnich	NIOSH V1		Minnich	NIOSH V1		DustControl		NIOSH V2	
Velocity	Hood Only	Hood Only	t-test	Enclosed	Enclosed	t-test	Enclosed	t-test	Enclosed	
500	0.67	0.75		0.68	0.62		0.64		0.62	
	0.66	0.74		0.69	0.61		0.64		0.62	
	0.67	0.74	0.0000§	0.69	0.61	0.0000§	0.63	0.0002‡	0.63	0.0001§
AVG	0.67	0.74		0.69	0.61					
1000	0.74	0.88		0.67	0.72		0.64		0.72	
	0.74	0.88		0.67	0.73		0.65		0.72	
	0.74	0.87	0.0003‡	0.67	0.73	0.0017†	0.63	0.0189*	0.72	0.0000§
AVG	0.74	0.88		0.67	0.73					
1500	0.72	0.89		0.67	0.73		0.64		0.73	
	0.71	0.88		0.68	0.73		0.64		0.71	
	0.72	0.88	0.0000§	0.67	0.73	0.0017†	0.64	0.0043†	0.73	0.0033†
AVG	0.72	0.88		0.67	0.73					
2000	0.52	0.86		0.49	0.53		0.47		0.53	
	0.52	0.88		0.51	0.53		0.49		0.52	
	0.53	0.88	0.0000§	0.50	0.53	0.0175*	0.48	0.0342*	0.53	0.0107*
AVG	0.52	0.87		0.50	0.53					
2500	0.69	0.84		0.63	0.69		0.61		0.69	
	0.70	0.86		0.64	0.70		0.63		0.69	
	0.70	0.86	0.0001§	0.64	0.70	0.0001§	0.63	0.0706	0.66	0.0207*
AVG	0.70	0.85		0.64	0.70					
3000	0.65	0.82		0.61	0.68		0.60		0.68	
	0.66	0.83		0.62	0.69		0.61		0.65	
	0.66	0.83	0.0000§	0.62	0.69	0.0001§	0.63	0.3652	0.66	0.0080†
AVG	0.66	0.83		0.62	0.69					
3500	0.64	0.80		0.59	0.66		0.58		0.66	
	0.65	0.81		0.60	0.66		0.59		0.66	
	0.65	0.80	0.0000§	0.60	0.66	0.0014†	0.61	0.3911	0.67	0.0001§
AVG	0.65	0.80		0.60	0.66					
4000	0.58	0.69		0.52	0.55		0.53		0.55	
	0.57	0.70		0.53	0.56		0.53		0.58	
	0.57	0.69	0.0000§	0.53	0.56	0.0016†	0.53	0.2261	0.55	0.0391*
AVG	0.57	0.69		0.53	0.56					
4500	0.58	0.69		0.53	0.56		0.53		0.56	
	0.57	0.69		0.54	0.56		0.53		0.56	
	0.57	0.69	0.0004‡	0.53	0.55	0.0039†	0.52	0.1370	0.55	0.0039†
AVG	0.57	0.69		0.53	0.56					

*p-value ≤0.05, †p-value ≤0.01, ‡p-value ≤0.001, §p-value ≤0.0001

Table A15. Transport Velocity. T-test parameters: two sample, unequal variances, 2-tail, normal distribution

Trial	Minnich	NIOSH V1		Minnich	NIOSH V1		DustControl		NIOSH V2	
Velocity	Hood Only	Hood Only	t-test	Enclosed	Enclosed	t-test	Enclosed	t-test	Enclosed	t-test
500	457	465		434	155		461		491	
	449	451		426	162		455		495	
	447	457	0.2643	421	160	0.0000§	451	0.0047†	488	0.0006‡
AVG	451	458		427	159		456		491	
1000	852	950		801	410		749		950	
	855	942		806	416		761		957	
	857	945	0.0000§	802	412	0.0000§	752	0.0018†	951	0.0000§
AVG	855	946		803	413		754		953	
1500	1236	1452		1181	1129		1284		1402	
	1228	1439		1190	1135		1280		1398	
	1239	1455	0.0000§	1192	1124	0.0002‡	1290	0.0000§	1405	0.0000§
AVG	1234	1449		1188	1129		1285		1402	
2000	1747	2011		1608	1727		1710		1869	
	1751	2010		1603	1721		1716		1870	
	1742	2001	0.0000§	1611	1729	0.0000§	1722	0.0000§	1873	0.0000§
AVG	1747	2007		1607	1726		1716		1871	
2500	2256	2436		2074	2317		1981		2444	
	2248	2446		2068	2318		1985		2438	
	2250	2441	0.0000§	2078	2324	0.0000§	1973	0.0000§	2449	0.0000§
AVG	2251	2441		2073	2320		1980		2444	
3000	2809	3040		2462	2871		2583		3405	
	2815	3034		2470	2860		2589		3411	
	2822	3035	0.0000§	2458	2874	0.0000§	2574	0.0000§	3406	0.0000§
AVG	2815	3036		2463	2868		2582		3407	
3500	3301	3698		3004	3295		2971		3695	
	3321	3679		3015	3288		2976		3698	
	3312	3684	0.0000§	3013	3284	0.0000§	2980	0.0016†	3699	0.0000§
AVG	3311	3687		3011	3289		2976		3697	
4000	4251	4842		3989	4476		4154		4045	
	4259	4846		3995	4481		4139		4035	
	4253	4840	0.0000§	3976	4485	0.0000§	4145	0.0000§	4038	0.0036†
AVG	4254	4843		3987	4481		4146		4039	
4500	4725	5243		4370	4858		4550		4693	
	4720	5251		4361	4864		4529		4699	
	4711	5241	0.0000§	4355	4855	0.0000§	4539	0.0000§	4695	0.0000§
AVG	4719	5245		4362	4859		4539		4696	

*p-value ≤0.05, †p-value ≤0.01, ‡p-value ≤0.001, §p-value ≤0.0001

Table A16. Transport Velocity. T-test parameters: two sample, unequal variances, 1-tail, normal distribution

Trial	Minnich	NIOSH V1		Minnich	NIOSH V1		DustControl		NIOSH V2	
Velocity	Hood Only	Hood Only	t-test	Enclosed	Enclosed	t-test		t-test	Enclosed	t-test
500	457	465		434	155		461		491	
	449	451		426	162		455		495	
	447	457	0.1322	421	160	0.0000§	451	0.0024†	488	0.0003‡
AVG	451	458		427	159		456		491	
1000	852	950		801	410		749		950	
	855	942		806	416		761		957	
	857	945	0.0000§	802	412	0.0000§	752	0.0009‡	951	0.0000§
AVG	855	946		803	413		754		953	
1500	1236	1452		1181	1129		1284		1402	
	1228	1439		1190	1135		1280		1398	
	1239	1455	0.0000§	1192	1124	0.0001§	1290	0.0000§	1405	0.0000§
AVG	1234	1449		1188	1129		1285		1402	
2000	1747	2011		1608	1727		1710		1869	
	1751	2010		1603	1721		1716		1870	
	1742	2001	0.0000§	1611	1729	0.0000§	1722	0.0000§	1873	0.0000§
AVG	1747	2007		1607	1726		1716		1871	
2500	2256	2436		2074	2317		1981		2444	
	2248	2446		2068	2318		1985		2438	
	2250	2441	0.0000§	2078	2324	0.0000§	1973	0.0000§	2449	0.0000§
AVG	2251	2441		2073	2320		1980		2444	
3000	2809	3040		2462	2871		2583		3405	
	2815	3034		2470	2860		2589		3411	
	2822	3035	0.0000§	2458	2874	0.0000§	2574	0.0000§	3406	0.0000§
AVG	2815	3036		2463	2868		2582		3407	
3500	3301	3698		3004	3295		2971		3695	
	3321	3679		3015	3288		2976		3698	
	3312	3684	0.0000§	3013	3284	0.0000§	2980	0.0008‡	3699	0.0000§
AVG	3311	3687		3011	3289		2976		3697	
4000	4251	4842		3989	4476		4154		4045	
	4259	4846		3995	4481		4139		4035	
	4253	4840	0.0000§	3976	4485	0.0000§	4145	0.0000§	4038	0.0018†
AVG	4254	4843		3987	4481		4146		4039	
4500	4725	5243		4370	4858		4550		4693	
	4720	5251		4361	4864		4529		4699	
	4711	5241	0.0000§	4355	4855	0.0000§	4539	0.0000§	4695	0.0000§
AVG	4719	5245		4362	4859		4539		4696	

*p-value ≤0.05, †p-value ≤0.01, ‡p-value ≤0.001, §p-value ≤0.0001

Table A17. Hood static pressure. T-test parameters: two sample, unequal variances, 2-tail, normal distribution

Trial	Minnich	NIOSH V1		Minnich	NIOSH V1		DustControl		NIOSH V2	
Velocity	Hood Only	Hood Only	t-test	Enclosed	Enclosed	t-test		t-test	Enclosed	t-test
500	0.0350	0.0280		0.0340	0.0400		0.0380		0.0320	
	0.0350	0.0250		0.0320	0.0500		0.0400		0.0315	
	0.0340	0.0240	0.0125*	0.0330	0.0500	0.0509	0.0400	0.0022†	0.0323	0.1977
AVG	0.0347	0.0257		0.0330	0.0467		0.0393		0.0319	
1000	0.1150	0.0810		0.1390	0.1200		0.1510		0.0840	
	0.1140	0.0820		0.1400	0.1100		0.1600		0.0843	
	0.1140	0.0800	0.0000§	0.1370	0.1100	0.0124*	0.1400	0.1786	0.0845	0.0002‡
AVG	0.1143	0.0810		0.1387	0.1133		0.1503		0.0843	
1500	0.2830	0.1790		0.3100	0.2640		0.3440		0.1950	
	0.2820	0.1770		0.2900	0.2700		0.3500		0.1946	
	0.2820	0.1760	0.0000§	0.2800	0.2500	0.0469*	0.3600	0.0098†	0.1948	0.0079†
AVG	0.2823	0.1773		0.2933	0.2613		0.3513		0.1948	
2000	0.5090	0.3350		0.5900	0.4940		0.6250		0.3800	
	0.5110	0.3400		0.6100	0.5000		0.6100		0.3815	
	0.5100	0.3370	0.0000§	0.6200	0.4900	0.0032†	0.6300	0.2415	0.3808	0.0015†
AVG	0.5100	0.3373		0.6067	0.4947		0.6217		0.3808	
2500	0.8220	0.5540		0.9970	0.8120		1.0330		0.5440	
	0.8240	0.5500		0.9910	0.8100		1.0500		0.5431	
	0.8230	0.5520	0.0000§	0.9890	0.8000	0.0000§	1.0600	0.0136*	0.5448	0.0000§
AVG	0.8230	0.5520		0.9923	0.8073		1.0477		0.5440	
3000	1.3080	0.8410		1.5230	1.2260		1.5650		1.2080	
	1.3050	0.8430		1.5200	1.2400		1.5700		1.2083	
	1.3060	0.8450	0.0000§	1.5200	1.2400	0.0001§	1.5800	0.0055†	1.2078	0.0000§
AVG	1.3063	0.8430		1.5210	1.2353		1.5717		1.2080	
3500	1.8630	1.1850		2.2190	1.7640		2.2570		1.4790	
	1.8650	1.1800		2.2200	1.7700		2.2800		1.4782	
	1.8660	1.1820	0.0000§	2.2210	1.7800	0.0001§	2.2400	0.0778	1.4796	0.0000§
AVG	1.8647	1.1823		2.2200	1.7713		2.2590		1.4789	
4000	2.9530	2.0940		3.6840	3.3280		3.5610		1.8640	
	2.9550	2.0910		3.6800	3.3400		3.5200		1.8645	
	2.9510	2.0890	0.0000§	3.6900	3.3500	0.0000§	3.5000	0.0111*	1.8643	0.0000§
AVG	2.9530	2.0913		3.6847	3.3393		3.5270		1.8643	
4500	3.7580	2.6440		4.6580	4.0200		4.4710		2.2410	
	3.7550	2.6500		4.6600	4.0500		4.4200		2.2425	
	3.7600	2.6490	0.0000§	4.6400	4.0400	0.0000§	4.4900	0.0073†	2.2460	0.0000§
AVG	3.7577	2.6477		4.6527	4.0367		4.4603		2.2432	

Table A18. Hood static pressure. T-test parameters: two sample, unequal variances, 1-tail, normal distribution

Trial	Minnich	NIOSH V1		Minnich	NIOSH V1		DustControl		NIOSH V2	
Velocity	Hood Only	Hood Only	t-test	Enclosed	Enclosed	t-test		t-test	Enclosed	t-test
500	0.0350	0.0280		0.0340	0.0400		0.0380		0.0320	
	0.0350	0.0250		0.0320	0.0500		0.0400		0.0315	
	0.0340	0.0240	0.0063†	0.0330	0.0500	0.0255*	0.0400	0.0011†	0.0323	0.0988
AVG	0.0347	0.0257		0.0330	0.0467		0.0393		0.0319	
1000	0.1150	0.0810		0.1390	0.1200		0.1510		0.0840	
	0.1140	0.0820		0.1400	0.1100		0.1600		0.0843	
	0.1140	0.0800	0.0000§	0.1370	0.1100	0.0062†	0.1400	0.0893	0.0845	0.0001§
AVG	0.1143	0.0810		0.1387	0.1133		0.1503		0.0843	
1500	0.2830	0.1790		0.3100	0.2640		0.3440		0.1950	
	0.2820	0.1770		0.2900	0.2700		0.3500		0.1946	
	0.2820	0.1760	0.0000§	0.2800	0.2500	0.0234*	0.3600	0.0049†	0.1948	0.0040†
AVG	0.2823	0.1773		0.2933	0.2613		0.3513		0.1948	
2000	0.5090	0.3350		0.5900	0.4940		0.6250		0.3800	
	0.5110	0.3400		0.6100	0.5000		0.6100		0.3815	
	0.5100	0.3370	0.0000§	0.6200	0.4900	0.0016†	0.6300	0.1208	0.3808	0.0007‡
AVG	0.5100	0.3373		0.6067	0.4947		0.6217		0.3808	
2500	0.8220	0.5540		0.9970	0.8120		1.0330		0.5440	
	0.8240	0.5500		0.9910	0.8100		1.0500		0.5431	
	0.8230	0.5520	0.0000§	0.9890	0.8000	0.0000§	1.0600	0.0068†	0.5448	0.0000§
AVG	0.8230	0.5520		0.9923	0.8073		1.0477		0.5440	
3000	1.3080	0.8410		1.5230	1.2260		1.5650		1.2080	
	1.3050	0.8430		1.5200	1.2400		1.5700		1.2083	
	1.3060	0.8450	0.0000§	1.5200	1.2400	0.0001§	1.5800	0.0028†	1.2078	0.0000§
AVG	1.3063	0.8430		1.5210	1.2353		1.5717		1.2080	
3500	1.8630	1.1850		2.2190	1.7640		2.2570		1.4790	
	1.8650	1.1800		2.2200	1.7700		2.2800		1.4782	
	1.8660	1.1820	0.0000§	2.2210	1.7800	0.0000§	2.2400	0.0389*	1.4796	0.0000§
AVG	1.8647	1.1823		2.2200	1.7713		2.2590		1.4789	
4000	2.9530	2.0940		3.6840	3.3280		3.5610		1.8640	
	2.9550	2.0910		3.6800	3.3400		3.5200		1.8645	
	2.9510	2.0890	0.0000§	3.6900	3.3500	0.0000§	3.5000	0.0056†	1.8643	0.0000§
AVG	2.9530	2.0913		3.6847	3.3393		3.5270		1.8643	
4500	3.7580	2.6440		4.6580	4.0200		4.4710		2.2410	
	3.7550	2.6500		4.6600	4.0500		4.4200		2.2425	
	3.7600	2.6490	0.0000§	4.6400	4.0400	0.0000§	4.4900	0.0037†	2.2460	0.0000§
AVG	3.7577	2.6477		4.6527	4.0367		4.4603		2.2432	

*p-value ≤0.05, †p-value ≤0.01, ‡p-value ≤0.001, §p-value ≤0.0001